

Fall 2006

# Microparticulate drug reformulation using electrostatic layer -by -layer assembly and co-entrapment with anionic phospholipids in calcium carbonate matrix

Krishna Gopal  
*Louisiana Tech University*

Follow this and additional works at: <https://digitalcommons.latech.edu/dissertations>

 Part of the [Pharmacology Commons](#)

---

## Recommended Citation

Gopal, Krishna, "" (2006). *Dissertation*. 541.  
<https://digitalcommons.latech.edu/dissertations/541>

This Dissertation is brought to you for free and open access by the Graduate School at Louisiana Tech Digital Commons. It has been accepted for inclusion in Doctoral Dissertations by an authorized administrator of Louisiana Tech Digital Commons. For more information, please contact [digitalcommons@latech.edu](mailto:digitalcommons@latech.edu).

**MICROPARTICULATE DRUG REFORMULATION USING  
ELECTROSTATIC LAYER-BY-LAYER ASSEMBLY  
AND CO-ENTRAPMENT WITH ANIONIC  
PHOSPHOLIPIDS IN CALCIUM  
CARBONATE MATRIX**

by

Krishna Gopal, B.Tech.

A Dissertation Presented in Partial Fulfillment  
of the Requirements for the Degree  
Doctor of Philosophy

COLLEGE OF ENGINEERING AND SCIENCE  
LOUISIANA TECH UNIVERSITY

November 2006

UMI Number: 3261292

### INFORMATION TO USERS

The quality of this reproduction is dependent upon the quality of the copy submitted. Broken or indistinct print, colored or poor quality illustrations and photographs, print bleed-through, substandard margins, and improper alignment can adversely affect reproduction.

In the unlikely event that the author did not send a complete manuscript and there are missing pages, these will be noted. Also, if unauthorized copyright material had to be removed, a note will indicate the deletion.

**UMI**<sup>®</sup>

---

UMI Microform 3261292

Copyright 2007 by ProQuest Information and Learning Company.

All rights reserved. This microform edition is protected against unauthorized copying under Title 17, United States Code.

ProQuest Information and Learning Company  
300 North Zeeb Road  
P.O. Box 1346  
Ann Arbor, MI 48106-1346

LOUISIANA TECH UNIVERSITY

THE GRADUATE SCHOOL

09/20/2006

Date

We hereby recommend that the dissertation prepared under our supervision by Krishna Gopal

entitled Microparticulate Drug Reformulation Using Electrostatic Layer-by-Layer Assembly

and Co-Entrapment With Anionic Phospholipids in Calcium Carbonate Matrix

be accepted in partial fulfillment of the requirements for the Degree of Doctor of Philosophy.

Yusuf K. You  
Supervisor of Dissertation Research  
Steve J.  
Head of Department  
Biomedical Engineering  
Department

Recommendation concurred in:

Michael J. McShane (Co-Chair)  
PNH

Steve J.

W. J.

David Mills

Advisory Committee

Approved: Paul Muradchandra  
Director of Graduate Studies

Approved: Timothy M. Conarty  
Dean of the Graduate School

Sam Noyes  
Dean of the College

## ABSTRACT

Non-invasive drug delivery systems for therapeutic drugs are gaining prominence. One such system, the nasal delivery system, shows good prospect for effective delivery of some drugs, however, it is yet to be well established for others. The preparation of a reformulated drug and studying its *in vitro* characteristics is a crucial step in the process of adapting the new drug for nasal delivery systems. The purpose of this research is to study the effect of electrostatic layer by layer assembly of polyelectrolytes on PROMAXX<sup>®</sup> insulin microparticles and to study the chemical, physical and corresponding release properties of the resulting formulations. PROMAXX<sup>®</sup> insulin microparticles of recombinant human insulin prepared and provided by Epic Therapeutics Inc<sup>®</sup>. During reformulation the temperature, pH, salt concentration and excipient concentrations were controlled to achieve maximum yield of final product and minimize raw material consumption. *In vitro* release studies were performed to study the release properties of various formulations prepared by electrostatic layer-by-layer assembly and compared with a standard insulin formulation. A key finding involved that the control release of insulin can be achieved by suitable selection of first polycation layer, and the consequent polyelectrolyte layers can be used to fine-tune the release. In addition, polyelectrolyte requirements were established for production of grams of final product.


To retard the permeability of thin films prepared with electrostatic layer-by-layer assembly, lipid bilayers were incorporated in layer by layer assembly. Study of diffusion properties of the composite multilayer films demonstrated that outermost lipid layer on hollow polyelectrolyte microcapsules acts as an effective diffusion barrier for FITC-dextran (MW 4300), which is comparable to insulin (MW 5800), and hence an important development towards imparting stealth and sustained release properties to low molecular weight drugs.

Hydrophobic drugs pose a problem for entrapment in polymeric matrices due to their poor solubility in aqueous media. In an effort to the study cores other than protein and drug microcrystals for nasal drug delivery, calcium carbonate microparticles incorporating phospholipids and hydrophobic molecules were prepared and characterized. The hydrophobic molecules were co-entrapped with anionic phospholipids in the calcium carbonate matrix with a near homogenous distribution of the molecules in the matrix, with loading up to 4 % (w/w) of calcium carbonate. Further, the anionic phospholipids influence the crystal morphology of calcium carbonate resulting in a decrease in release of hydrophobic molecules due to decreased rate of re-crystallization.

## APPROVAL FOR SCHOLARLY DISSEMINATION

The author grants to the Prescott Memorial Library of Louisiana Tech University the right to reproduce, by appropriate methods, upon request, any or all portions of this Dissertation. It is understood that "proper request" consists of the agreement, on the part of the requesting party, that said reproduction is for his personal use and that subsequent reproduction will not occur without written approval of the author of this Dissertation. Further, any portions of the Dissertation used in books, papers, and other works must be appropriately referenced to this Dissertation.

Finally, the author of this Dissertation reserves the right to publish freely, in the literature, at any time, any or all portions of this Dissertation.

Author   
Date 10/31/2006

*Dedicated to my parents Suryakumari Mantripragada and  
Sambasiva Mantripragada and  
my sister Ratna Srivalli.*



## TABLE OF CONTENTS

|  |     |
|--|-----|
| ABSTRACT.....  | iii |
| LIST OF TABLES.....  | x   |
| LIST OF FIGURES.....   | xi  |
| ACKNOWLEDGMENTS.....   | xiv |
| CHAPTER 1 INTRODUCTION.....  | 1   |
| 1.1 Microencapsulation.....  | 2   |
| 1.1.1 Microcapsules and Microparticles.....                          | 2   |
| 1.2 Importance of Size in Microencapsulation.....                    | 4   |
| 1.3 Objectives and Novel Aspects.....                                | 5   |
| 1.4 Organization of Chapters.....                                    | 9   |
| CHAPTER 2 BACKGROUND AND THEORY.....                                 | 11  |
| 2.1 Introduction.....  | 11  |
| 2.2 Market Outlook.....  | 11  |
| 2.3 Insulin Reformulations.....                                      | 12  |
| 2.3.1 Diabetes, Insulin and the Pharmaceutical Industry.....         | 12  |
| 2.3.2 Physiochemical Properties of Insulin.....                      | 14  |
| 2.3.3 Design of Insulin Drug Reformulation.....                      | 15  |
| 2.3.4 Current Insulin Drug Reformulations.....                       | 16  |
| 2.3.4.1 Oral delivery.....   | 18  |
| 2.3.4.2 Nasal delivery.....  | 20  |
| 2.3.4.3 Subcutaneous/musculo-skeletal injection.....                 | 23  |
| 2.3.4.4 Transdermal and other intelligent drug delivery systems..... | 26  |
| 2.4 Phospholipids Retard Diffusion of LbL Thin Films.....            | 29  |
| 2.5 Calcium Salts for Delivery of Hydrophobic Drugs.....             | 33  |
| 2.6 Instrumentation: Theory and Practice.....                        | 35  |
| 2.6.1 Quartz Crystal Microbalance.....                               | 35  |
| 2.6.2 Zeta-Potential and the Theory Involved.....                    | 39  |
| 2.6.3 Confocal Microscopy.....                                       | 46  |
| 2.6.4 Thermogravimetric Analysis.....                                | 50  |

|   |        |
|---|--------|
| CHAPTER 3 SURFACE MODIFICATION OF INSULIN<br>MICROPARTICLES USING<br>ELECTROSTATIC LAYER-BY-LAYER<br>ASSEMBLY ..... | 52     |
| 3.1 Introduction.....   | 52     |
| 3.2 Experimental Methods .....  | 55     |
| 3.2.1 Materials. ....   | 55     |
| 3.2.2 Layer-by-Layer Coating of Insulin Microspheres with<br>Multiple Polyelectrolyte Layers.....                   | 56     |
| 3.2.3 Quartz Crystal Microbalance Measurements.....   | 57     |
| 3.2.4 Microparticles Surface Potential Measurements .....   | 57     |
| 3.2.5 Confocal Laser Scanning Microscopy. ....  | 58     |
| 3.2.6 <i>In Vitro</i> Release Study. ....   | 58     |
| 3.3 Results and Discussion .....  | 59     |
| 3.3.1 Electrostatic LbL Assembly in the Presence of PEG.....  | 59     |
| 3.3.2 Influence of Temperature on LbL Assembly in the Presence<br>of PEG.....                                       | 61     |
| 3.3.3 Coating PROMAXX <sup>®</sup> Insulin-Microspheres with<br>Polyelectrolytes.....                               | 63     |
| 3.3.3.1 pH 5.8, positive core .....   | 64     |
| 3.3.3.2 pH 7.0, negative core .....   | 65     |
| 3.3.4 Optimization of the Nanoencapsulation Conditions. ....  | 67     |
| 3.3.4.1 pH 7.0, negative core .....   | 68     |
| 3.3.4.2 pH 5.8, positive core .....   | 69     |
| 3.3.5 Polyelectrolyte Interaction with Microparticles.....  | 69     |
| 3.3.5.1 At pH 7.0.....  | 69     |
| 3.3.5.2 At pH 5.8.....  | 70     |
| 3.3.6 Modification of Microparticle Solubility.....   | 70     |
| 3.3.6.1 pH 5.8, positive core .....   | 71     |
| 3.3.6.2 pH 7.0 negative core .....  | 72     |
| 3.3.7 Effect of Polyion Concentration on Release of Insulin from<br>Microparticles .....                            | 75     |
| 3.4 Conclusions.....  | 76     |
| <br>CHAPTER 4 LAYER-BY-LAYER ASSEMBLY USING<br>PHOSPHOLIPIDS AS A DIFFUSION BARRIER.....                            | <br>78 |
| 4.1 Introduction.....   | 78     |
| 4.2 Experimental .....  | 79     |
| 4.2.1 Materials .....   | 79     |
| 4.2.2 Preparation of Unilamellar Liposomes .....  | 80     |
| 4.2.3 Preparation of Polyelectrolyte Solutions .....  | 80     |
| 4.2.4 Assembly on Quartz Crystal Microbalance .....   | 80     |
| 4.2.5 LbL Assembly on PMA Microparticles for $\zeta$ -Potential<br>Studies.....                                     | 81     |

|  |     |
|--|-----|
| 4.2.6 Phospholipid Coatings on Hollow PAH/PSS Microcapsules<br>and Measurement of Diffusion Coefficient of the Capsule<br>Wall.....                  | 81  |
| 4.3 Results and Discussion .....   | 82  |
| 4.3.1 Quartz Crystal Microbalance Study of Lipid-Polyelectrolyte<br>Multilayers.....   | 82  |
| 4.3.2 Analysis of $\zeta$ -Potential Measurements.....   | 84  |
| 4.3.3 Diffusion Properties of Lipid Coated Hollow Polyelectrolyte<br>Microcapsules .....   | 86  |
| 4.4 Conclusions.....   | 89  |
| <br>   |     |
| CHAPTER 5 COMPOSITE PHOSPHOLIPID -<br>CALCIUM CARBONATE MICROPARTICLES CO-<br>ENTRAPMENT OF ANIONIC PHOSPHOLIPIDS<br>AND HYDROPHOBIC MOLECULES ..... | 90  |
| 5.1 Introduction.....  | 90  |
| 5.2 Experimental.....  | 92  |
| 5.2.1 Materials. ....  | 92  |
| 5.2.2 Preparation of Calcium Carbonate Particles Incorporating<br>Phospholipids in the Matrix.....   | 93  |
| 5.2.3 Preparation of Calcium Carbonate Microparticles Without<br>Phospholipids in the Matrix.....  | 93  |
| 5.2.4 Preparation of Calcium Carbonate Microparticles with<br>Hydrophobic Molecule Entrapped in the Matirix.....                                     | 94  |
| 5.3 Results and Discussion .....   | 94  |
| 5.3.1 Characterization of Morphology and Microstructure .....  | 94  |
| 5.3.2 Effect of Molar Ratio of Reactants .....   | 97  |
| 5.3.3 Thermogravimetric Analysis of Calcium Carbonate<br>Microparticles Prepared by Different Methods .....  | 100 |
| 5.3.4 Long Term Stability of the Calcium Carbonate<br>Microparticles .....   | 102 |
| 5.3.5 Incorporation of Hydrophobic Molecules in Calcium<br>Carbonate Matrix to Simulate a Model Drug .....   | 103 |
| 5.4 Conclusion .....   | 103 |
| <br>   |     |
| CHAPTER 6 CONCLUSIONS AND FUTURE WORK.....   | 105 |
| 6.1 Conclusions.....   | 105 |
| 6.2 Future work.....   | 109 |
| <br>   |     |
| REFERENCES .....   | 111 |
| <br>   |     |
| VITA .....   | 121 |

## LIST OF TABLES

|  |    |
|--|----|
| Table 1.1. Classification of microencapsulation methods [1].....   | 2  |
| Table 1.2. Particle dimension estimates in drug delivery [1]. .....  | 4  |
| Table 2.1. Commercial development of pulmonary insulin systems [28]. .....   | 23 |
| Table 2.2. Injectable insulin formulations [29].....   | 24 |
| Table 3.1. Bilayer thickness (in nm) for polycation / polyanion assemblies in 16%<br>PEG-0.7% NaCl, pH 5.8, room temperature, 15 min per layer. .... | 61 |
| Table 3.2. Bilayer thickness (in nm) for polycation / polyanion assemblies in 16%<br>PEG-0.7% NaCl, pH 5.8, 2 °C, 60 min per layer. ....             | 62 |
| Table 4.1. Thickness of lipid/polyelectrolyte bilayers.....  | 83 |

## LIST OF FIGURES

|   |    |
|---|----|
| Figure 1.1. Various configurations of, (a) microcapsules and (b) microspheres [1].  | 3  |
| Figure 2.1. Hierarchy of reformulation [4].   | 12 |
| Figure 2.2. Primary structure of human insulin. The shaded regions are involved in self association [8].  | 14 |
| Figure 2.3. Overview of Insulin Formulations.   | 17 |
| Figure 2.4. LbL schemes for polymers, proteins, nanoparticles ( <i>top</i> ). Preparation of hollow polyelectrolyte capsules ( <i>bottom</i> ).   | 30 |
| Figure 2.5. Biocompatible polyelectrolytes in Layer-by-Layer assembly.  | 31 |
| Figure 2.6. Schemes showing the alternate deposition of polyelectrolytes and phospholipids. Such architectures can impart special properties to LbL films like diffusion control and biocompatibility.  | 33 |
| Figure 2.7. Transverse shear wave in a quartz crystal microbalance where $t_q$ is thickness of the quartz crystal, $t_f$ is the thickness of the film.  | 36 |
| Figure 2.8. Relative magnitudes of potentials of interest.  | 42 |
| Figure 2.9. The domain within which most investigations of aqueous colloidal systems lie in terms of particle radii and 1:1 electrolyte concentration. The diagonal lines indicate the limits of the Hückel and the Helmholtz-Smoluchowski Equations. | 45 |
| Figure 2.10. FRAP experimental schematic for estimation of diffusion coefficient of microcapsules.  | 47 |
| Figure 2.11. Principle of thermogravimetric analysis: a sample is heated at a fixed rate and mass changes are recorded with changes in temperature.   | 51 |
| Figure 3.1. A schematic illustration of the assembly of polyelectrolyte layers on insulin PROMAXX <sup>®</sup> microspheres at pH 7.0.  | 55 |

|   |    |
|---|----|
| Figure 3.2. Quartz crystal microbalance data for assembly of different polyelectrolytes from 1 mg/mL solutions in 16 % PEG-0.7 % NaCl buffer, pH 5.8 at room temperature (a) and over ice (b). Experimental errors are $\pm 0.5$ nm.....  | 60 |
| Figure 3.3. Surface charge of microparticles after deposition of different bilayers at pH 5.8 (a); and pH 7.0 (b).....  | 64 |
| Figure 3.4. Surface charge alternation for insulin microparticles coated with multiple polyelectrolyte layers at, (a) pH 5.8 and (b) pH 7.0.....  | 66 |
| Figure 3.5. $\zeta$ -potential of microparticles after LbL assembly at pH 7.0 on insulin microparticles in solutions with different concentrations. Closed diamonds represent ProtS. Open circles and closed triangles represent ChS and CMC respectively, on particles that were coated with ProtS at 1.5mg/ml. Closed squares represent particles that were first coated with ProtS at 1.5mg/ml, followed by CMC at 1.5mg/ml and finally a second layer of ProtS..... | 68 |
| Figure 3.6. Confocal images of insulin microparticles coated with, a) FITC-ProtS layer in 16 % PEG-0.7 % NaCl, pH 7.0; and (b) PSS/FITC-PLys at pH 5.8. ....  | 70 |
| Figure 3.7. Cumulative <i>in vitro</i> release of insulin from microparticles coated with CMC and ProtS up to two bilayers at pH 5.8. The control is uncoated microparticles suspended in PEG buffer at pH 5.8.....   | 71 |
| Figure 3.8. Cumulative <i>in vitro</i> release of insulin from microparticles coated with single layer of polycation at pH 7.0. The control is uncoated insulin microparticles. ....  | 72 |
| Figure 3.9. Cumulative <i>in vitro</i> release of insulin from microparticles coated with ProtS as the first layer and subsequent layers of polyanions- PAsp and CMC at pH 7.0. The control represents uncoated microparticles.....   | 73 |
| Figure 3.10. Concentration dependence of outermost polyelectrolyte layer on insulin release <i>in vitro</i> after 48 hours from insulin microparticles coated with different polyelectrolyte concentrations in 16 % PEG-0.7 % NaCl pH 7.0. ....   | 75 |
| Figure 4.1. $\zeta$ -Potential analysis of polyelectrolyte/lipid assemblies on PMA/(PAH/PSS) <sub>2</sub> microparticles, the first layer corresponding to respective polycation (Top): lipid – DPPA-DPPC 20% w/w with polyelectrolytes. (Bottom): lipid – PG-PC 20% w/w with polyelectrolytes.....   | 85 |
| Figure 4.2. Lipid coating on (PAH/PSS) <sub>5</sub> to show lipid coating on microcapsules. ....  | 86 |

- Figure 4.3. Fluorescence recovery of (PSS/PAH)<sub>5</sub> capsules coated with different lipid mixtures: (1) uncoated, (2) PG-PC 20% coated, (3) DPPA-DPPC 20% coated. The intensities of capsule interior are shown relatively that of surrounding solution.....87
- Figure 4.4. Fluorescence recovery after photobleaching for different capsules in a 10  $\mu$ M solution of FITC-dextran of MW 4300: a) an uncoated (PSS/PAH)<sub>5</sub> capsule, b) a capsule coated with one bilayer of PG-PC (20 % w/w) and c) a capsule coated with one bilayer of DPPA- DPPC (20% w/w). .....88
- Figure 5.1. Scheme for entrapment of hydrophobic drugs in mineral matrix. The hydrophobic molecules are localized in the hydrophobic tail regions of the phospholipids molecules. The hydrophilic head interacts with the mineral matrix.....92
- Figure 5.2. Representative SEM images of calcite microcrystals prepared by reaction of 1 mL 0.01 M CaCl<sub>2</sub> + 1 mL 0.375M NH<sub>4</sub>HCO<sub>3</sub> + 2 mL of DI water (a). Porous CaCO<sub>3</sub> microparticles by first reacting 2 mL of 1 mg/mL DPPA +1 mL 0.01 M CaCl<sub>2</sub> + (after 10 min) 1 mL of NH<sub>4</sub>HCO<sub>3</sub> (b), these microparticles contain 3%(w/w) phospholipids in matrix. ....95
- Figure 5.3. X-ray diffraction pattern of calcium carbonate microparticles. The top graph shows the X-ray diffraction pattern of calcite with the principal peaks highlighted [117]. The bottom graph shows the X-ray diffraction pattern of calcium carbonate microparticles synthesized in the presence of DPPA (V-veterite, C-calcite). ....97
- Figure 5.4. Effect of the ratio of Ca<sup>2+</sup> to HCO<sub>3</sub><sup>-</sup> ions on the size of calcium carbonate microparticles based on 0.375 M concentration of NH<sub>4</sub>HCO<sub>3</sub> in total volume, with DPPA concentration constant at 0.2 mg/mL.....98
- Figure 5.5. CLSM image of cross-section of (a) calcium carbonate microparticles incorporating FITC-EA; in phospholipid deficient medium the non-uniform distribution of phospholipids in the matrix is observed (inset) and (b) prepared by reaction of CaCl<sub>2</sub> and NH<sub>4</sub>HCO<sub>3</sub> in the presence of (DPPA 20%(w/w) -DPPC mixture containing [Ru(dpp)<sub>3</sub>]<sup>2+</sup> which is a hydrophobic molecule localized in the hydrophobic region of fatty acid side chain.....100
- Figure 5.6. Thermogravimetric analysis of (A) calcite and DPPA and (B) calcium carbonate microparticles prepared in the presence of DPPA, the change in weight is shown as percentage total weight (inset) (1) and mixture of calcite and DPPA (2). The temperature was increased at 5°C/minute. ....101

## ACKNOWLEDGMENTS

I am deeply indebted to my advisors Dr. Yuri Lvov and Dr. Michael J. McShane for their continued guidance and encouragement throughout the duration of my Ph.D. I would like to thank our collaborators Dr. Melgardt de Villiers and his student Ning Li who were at University of Louisiana at Monroe (currently at University of Wisconsin, Madison.), for useful discussions and suggestions in the work related to calcium carbonate microcores. Epic Therapeutics Inc<sup>®</sup> (Baxter Healthcare Corporation) and the people there– Julia Rashba-Step, Ramin Darvari and Quinmin Lin without whom the work with insulin microcores would not have been possible. My advisory committee members Dr. Steven A. Jones, Dr. David K. Mills, and Dr. Walter Besio have been a great guidance and help during my research, I thank them for letting me use their labs when the need arose.

I would like to thank our lab postdocs Dr. Tatsiana Shutava and Dr. Zonghuan Lu who have been a constant source of knowledge, research papers, funny anecdotes, and fruitful discussions in research. Erich Stein, Dr. Patrick Grant, and Dr. Quincy Brown, though not students of our group, have been most helpful, be it with instrument training or brainstorming. I would like to thank Malcolm Prouty in particular for proofreading numerous documents I pushed under his nose. I am grateful to Dmitry Shchukin for the help rendered with SEM and X-Ray diffraction experiments.



I would like to acknowledge financial assistance from Epic Therapeutics Inc, the National Institutes of Health (RO1 EB000739-01) and the National Science Foundation (0210298).

I would like to thank other members of my lab, and the IfM staff for not only help received towards my Ph.D but also in many areas although not of academic interest made my stay at Louisiana Tech fondly memorable.

# CHAPTER 1

## INTRODUCTION

Over the last ten decades healthcare has improved considerably throughout the world, improving life expectancy of humankind. Advances in science and technology have provided amenities for a comfortable living, which coupled with a sedentary lifestyle have led to an increasing number of people who suffer from diabetes. Pharmaceutical companies are trying to cope with increased demand for new drugs and better delivery systems for existing drugs.

Major players in the drug market are characterized by two main traits, namely the discovery of new drugs, or reformulation of existing drugs. The drug delivery market is intensely competitive and survival of a company depends on the ability to innovate and obtain patent protections for new developments and enhanced products. The cost of developing a new drug from discovery to marketing is close to a billion dollars. Therefore, emphasis on improvement of delivery methods is inevitable for the industry due to economic reasons. Lately, more attention is being given to particulate delivery systems with known size distributions to achieve better predictable pharmacodynamics and pharmacokinetics. An increasing number of patents are being filed for novel microencapsulation techniques themselves. This work is an effort to achieve that

competitive edge through product enhancement and innovation through the study of fundamental processes involving surface chemistry changes at nano and microscale.

## **1.1 Microencapsulation**

Microencapsulation is not a new concept and has been in use since the early 20<sup>th</sup> century. Numerous methods exist for encapsulation of many active agents, with wide-ranging applications including but not limited to food, consumer products, cosmetics, and pharmaceuticals. Microencapsulation in most instances aims to protect the encapsulated material and/or to enhance its stability. Many microencapsulation schemes involve the entrapment of simple molecules and usually entail harsh processing conditions such as high temperatures, and use of non-aqueous solvents and surfactants.

### **1.1.1 Microcapsules and Microparticles**

A general summary of microencapsulation methods is presented in Table 1.1.

Table 1.1. Classification of microencapsulation methods [1].

| <b>Process</b>             | <b>Coating material</b>              | <b>Suspended medium</b> |
|----------------------------|--------------------------------------|-------------------------|
| Interfacial polymerization | Water-soluble and insoluble monomers | Aqueous/organic solvent |
| Complex coacervation       | Water-soluble polyelectrolyte        | Water                   |
| Coacervation               | Hydrophobic polymers                 | Organic solvent         |
| Thermal denaturation       | Proteins                             | Organic                 |
| Salting-out                | Water-soluble polymer                | Water                   |
| Solvent evaporation        | Hydrophilic or hydrophobic polymers  | Organic or water        |
| Hot melt                   | Hydrophilic or hydrophobic polymers  | Aqueous/organic solvent |
| Solvent removal            | Hydrophilic or hydrophobic polymers  | Organic solvents        |
| Spray-drying               | Hydrophilic or hydrophobic polymers  | Air, nitrogen           |
| Phase separation           | Hydrophilic or hydrophobic polymers  | Aqueous/organic         |

The microencapsulation methods described in Table 1.1 produce particles generally characterized as microcapsules or microspheres. Microcapsules can be defined as a continuous envelope enclosing a well defined core and microspheres as solid particles with a homogenous or a heterogeneous core. The alternate architectures of

microcapsules and microspheres produced through the microencapsulation methods listed in Table 1.1 are shown in .

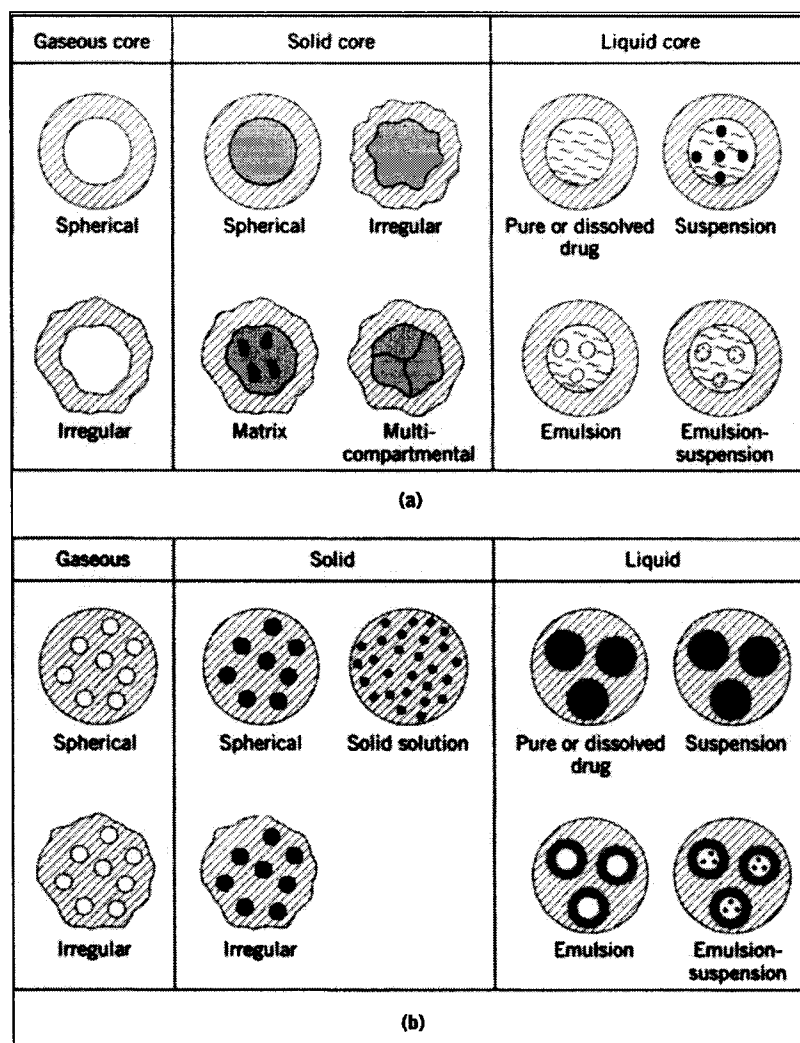


Figure 1.1. Various configurations of, (a) microcapsules and (b) microspheres [1].

Microcapsules consist of different solid, liquid or gaseous active material entrapped in a solid shell (a). Microspheres on the other hand have a solid matrix with active material dispersed as gas bubbles, liquid droplets, emulsions, or solid particles dispersed in the microsphere matrix. In this work two types of particles will be discussed

widely microcapsules of emulsion-suspension type with a semi-solid core such as insulin, and microspheres with solid solution type in which organic micelles occur discreetly in a solid calcium carbonate core ( ).

More recently, many new drugs coming in the market are large biomolecules such as proteins, peptides, DNA and oligonucleotides. The use of harsh treatment with such active agents could potentially result in degradation of the active agent, subsequently causing loss of bioactivity.

### **1.2 Importance of Size in Microencapsulation**

A wide range of sizes is permissible for particle size in drug delivery depending on the drug delivery method employed and the nature of active formulation. Table 1.2 summarizes the typical size ranges of pharmaceutically relevant particle sizes and their nomenclature.

Table 1.2. Particle dimension estimates in drug delivery [1].

| <b>Particle Size (<math>\mu\text{m}</math>)</b> | <b>Examples</b>  |
|---|--|
| 0.001-0.5                                       | Proteins, polymers, oligonucleotides, DNA, micelles, microemulsions, colloidal suspensions |
| 0.5-10  | Suspensions, fine emulsions, micronized drugs  |
| 10-50   | Coarse emulsions, flocculated suspensions  |
| 50-150  | Fine powders   |
| 150-1,000                                       | Coarse powders   |
| 1,000-3,400                                     | Granules   |

Currently, micronized drugs and microemulsions with narrow particle size ranges are becoming favored over larger particulate and/or polydisperse systems in both industrial and academic research. Small particles with a narrow size distribution have

more predictable release profiles and increased bioavailability. The micronized drug delivery with particles in the 0.5-10  $\mu\text{m}$  range also show promise for nasal and pulmonary delivery of drugs [1].

### **1.3 Objectives and Novel Aspects**

This work represents an advancement in a particulate drug delivery system with the emphasis on peptide delivery using layer-by-layer (LbL) electrostatic self-assembly and entrapment of hydrophobic molecules in an inorganic matrix. This work advances both particle-based drug delivery and the LbL technique itself. Further, it demonstrates for the first time the electrostatic LbL assembly of nanofilm coatings in the presence of high concentration of inert and semi-interacting polymer- poly(ethelenglycol).

This work demonstrates the use of economical but milder methods like the electrostatic LbL assembly, use of an aqueous medium, phospholipids, and biologically safer minerals such as calcium carbonate for preparing microparticles with reliably controlled particle size distribution.

This dissertation consists of two parts, the surface modification of insulin microparticles PROMAXX<sup>®</sup>, and the synthesis of calcium carbonate microparticles. Specific aims and the design of experiments to achieve the objectives will be thoroughly treated in the following discussion.

#### **Hypothesis I**

The assembly of LbL multilayers on insulin microparticles can be used to achieve a sustained release of drug from the microparticle, impart proteolytic resistance, achieve microparticle stabilization by preventing aggregation, stabilization of insulin tertiary

structure through complex formation with polyelectrolytes and achieve an outermost biocompatible coating to minimize immune response.

The work with insulin microparticles involved the surface modification of insulin microparticles, as achieved through the use of LbL assembly. LbL assembly was chosen because LbL assembly has significant advantages over other methods as it can be employed in an aqueous media to deposit nanometer-thick ultrathin films with a wide choice of materials. The conditions of LbL assembly can be achieved under mild conditions over a wide range of temperatures.

To achieve the objectives above, said a number of aspects related to LbL assembly need to be investigated. The first step involves choice of materials to perform LbL assembly, followed by determining suitable temperature, assembly buffers, pH of assembly, and centrifuge speed. Choice of materials was limited to biopolymers such as polyaminoacids, polysaccharides, polyamides, phospholipids, and naturally occurring peptides in either modified or unmodified form. However some experiments needed to be performed with synthetic polyelectrolytes to establish the feasibility, and to compare assembly results with biopolymers. This choice of biological polymers could offer better biocompatibility compared with synthetic polymers. To establish the assembly conditions and materials the first step involves the study and characterization of LbL assembly on flat substrates, and on microparticles. Such a study would enable the characterization of the effects of different material and concentration on the release of insulin microparticles.

A simple mathematical model accounting for the release properties of different polyelectrolyte layers, the number and order of layers would be impractical because of variable interactions of protein-polyelectrolyte complexes. Such interactions depend on

the functional groups of polyelectrolyte with the functional groups on the insulin molecule, and the protein-polyelectrolyte complex can be reversible or irreversible. The temperature and pH of assembly and consequent release studies also affect the drug release from the microparticle. Therefore, analysis of experimental data has been used to optimize the LbL process, establishing various parameters required for scaleup.

In this work, to scaleup the process for production of grams of final product (pilot plant scale), the concentrations of polyelectrolytes, pH, temperature, centrifuge, assembly medium and number of process steps need to be established and standardized for unit weight of insulin microparticles. These parameters need to be established by experimentation. This physical and chemical characterization of microparticles prepared with different polyelectrolytes, at different assembly conditions, and the consequent release properties are expected to provide an insight into the most suitable polyelectrolytes for *in vivo* testing.

Controlled experimental conditions have been used in this work, and the experimental data generated have been used to optimize the final process scaleup, thus establishing concentrations of polyelectrolytes and the resulting surface and release properties of the drug microparticles.

### **Hypothesis II**

Phospholipid-polyelectrolyte composite films can effectively modulate diffusion properties of molecules smaller than MW 10,000.

As an advancement of the work on insulin drug formulation, the use of phospholipids in combination with polyelectrolytes can effectively modulate the diffusion properties of LbL nanofilms.



Such a scheme could minimize the number of process steps for nanofilms acting as a simple diffusion barrier [2], in addition to providing a biocompatible outermost coating. However, before it's in insulin formulation, the optimization of suitable phospholipids compositions, and study of the multilayer-phospholipid-polyelectrolyte thin film properties is the fundamental step. Assembly of single phospholipid layer on polyelectrolyte multilayers has been demonstrated by Moya et al. [3]; however, multilayer polyelectrolyte/phospholipid assemblies have not been demonstrated. To study these properties, qualitative and quantitative techniques are required to establish phospholipids compositions and corresponding LbL film properties. In addition the optimized material composition and assembly conditions can be effectively used to design and test the diffusion properties of such thin films using a model compound similar to insulin. Thus, the refined technique could effectively be employed in modulating the diffusion properties of insulin.

The second objective is to develop a particulate drug delivery system stems from the need to develop suitable carriers for hydrophobic drugs. Most nasal delivery systems are based on polymeric microparticles, and face a major drawback due to poor systemic clearance of inert polymeric materials. Moreover, suitable dispersion mediums for polymer-based microparticles involve liquids, which consequently involve significant handling costs, and custom delivery devices. Mineral particulate systems for drug delivery are a recent development and well suited for delivery of drugs with existing nasal delivery devices. Calcium carbonate, apatite, and hydroxyapatite are three mineral particulate delivery systems gaining prominence because of their biocompatible nature. Among these calcium carbonate microparticles show promise due to their biodegradation

rates. Adsorption of drug on surface of microparticles and delivery *in vivo* has been shown to be effective for hydrophilic drugs. However, delivery of hydrophobic drugs using calcium carbonate needs to be developed.

### **Hypothesis III**

Hydrophobic molecules can be entrapped in calcium carbonate matrix.

This work involves the development of one such system and establishes the proof of concept for entrapment of hydrophobic molecules in the calcium carbonate matrix. Calcium carbonate microparticles incorporating phospholipids in the matrix and consequently the co-entrapment of hydrophobic molecules are demonstrated. The characterization of the microparticles using various analytical techniques, such as thermogravimetric analysis, SEM and XRD is described. Establishing proof of concept for entrapment of hydrophobic molecules was achieved using a model hydrophobic fluorescent dye.

A system employing the use of phospholipids for entrapment of a species in calcium carbonate matrix is flexible and can in principle be employed to entrap not only hydrophobic drugs but also hydrophilic and peptide drugs. Large drug molecules such as proteins exhibit marked surface active property in that they partition or preferentially adsorb on surfaces at an interface; thus it is possible to entrap such molecules using the proposed scheme.

### **1.4 Organization of Chapters**

This dissertation has been organized in chapters so that Chapters 3, 4, and 5 are self contained. Some degree of redundancy has been retained to make these chapters more readable as a contiguous piece work. Chapter 2 covers the background and theory

of the material presented in Chapters 3, 4, and 5 as well as the principles behind the instrumentation and computation involved. Chapter 6 summarizes the entire work and provides recommendations for future work. Chapter 3 describes applicability of an established technique – the electrostatic LbL assembly to enhance a pharmaceutical product PROMAXX<sup>®</sup>. Chapter 4 describes enhancement of the LbL technique by use of phospholipids. Chapter 5 describes the use of phospholipids to develop a novel technique to entrap small hydrophobic materials in an inorganic and relatively inert calcium carbonate matrix.

## **CHAPTER 2**

### **BACKGROUND AND THEORY**

#### **2.1 Introduction**

In this chapter the literature concerning the insulin formulations, the LbL technique, and inorganic/organic matrices is reviewed with respect to drug delivery. Relevant instrumentation and theory used are presented to better understand the multiple but succinct references to the same in the following three chapters.

#### **2.2 Market Outlook**

Pharmaceutical companies market drugs based on less-than-perfect delivery systems or formulations, with their prime concern being limited to the safety and efficacy of the drug. Moreover, alternate development of drug delivery platforms and formulations is inhibited by patent protections. To overcome these drawbacks more and more pharmaceutical companies are partnering with drug delivery companies to co-develop marketable products. During the term of patent protection the parent company is guaranteed artificially inflated revenue for brand-name drugs, and patent expiration results in rapidly declining sales due to a host of generic drug manufacturers selling at a fraction of the price. Clinicians and patients may prefer reformulated brand-name drugs, possibly due to increased value or improved product, and the reformulation may in turn

lead to patent extension. Patent expiry also creates a window for competing firms to improve drug formulations. Selecting a drug candidate for reformulation is governed by the market value it generates. Figure 2.1 shows the attractiveness of reformulation for a general drug[4].

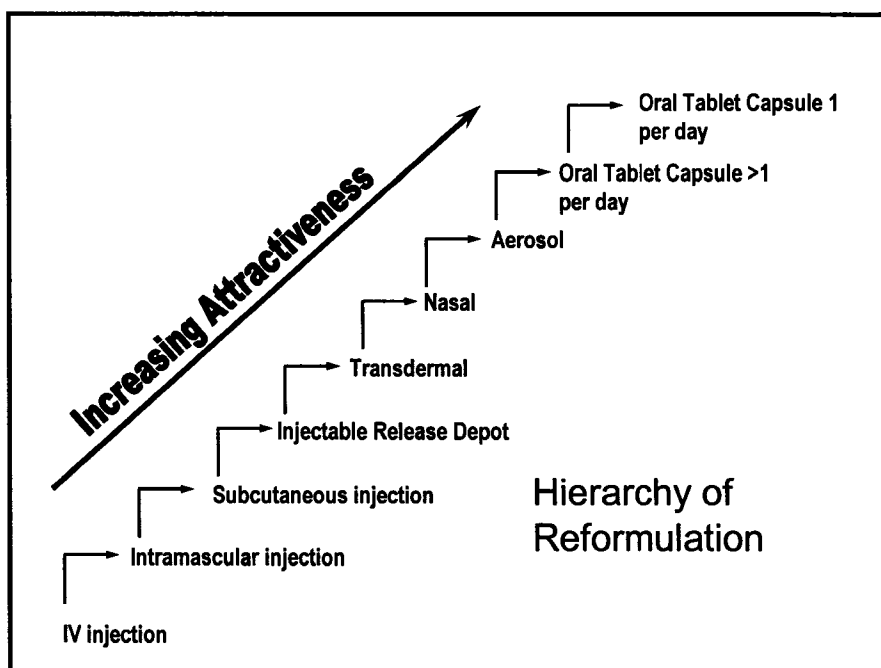


Figure 2.1. Hierarchy of reformulation [4].

## 2.3 Insulin Reformulations

### 2.3.1 Diabetes, Insulin and the Pharmaceutical Industry

Diabetes, a chronic metabolic disorder, continues to be a global epidemic, affecting more than 170 million people (WHO) globally and increasing at an alarming rate. Type I diabetes results from inability of the body to produce insulin. This form of diabetes is treated with insulin injections. During the eventual course of type II diabetes (due to insulin resistance) insulin injections need to be administered to control the

progress of the disease [5]. Thus, currently the most viable form of treatment for diabetes for over four decades is injectable insulin. Insulin formulations, both slow-acting and fast-acting, are widely in use. Insulin formulations are usually injected subcutaneously, although more recently nasal, oral and transdermal delivery techniques are being developed. However, these variants have had limited success due to various problems such as dosage, bioavailability, and problems with prolonged use. Two popular injectable insulin formulations of insulin are Humulin<sup>®</sup> (Eli Lilly) and Glucophage<sup>®</sup> (Bristol-Myers Squibb) which generated a combined \$1.5 billion in sales worldwide in 1997 alone and went off-patent in 2000 [6]. Many more drugs will go off-patent in 2005-2008, leading to a host of generic drug manufacturers fighting for a market share. Thus, market pressures for discovery of new drugs or reformulation of old drugs play an important role in determining the major players in the drug market [4].

Insulin was discovered in 1920s [7], and its method of administration has changed little since then. The purity and quality of the final product have, however, improved greatly with the advent of recombinant DNA technology. Control of blood glucose levels is the primary goal of insulin administration. Most commercial formulations achieve fast release ~30 min-2 hr to prolonged ~ 1 day of therapeutic levels of insulin. The fast-acting products/formulations target glucose levels immediately following a meal, and the long-acting formulation targets the basal glucose level. Depending on the individual, physicians prescribe a combination of both fast and slow formulations to achieve optimal glycemic control and minimize the number of injections required. Although techniques for delivering peptide drugs have evolved over the period of time the principal components of the formulation remain the same, namely zinc, protamine and insulin,

which are commonly used in most formulations. Insulin is an attractive and widely researched drug; numerous publications and patents exist on its formulations.

### **2.3.2 Physiochemical Properties of Insulin**

Human insulin is a 51 amino acid peptide with molecular weight of 5700 and isoelectric point ranging from 5.3-5.4. However, the isoelectric point of insulin varies depending on conjugation, self-association, and modifications in amino acid sequence, or isoforms. Various sources suggest that the value of isoelectric point of insulin can be in the broad range from 5.2-5.9. The human insulin molecule consists of two peptide chains (A-21 amino acids and B-30 amino acids) linked by two disulfide bonds. The primary structure of human insulin is shown in Figure 2.2.

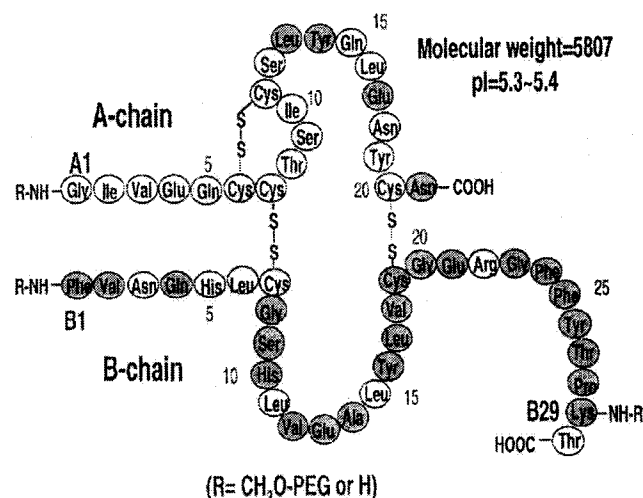


Figure 2.2. Primary structure of human insulin. The shaded regions are involved in self association [8].

The shaded regions show insulin self-association sites implicated in the formation of dimers or hexamers. Insulin usually assembles to dimers at acid and neutral pH; in the presence of zinc it forms hexamers [8]. It is slightly soluble in water and practically

insoluble in alcohol, chloroform or ether. Because of its amphoteric nature it forms soluble salts with weak acids and alkalis.

### **2.3.3 Design of Insulin Drug Reformulation**

Proteins are macromolecules and differ from conventional small molecule drugs in that they are fragile systems with a complex architecture, and changes in the local environment of the protein can cause severe changes in the structure and function of the protein-drug, rendering it ineffective for treatment. The biological activity of the protein is retained only when the integrity of their structure is maintained. Administration of native protein alone does not achieve desired results because of rapid degradation processes that occur in biological systems due to proteolytic activity and rapid uptake and elimination. Therefore, it becomes imperative to design controls into the dosage form to achieve predictable and well-defined pharmacokinetics. Particulate delivery systems are more attractive to native enzyme because of enhanced protein and peptide stability, reduced protein degradation, increased chemical and biological stability, and increased bioavailability. The particulation of drugs can be achieved by spraying and drying techniques, use of solvent mixtures, and homogenizing [9]. During particulation, additives are added to the protein, and careful choice of materials reduces adverse effects [10, 11].



### **2.3.4 Current Insulin Drug Reformulations**

Insulin formulations and their variations can be broadly classified based on their solubility *in vivo* as fast-acting or slow-acting formulations. The excipients primarily act by conjugating/complexing with the insulin molecules in ways that enable either rapid release (phenolic compounds), or slow-release (protamine, zinc, pegylation), of insulin molecule from the complex. In addition to excipients, some formulations also regulate pH of formulation as a means to crystallize/solubilize insulin and thus achieving the desired release rate. Although different formulations contain variable concentrations of excipients, the general constituents of the formulations are summarized in Figure 2.3. Alternatively, insulin delivery platforms can be categorized by method of administration as

- (a) Oral/Gastrointestinal.
- (b) Nasal/Mucosal.
- (c) Subcutaneous/Musculoskeletal.
- (d) Transdermal and other intelligent drug delivery systems.

Each of these systems is discussed in greater detail, highlighting the current state of research and the most promising avenues.

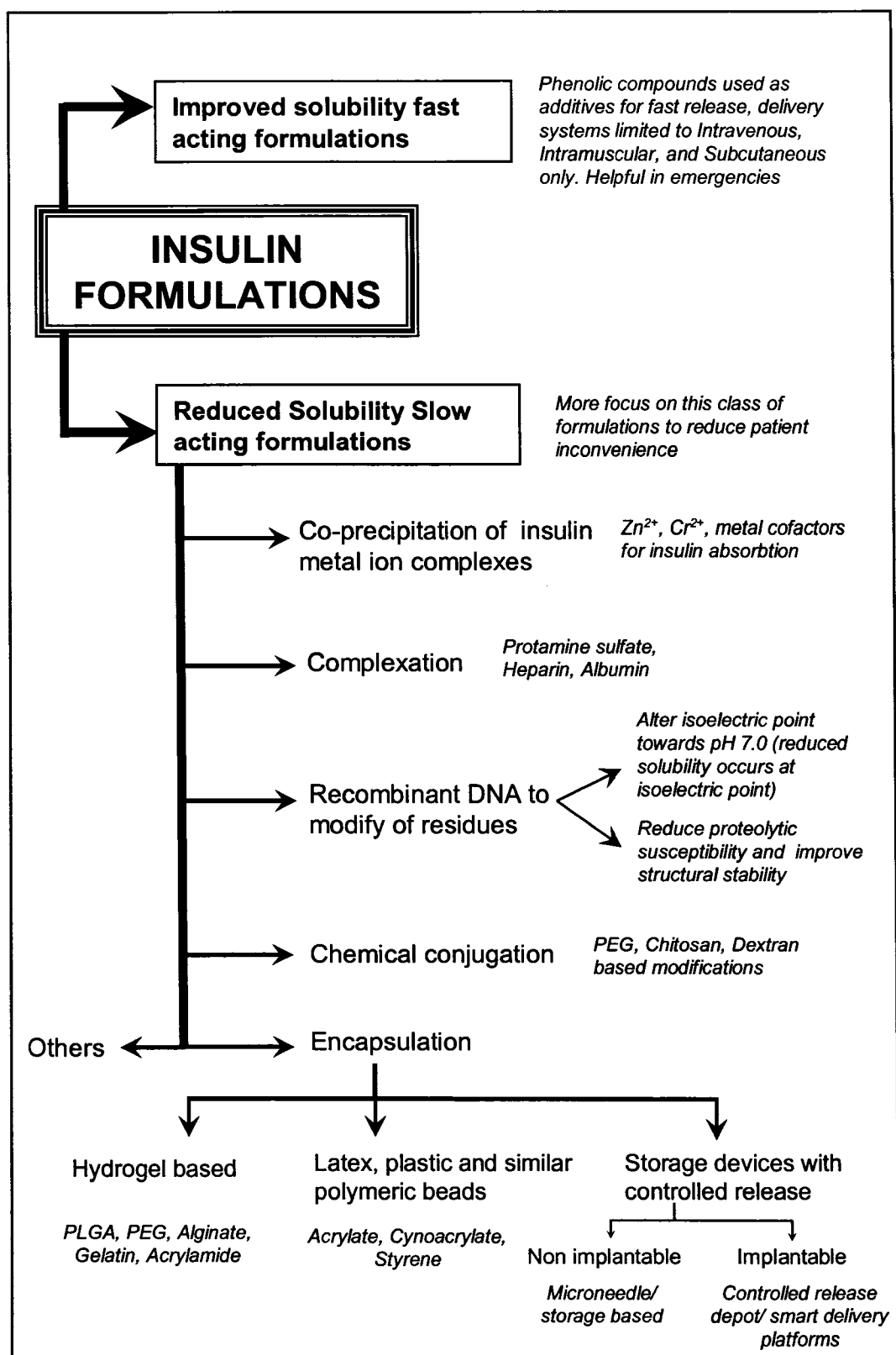


Figure 2.3. Overview of Insulin Formulations.

#### 2.3.4.1 Oral delivery

From the reformulation hierarchy in Figure 2.1 it can be inferred the oral delivery of insulin is the most attractive. The first attempt to formulate insulin for oral delivery was by Oppenheim et al. [12] who prepared insulin formulation composed of particles in the ~200 nanometer range without polymers, where the insulin was cross-linked using glutaraldehyde. Damgé et al. [13] loaded insulin into poly(alkyl cyanoacrylate) (PACA) nanocapsules by interfacial polymerization technique in which a mixture of insulin, isobutyl cyanoacrylate (IBCA), Mygliol<sup>®</sup> were added to an aqueous solution of poloxamer 188. This procedure resulted in interfacial anionic polymerization and formation of nanoparticles ~220 nm in size. The encapsulation efficiency was 55% and the suspension was used without any further purification for *in vivo* tests. Michel et al. [14] also prepared poly(isobutyl cyanoacrylate) (PIBCA) nanospheres by the conventional emulsion polymerization technique [15]. The particles had a mean size of 150 nm. The insulin microspheres lacked protection against proteolytic enzymes when suspended in water but were resistant to proteolytic action when dispersed in Mygliol<sup>®</sup>. Therefore, in the particles prepared with the emulsion polymerization technique, hydrophilic peptides tend to diffuse out to the surface of the particles which impedes the protection of the peptide.

Although partial adsorption in gastrointestinal tract was speculated for glutaraldehyde cross-linked insulin preparations, *in vivo* tests by Oppenheim et al. [12] were ineffective because glutaraldehyde denatures the insulin and causes loss of bioactivity. Moreover, the nanoparticles were predictably degraded by proteolytic enzymes of the gastric tract. Although, this formulation achieved a 15-20% reduction of

glucose level in mice, which is nonetheless marginal for a commercially viable product. In the work of Damgé et al. [13], a single 100 IU/Kg administration of insulin-loaded IBCA nanospheres resulted in reduction of glycemia by 65% in normal dogs with a glucose overload after 3 days of oral administration. Reduction reached 72% after nine days and 48% after 15 days. The glycemia returned to normal levels 21 days after administration. Damgé et al. [13] claimed that this impressive prolonged effect was caused by altered biodistribution after oral administration of insulin-loaded nanoparticles. They also claimed that if sufficient number of intact nanocapsules were absorbed, nanocapsules would be localized in liver and spleen due to rapid phagocytosis. However, the purification and preservation of insulin-loaded IBCA nanocapsules poses a significant problem and is consequently poorly adapted for clinical use. To overcome this problem PIBCA based nanospheres were prepared by Michel et al. [14]. The PIBCA based formulation was effective after subcutaneous injection but induced no biological effect after oral administration.

The most promising work on oral delivery systems was done by Morishita et al. [16-18] who investigated pH-sensitive particles that would dissolve in various segments of digestive tract, in particular the jejunum or the ileum, where protease activities are lower. Morishita et al. incorporated insulin with or without protease inhibitor, which was dissolved in a small amount of HCl (0.1 N). Ethanol and methacrylic acid copolymer (type A, Eudragit<sup>®</sup> L100 soluble at pH >6, or type B, Eudragit<sup>®</sup> S100 soluble at pH >7 Röhm, Darmstadt, Germany) were added with stirring. This solution was emulsified into liquid paraffin, phase separated with gelatin solution (0.5% w/w), and the particles isolated. The isolated particles were coated with Eudragit<sup>®</sup> L100 to avoid dissolution of

the drug that was adsorbed on the surface of the particle. The total encapsulation efficiency of insulin was 78%. Good protection against pepsin was achieved; protection against trypsin and  $\alpha$ -chemotrypsin was achieved with protease inhibitors. *In vivo* tests indicated that Eudragit<sup>®</sup> L microspheres had enhanced biological activity in fasting wistar rats (16-20 hr fasting).

The primary advantage of oral administration is the availability of the widest array of materials for formulation compared with all other routes of delivery; biocompatibility is limited to “edible substances”. The disadvantage of current approaches to oral delivery is the extremely high doses of insulin required, for even a low therapeutic effect compared with parenteral doses. Although the work looks promising in rodents and dogs, it is yet to be well tested in human subjects. Overall, the oral delivery formulations are still in the natal stages.

#### **2.3.4.2 Nasal delivery**

Evolution of new materials has stimulated interest in alternate drug delivery systems other than oral and injectable routes, and nasal drug delivery is an emerging field. Nasal dosage forms consist of preparations containing dispersed or dissolved drugs which can be either squeezed or sprayed into the nose, or applied topically as a gel (vitamin B<sub>12</sub>) [19, 20]. The drugs target the nasal mucosa where they deposit and are absorbed. The nasal mucosa and epithelium primarily act as a lipophilic transport barrier, and transport across the membrane is related to the water partition coefficient [21]. Strategies to optimize the use of mucoadhesives for nasal delivery of insulin include (a) preparing the formulations as micro- or nanospheres, (b) incorporation of absorption enhancers and (c) combination of different polymers [22]. The formulation design should

also consider factors such as pH, ionic strength, surface active agents, viscosity, and drug concentration [23]. Enhancers are used in nasal formulations to improve drug absorption across the nasal membrane. The most evaluated compounds as enhancers are surfactants (laureth-9), bile salts (glyco-taurocholate, deoxycholate), chelators (EDTA, citric acid), fatty acid salts (oleic, caprylic, capric, and lauric), phospholipids (L- $\alpha$ -lysophosphatidylcholine (DDPC), didecanoyl-PC, fusidates (sodium taurodihydrofusidate, STDHF), glycyrrhetic acid derivatives (carbenoxolone, glycyrrhizinate), cyclodextrins ( $\alpha$ -,  $\beta$ -,  $\gamma$ -cyclodextrins), hydroxypropyl- $\beta$ -cyclodextrin and dimethyl- $\beta$ -cyclodextrin (DM $\beta$ CD), randomly methylated  $\beta$ -cyclodextrin (RAMEB), chitosan, and particulate carriers (microcrystalline cellulose, starch microspheres, and liposomes). Some of these compounds are also used in fast-acting formulations of insulin [9].

Controlled studies in humans using phospholipid DDPC as an insulin enhancer have shown that nasal mucosal physiology was unaffected after intranasal administration, but that insulin bioavailability was low, despite intranasal doses about 20 times higher than subcutaneous doses [24]. Cyclodextrins are another class of compounds that show great promise in nasal drug delivery. They interact with polar/amphoteric molecules and also adsorb with specific lipids in biological membranes thus acting both as a carrier, and enhancer for hydrophobic drugs. *In vivo* studies by Merkus et al. [25] in rats have demonstrated that the addition of 5%  $\alpha$ -CD to a nasal preparation of insulin resulted in an absolute bioavailability of approximately 30%; on the contrary,  $\beta$ - and  $\gamma$ -CDs did not affect insulin absorption. However, DM $\beta$ CD gave rise to a large increase in insulin absorption, with a bioavailability of 100%. Contrasting results were obtained in

experiments with rabbits and human volunteers in which no absorption-enhancing effect of CDs for insulin was observed, with a bioavailability of approximately 3-5% [1, 25]. Thus, the effectiveness of CDs depends on both the drug and the animal being tested. Another prospective mucoadhesive formulation is chitosan, a positively charged high molecular weight polymer. For chitosan-based formulations Dyer et al. [22] showed that the most effective formulation for absorption is a chitosan powder delivery system, found to be better than chitosan nanoparticles and chitosan solution formulations, respectively. Callens and Remon reported that nasal administration of insulin formulated with drum-dried waxy maize starch (DDWM) or maltodextrins and Carbopol 974P, had the highest absolute bioavailability (14.4% for a mixture consisting of DDWM/Carbopol 974P 90/10) [26]. However use of the formulation over a week in sheep showed reduced bioavailability due to high viscosity of the mucoadhesive formulation [27].

Thus, the bioavailability of the administered drug is a major problem in the nasal delivery of insulin formulation. However, development of pulmonary insulin delivery systems by commercial vendors is reaching critical and near market stages (Table 2.1).

Table 2.1. Commercial development of pulmonary insulin systems [28].

| <b>Pulmonary Insulin Delivery Systems under Development</b> |                             |  |   |
|---|-----------------------------|--|---|
| <b>Dosage Form</b>  | <b>Trade Name</b>           | <b>Company</b>                           | <b>Development Stage</b>  |
| Solution  | AERx iDMS                   | Novo Nordisk, Aradigm                    | Phase III clinical trial in progress  |
|   | Aerodose                    | Aerogen                                  | Phase II clinical trial completed; development halted in January 2003   |
| Powder  | Exubera                     | Pfizer, Aventis, Nektar                  | Phase III clinical trial completed; long-term safety studies ongoing; marketing authorization application filed with European Medicine Evaluation Agency in March 2004; new drug application filed with FDA in 2005 |
|   | ProMaxx AIR                 | Epic Therapeutics<br>Eli Lilly, Alkermes | Preclinical studies<br>Phase II clinical trial in progress  |
|   | Spiros                      | Eli Lilly, Dura Pharmaceuticals          | Discontinued after merger between Dura Pharmaceuticals and Elan Pharmaceuticals   |
|   | Technosphere Insulin System | MannKind Corporation                     | Late Phase II clinical trial ongoing; Phase III clinical trial initiated in Europe  |

The bioavailability of commercial variants is in the range of 13-30%, slightly higher than reported in research papers. Many enhancers used in the formulations for nasal delivery are known to be biocompatible, and adverse reactions are limited compared with intra-venous, intra-muscular, subcutaneous administration.

#### **2.3.4.3 Subcutaneous/musculo-skeletal injection**

This is the most widely used and established form of insulin administration. Insulin formulations, depending on action, have common names and they have established pharmacokinetic characteristics. These formulations fall in one of the broad types based on duration of action as illustrated in Table 2.2.



Table 2.2. Injectable insulin formulations [29].

| <b>PHARMACOKINETIC CHARACTERISTICS OF INSULIN FORMULATIONS (TIME IN HOURS)</b> |              |             |                 |
|--|--------------|-------------|-----------------|
| <b>Type of Insulin</b>   | <b>Onset</b> | <b>Peak</b> | <b>Duration</b> |
| Slow-acting  |              |             |                 |
| Ultralente   | 3-5          | 10-16       | 18-24           |
| Glargine   | 1-2          | NA          | 24              |
| Intermediate-acting  |              |             |                 |
| NPH  | 1-2          | 6-10        | 12-20           |
| Lente  | 2-4          | 6-12        | 12-20           |
| Short-acting   |              |             |                 |
| Regular  | 0.5-1        | 2-4         | 4-8             |
| Lispro/aspart  | immediate    | 0.5-2       | 3-4             |

Most individuals are prescribed a combination of two or more types of insulin for optimal glycemia control. The pharmacokinetic profiles of individual insulin products however, differ significantly [30]. The ultralente insulin formulations are slow-acting and typically consist of zinc cross-linked hexameric insulin with or without protamine.

Insulin can be co-crystallized with zinc atoms to obtain numerous types of stable crystals with longer time actions than soluble or amorphous, uncrystallized insulin. The fish protein protamine has been used as insulin complexing agent to prolong the time action of insulin. Insulin glargine, insulin lispro, and insulin aspart are insulin analogues which have modified amino acids and hence complex with zinc and protamine differently. The NPH insulin is a protamine insulin complex and is intermediate acting. The fast-acting analogues are usually co-crystallized with zinc and phenolic molecules, and diffusion of the phenolic molecule away from site of injection causes the insulin-zinc crystal to break apart yielding monomers and hence the instantaneous action. Individual manufacturers add various stabilizing additives during the formulation including albumin,

sugars, polyols, chelating agents and inorganic salts– to confer stability in solution, frozen and dried states as required.

Polymeric drug delivery has been studied for the past 30 years but few commercial products have come to market. It is gaining importance because of recent advances in polymeric materials and advantages offered by polymeric micro and nanoparticles for delivery of peptides. Polymeric materials are attractive for drug delivery because they afford protection to peptide drugs, prolong release, and have controllable biodegradability. Commonly used materials for encapsulation of proteins are poly(l-lactic acid) (PLLA) and its copolymers with d-lactic acid or glycolic acid, which provide a wide range of degradation periods from weeks to years [31]. Most researchers use solvent evaporation or a modification thereof to prepare microparticles for controlled release [32, 33]. Emulsion, extrusion and spraying techniques can cause protein damage because they involve use of one or more of the following– organic solvents, elevated temperature, vigorous agitation and detergents. Controlled phase separation and use of aqueous biphasic mixtures have also been employed to achieve micro- and nanoparticles.

Pfizer® in collaboration with Nektar® and Aventis® has developed a formulation based on pegylated insulin for nasal and possible IV delivery and recently launched their product Exubera™. However, it is not yet widely available.

Subcutaneous injection for diabetic treatment is currently the most effective control for both Type I diabetes and eventually Type II diabetes. For this method of administration, only FDA approved polymeric materials can be used in the formulation, which limits the formulation composition because few polymers have been approved for such use.

#### **2.3.4.4 Transdermal and other intelligent drug delivery systems**

Minimally invasive insulin pumps are primarily used to treat the basal glycemia, and some are programmable to release drug at specified periods of time. Insulin is delivered transdermally using either a pressure activated, or an ionotropic, or an ultrasonically modulated device.

Pulsatile systems involving insulin in an ethylene-vinyl acetate copolymer (EVAc) matrix loaded with magnetic beads have been used to control the release of insulin *in vivo* in rats by application of an oscillating magnetic field. The release rate is dependent on the magnitude of the magnetic field and rigidity of the matrix. Similar results were observed with alginate-protein matrices [34-40].

An ultrasonically controlled polymeric delivery system in which release rates of substances can be repeatedly modulated at will, from a position external to the delivery system were tested by Kost et al.[41]. Both bioerodible and nonerodible polymers were used as drug carrier matrices. The bioerodible polymers evaluated were polyglycolide, polylactide, poly(bis(p-carboxyphenoxy) alkane anhydrides and their copolymers with sebacic acid. The releasing agents were p-nitroaniline, p-aminohippurate, bovine serum albumin, and insulin. Non-bioerodable system consisting of EVAc-insulin was also tested. *In vitro* and *in vivo* experiments in rats indicate feasibility of such a system. The release was modulated by the ultrasonic frequency, intensity and duration. Instantaneous release of encapsulated material over two minutes was achieved upon application of ultrasound [41]. Over 40 years, numerous clinical reports have been published concerning phonophoresis [42]. This technique is based on the basic principle that the

drug to be transdermally transferred is placed topically, followed by application of ultrasound. However, this method is not yet well established for protein drugs.

Competitive binding of glycosylated insulin to glucose and a saccharide binding protein such as Concanavalin A as a release mechanism for regulated insulin delivery were first proposed by Brownlee and Cerami [43]. *In vivo* experiments in diabetic dogs show promising results.

Another such smart system involves a saccharide sensitive gel that swells in the presence of glucose. The gel consists of a covalently cross-linked polymer network of N-isopropylacrylamide in which the lectin and Con A are immobilized [44]. Other such smart systems involving intelligent glucose responsive chemistries have been demonstrated *in vitro*, but promising *in vivo* results are unavailable.

It would be fascinating and exciting to demonstrate the efficacy and long-term stability of smart chemistries *in vivo*. Fouling and lack of biocompatibility could be a potential problem in such systems after a prolonged period of time. However, smart systems currently available are underdeveloped for induction into the market. Glucose pumps are, to the best of my knowledge, the only commercially available devices for insulin delivery that have a minimally invasive approach. Popular vendors of glucose pumps include Animas Corp, Medtronic MiniMed Inc, Disetronic Medical Systems, Inc, and Deltec Cosmo.

**Discussion:** The nasal/aerosol-based delivery of insulin would be better than other methods of administration and this modality may become practically possible in the near future, considering current research levels in major firms. Time-release rates for the insulin formulations by themselves cannot be judged as good or bad because both short-

and long-acting formulations may be necessary based on patient requirements. However, prolonged oral formulation of IBCA nanocapsules is most attractive in terms of control of basal glycemia because prolonged bioavailability of insulin for a single dose have not been achieved by systemic injection or other non-invasive methods.

The nasal/aerosol system has some drawbacks in its current form in terms of bioavailability of the drug after administration. However, it is theoretically possible to achieve quick-acting formulations because the rate of drug uptake in the lungs is exceeded only by intravenous injection. Oral delivery is nearly impractical for fast-acting formulations unless a very low molecular weight insulin analogue is discovered which is extremely resistant to proteolytic activity. Intravenous and subcutaneous drug delivery are painful, and patient compliance is not always good. It is particularly stressful for children.

**Design Criteria for Coatings:** As LbL-based insulin microparticles are primarily targeted for *in vivo* delivery, it is of paramount importance that all components must be completely biocompatible and produce no adverse reactions in diabetics. This project involves the development of long-acting insulin formulation, so it is important to have a tunable release of the drug with prolonged bioavailability. The outermost LbL layer should be designed to impart proteolytic resistance to the insulin microparticle. The coating should impart physical and chemical stability to the encapsulated insulin. Finally the procedure developed must be scalable and optimized with respect to concentrations of prospective polyelectrolytes to minimize the use of the same. Repeatability and consistency of product and method are essential for the final product.

During the surface modification using LbL assembly, low temperatures should be maintained to prevent protein denaturation and/or complexation. Extremely low pH values (<4.0) should be avoided because they lead to increased solubility of PROMAXX<sup>®</sup> microparticles (insulin-zinc) that were used in this work. Phosphate salts and/or compounds containing phosphate groups should be avoided because phosphate moiety has a tendency to bind with zinc-complexed insulin, leading to reduced solubility and marked changes of pharmacokinetic activity of the final formulation. It is also important to avoid any other contaminants and non-sterile media in samples to be dissolution tested.

#### **2.4 Phospholipids Retard Diffusion of LbL Thin Films**

Electrostatic LbL has earned significant focus over the last decade because of the simplicity of the technique. It has evolved from the study of the fundamental science of LbL thin films to applications in real world product development. One practical area of interest is drug delivery. The basic scheme of the LbL assembly is shown in Figure 2.4. Thin films of opposite charge are deposited on a solid substrate by electrostatic assembly in an alternate manner to achieve sequential growth of thickness with each deposited layer. LbL assembly can be used to deposit thin films from a wide range of materials from metal complexes and polymers to proteins and nanoparticles (Figure 2.4 (*top*)), or to prepare hollow multilayer capsules (Figure 2.4 (*bottom*))[45-47].

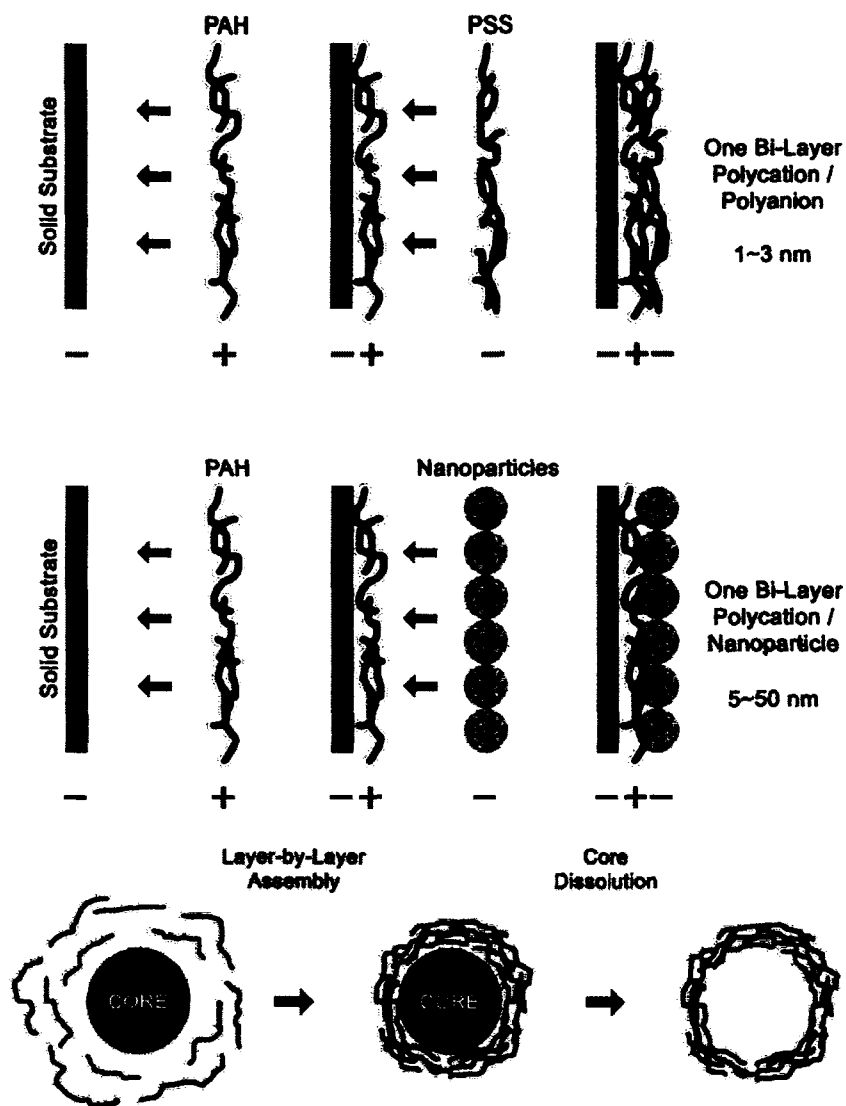


Figure 2.4. LbL schemes for polymers, proteins, nanoparticles (*top*). Preparation of hollow polyelectrolyte capsules (*bottom*).

The versatility of the process allows the use of LbL technique on both template particles and flat surfaces, irrespective of the size of the object. It can be used to design hollow capsules or thin films, and the choice of materials is extensive and limited by the charge on the polymer, nanoparticle or protein. Thorough reviews of the technique have been elaborated elsewhere [45, 48-52]. More recently, drug delivery applications were elaborated by the deposition of multilayer thin films on the drug microparticles [53-56].

The primary focus of these works is the design of multilayer thin film coatings on drug crystals and the tuning of release properties by increasing the number of polyelectrolyte bilayers on the drug microcrystal. The universality of the idea implies no fundamental restriction on the choice of materials and the possibility of designing ultrathin ordered films in the range of 5-500 nm, with the precision of greater than one nanometer and a definitive knowledge of molecular composition.

The material selection for biomedical and pharmaceutical applications is large and expanding rapidly to include numerous biocompatible polyelectrolytes. Some of the more commonly used polyelectrolytes for LbL assembly are shown in Figure 2.5.

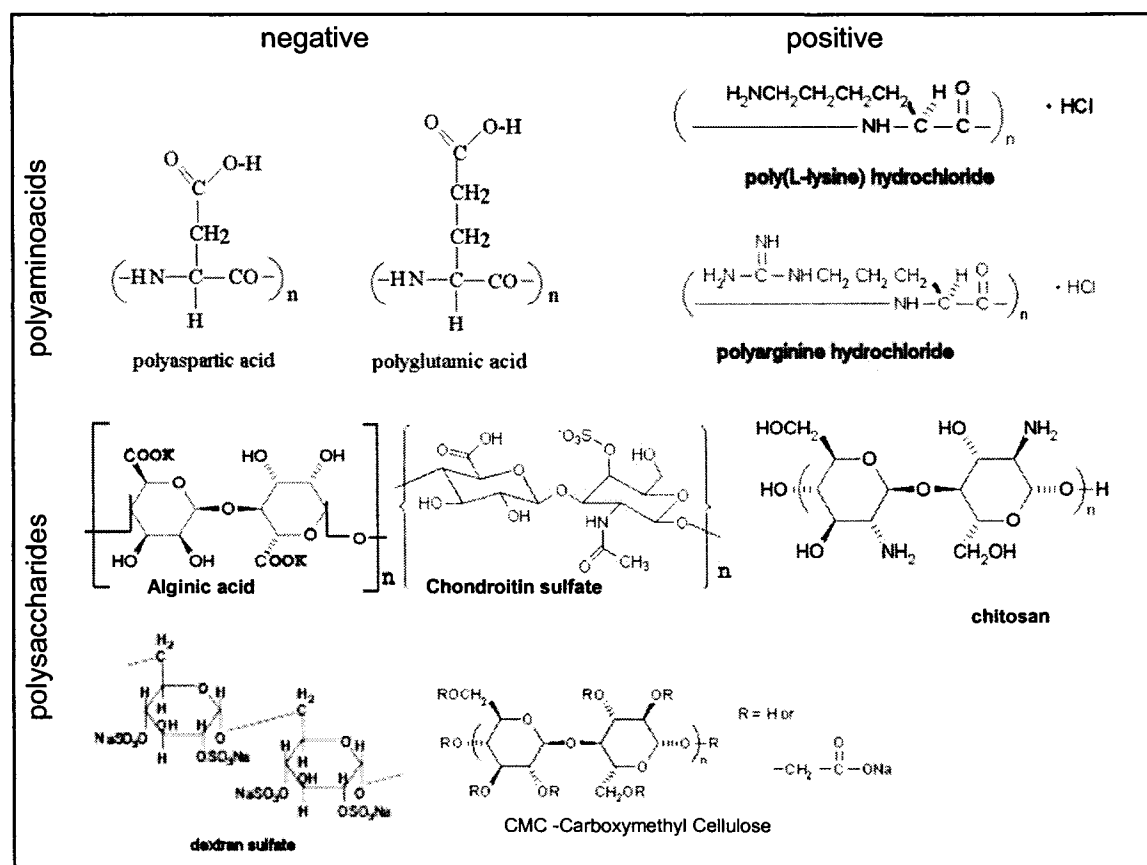


Figure 2.5. Biocompatible polyelectrolytes in Layer-by-Layer assembly.



Although the LbL technique is versatile and can be used in a wide array of schemes it is time consuming and laborious to deposit multilayer films. The method is not amenable to scaleup due to the large number of process steps involved. Therefore, there is a need for using materials that will modulate the desired property, such as diffusion, by an order of magnitude and to reduce number of process steps.

One prospective material in the field of drug delivery could be the use of phospholipids. Phospholipids have long been used in the pharmaceutical industry to deliver drugs *in vivo*. Moreover the diffusion properties of lipid bilayers for hydrophilic and water soluble molecules is low. Combining LbL assembly and liposome technology could yield benefits that will combine the advantages of both the technologies. The LbL technique enables the design of microcapsules of precise size, and liposomes could be used to tune the diffusion of these microcapsules. The concept is presented pictorially in Figure 2.6, where a charged solid core can first be coated with two bilayers of oppositely charged polyelectrolytes followed by alternate deposition of negatively charged phospholipids admixed with DPPC alternated with a positively charged polyelectrolyte. Such a scheme can be exploited to coat drug microparticles such as insulin to retard diffusion of drug from the core. To elaborate the scheme, a sacrificial core could be employed to produce a hollow polyelectrolyte capsule which can be used to permeate active drug followed by phospholipid/polyelectrolyte coating to entrap the drug for sustained delivery.

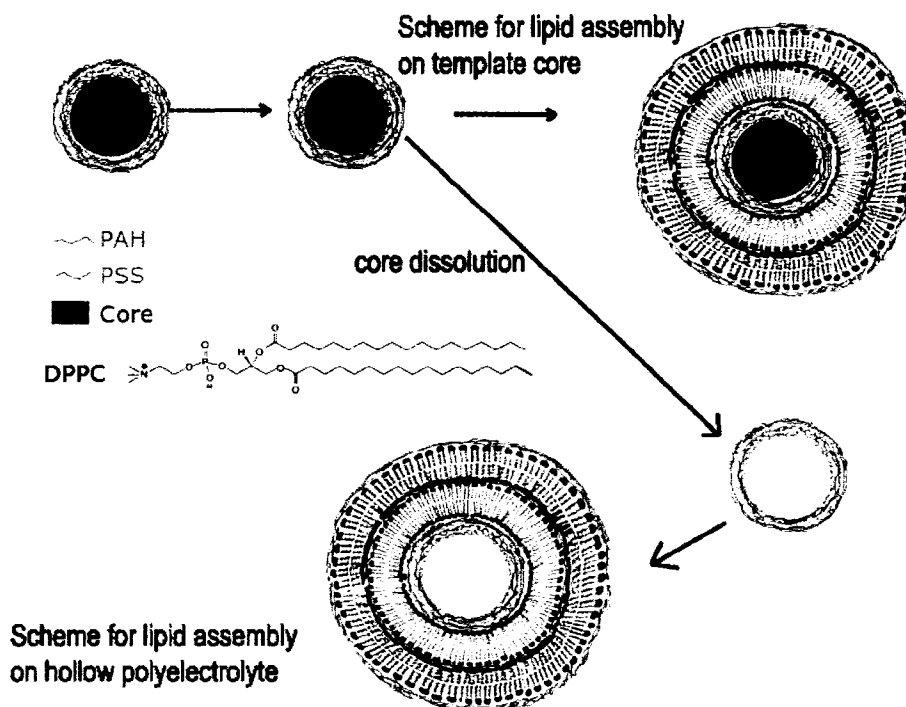


Figure 2.6. Schemes showing the alternate deposition of polyelectrolytes and phospholipids. Such architectures can impart special properties to LbL films like diffusion control and biocompatibility.

### 2.5 Calcium Salts for Delivery of Hydrophobic Drugs

Many anticancer drugs such as dexamethasone, paclitaxil, and some chemotherapeutic drugs are hydrophobic in nature and thus have extremely poor solubility in water. These drugs are typically administered by an intravenous injection of a liposome-based formulation. Although new methods are being developed for delivery of these drugs, such as the use of pegylated amphiphilic molecules, these techniques remain distant from the market and are still in preclinical trials. Effective administration of these drugs eliciting low systemic toxicity could be possible through the use of a nasal delivery platform with the use of micro- and nanoparticles. Alternatively, nanoparticle-based delivery mechanisms with slow biodegradability could be prospectively exploited

if such drugs were entrapped in a mineral matrix of calcium carbonate. Such a system has been demonstrated in a rat model by Uneo et al. [57] for hydrophilic drugs and peptides.

Microparticles have been used for drug delivery for the last couple of decades. Most of the micro- and nanoparticles are organic[58] and some are inorganic [58, 59]. The use of calcium mineral salts incorporating drugs in the form of nano-microparticles of calcium carbonate ( $\text{CaCO}_3$ ), calcium phosphate ( $\text{Ca}(\text{H}_2\text{PO}_4)_2$ ), tricalcium phosphate ( $\text{Ca}_3(\text{PO}_4)_2$ ) and hydroxyapatite ( $\text{Ca}_5(\text{PO}_4)_3\text{OH}$ ), have been used in drug delivery [60, 61].  $\text{CaCO}_3$  has been reported useful as a carrier of hydrophilic drugs and insulin because of easy production and slow biodegradability [62-64]. In most of the work using calcium salt microparticles for drug delivery, the drug has been adsorbed on the surface of the micro- and nanoparticles. In a recent report Uneo et al. [57] have shown that both hydrophilic and peptide drugs can be incorporated into calcium carbonate nanoparticles. The authors further showed the feasibility of delivering the drug intravenously in rats without eliciting a systemic toxicity. Among all the minerals used for delivery of drugs *in vivo*, calcium carbonate has the highest lethal dose limit (~150 mg/kg body weight), making it one of the most promising candidates for drug delivery. It surpasses inert materials such as titanium dioxide, silica and apatite in terms of body tolerance.  $\text{CaCO}_3$  is a food supplement and can be incorporated in the biochemical pathways, thus facilitating easy clearance from the body.

Most of the work relating to  $\text{CaCO}_3$  has been in the area of study of its mineral polymorphs and crystallization mechanisms. Ozin et al. [65, 66] have studied in great detail the biomineralization scheme of calcium salts, particularly carbonate, apatite, and hydroxyapatite in association with biological materials such as amphiphiles, proteins, and

polymers. Although incorporation and adsorption of hydrophilic drugs and peptides into the microparticles [53, 57] have been well studied and elaborated, the adsorption of hydrophobic drugs has not. Because most new drugs for the treatment of cancer are hydrophobic, design of effective and convenient drug delivery methods are important.

To study the physical and chemical changes at micro- and nanoscale requires appropriate instrumentation and suitable analysis of the results. The next section deals with the changes to standard measurement techniques and theory associated with it. The study of ultrathin films on flat surfaces needs characterization capable of measuring nanometer thickness changes such as quartz crystal microbalance QCM. Changes in colloidal particles coated with nanometer thick films can be characterized by studying the alternation of surface charge.

## **2.6 Instrumentation: Theory and Practice**

### **2.6.1 Quartz Crystal Microbalance**

QCM technique is capable of measuring thickness changes less than a nanometer, and mass changes less than a nanogram.

The following notation has been used for this subsection on the QCM.

Symbol definitions:

$\lambda$  - acoustic wavelength

$V_r$  - speed of acoustic wave

$t$  - quartz thickness

$F_0$  - resonance frequency of the quartz crystal

$M$  - Mass of quartz (between the electrodes)

$A$  - area between the electrodes

$\rho$  - density of quartz.

$\mu_q$  - quartz shear modulus

Figure 2.7 is a schematic of the QCM, showing a transverse section of the quartz crystal with electrodes plated on the top and bottom of the crystal.

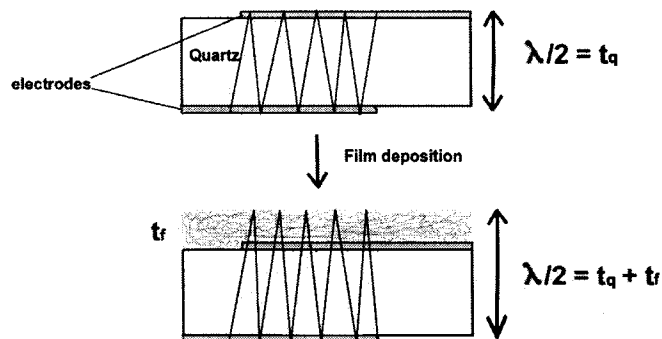


Figure 2.7. Transverse shear wave in a quartz crystal microbalance where  $t_q$  is thickness of the quartz crystal,  $t_f$  is the thickness of the film.

The piezoelectric effect of quartz is well known, when two electrodes are put at different potentials, an electric field results across the QCM, i.e., in the "y direction". Such an electric field in the "y direction" couples to shear motion "around" the z-axis, and vice versa. The end result is that shear waves in the quartz, in which the mechanical displacement is in the "x direction", also called the electric axis, are coupled to voltage between the electrodes. This phenomenon is used to study deposition of ultrathin films on quartz substrate.

In a quartz crystal which is cut along the A-T axis and coated with a fine layer of metal to act as electrode, a potential applied to the electrodes of a QCM produces an acoustic wave along the transverse direction, as depicted in Figure 2.7, of wavelength  $\lambda$ .

The Sauerbrey Equation can be derived as follows.

The wavelength is related to the thickness of the quartz can be represented by the following relation

$$\lambda / 2 = t \quad (1)$$

Also,

$$\lambda = V_r / F_0 \quad (2)$$

$$F_0 = V_r / 2t. \quad (3)$$

For a unit change in frequency,

$$\Delta F = \frac{-V_r \Delta t}{2t^2}. \quad (4)$$

From equations  $M = tA\rho$ ,  $\Delta t = \Delta M / A\rho$ ,  $t = V_r / 2F_0$  and (1), (2) and (3) in Equation (4) we obtain

$$\frac{\Delta F}{F_0^2} = \frac{-2\Delta M}{V_r A\rho} \quad (5)$$

This equation is called the Sauerbrey Equation.

We can write  $V_r = \sqrt{\mu_q / \rho}$ , where for quartz  $\mu_q = 2.95 \times 10^{11} \text{ dyn/cm}^2$  and  $\rho = 2.65 \text{ g/cm}^3$ , and  $F_0 = 9 \times 10^6 \text{ Hz}$  and  $A = 0.16 \text{ cm}^2$  for quartz crystals used in this work.

Substitution of these values into Equation (5) results in a working equation for measurement of the film thickness.

**Discussion:** The entire derivation above, and consequently the validity of Sauerbrey Equation, is based on the assumption that the material adsorbed on the quartz

crystal is a rigid body (it vibrates/resonates in sync with the quartz crystal), so the change in frequency is directly correlated to the deposition of mass.

This derivation does not depend on the properties of the materials being adsorbed. For practical purposes, such as adsorption of polyelectrolytes and nanoparticles, these properties are unimportant because the mass of material adsorbed is  $< 1\%$  of the mass of resonator itself. This mass is equivalent to  $\sim 200$  nm thick film of polymers.

Biological materials however are not rigid bodies but behave as viscoelastic materials. Therefore, there is a delay from the time of application of shear to the onset of deformation, so the stress/strain relation is not linear. For such materials, the change in frequency is not proportional to the mass adsorbed. In typical situations the mass is overestimated due to frequency attenuation. Therefore, real time decay of the resonant frequency is used to estimate the changes in mass of the adsorbed material where deposition in aqueous mediums can be studied.

However, in this work QCM resonance frequency changes have been used to estimate thin film deposition with biological samples as well. To take into account the above constraints, it has been shown by Kankare [67] that for films with a thickness less than 45 nm, viscoelastic material such as proteins and hydrated polymers behave as a rigid body because in such circumstances the film consists  $< 0.1\%$  mass of the quartz crystal and the errors are not significant. Hence, for QCM studies of biological (soft) materials it is not advisable to go beyond this limit.

### **2.6.2 Zeta-Potential and the Theory Involved**

The equations, some statements and figures in this subsection have been reproduced from the book titled Paul C Hiemenz, Principles of Colloid and Surface Chemistry, 2<sup>nd</sup> Ed.

Marcel Dekker, 1986. Discussion relevant to the current work is provided by the author.

A colloidal particle has surface charge attributed to it due to the presence of charged functional groups such as carboxylate, amine, hydroxyl, oxide, and others. Such groups cause discrepancy in surface charge of a colloidal particle or protein, and the net surface charge of the particle as a result of all the positive and negative charges on the surface is studied using zeta-potential.

The zeta-potential is a derived value and involves the combined effects of motion and electrical phenomena. Zeta-potential is therefore an electrokinetic phenomenon and is empirically equivalent to the double layer potential, and has a direct bearing on the colloid stability.

To begin the analysis of the formulas leading to zeta-potential and understand the limitations we have to begin from the Debye-Hückel Approximation:

The variation of potential with distance from a charged surface of arbitrary shape is described by the Poisson Equation

$$\frac{\partial^2 \psi}{\partial x^2} + \frac{\partial^2 \psi}{\partial y^2} + \frac{\partial^2 \psi}{\partial z^2} = -\frac{\rho^*}{\epsilon} \quad (6)$$

Where,

$\psi$  is the potential,  $\rho^*$  is the charge density (coulomb/m<sup>3</sup>) and,  $\epsilon$  is the dielectric constant ( $\epsilon_0 \epsilon_r$ ) is product of permittivity of free space and permittivity of the medium.



Equation (6) can be reduced to a one-dimensional form as for charge distribution from a planar surface

$$\frac{\partial^2 \psi}{\partial x^2} = -\frac{\rho^*}{\epsilon}. \quad (7)$$

The charge density can be expressed in terms of potential with the Boltzmann factor as applied to *ions*.

$$\frac{n_i}{n_{i0}} = \exp\left(\frac{-z_i e \psi}{kT}\right) \quad (8)$$

where  $n_i$  is the number of ions of type  $i$  per unit volume near the surface, and  $n_{i0}$  is the bulk concentration.  $e$  is the charge of an electron,  $k$  is the Boltzmann constant,  $T$  is the temperature in Kelvin and  $z_i$  is the valence of the ion and is either a positive or negative integer. Thus charge density can be expressed as

$$\rho^* = \sum_i z_i e n_i = \sum_i z_i e n_{i0} \exp\left(\frac{-z_i e \psi}{kT}\right). \quad (9)$$

Combining Equations (7) and (9) we have

$$\frac{\partial^2 \psi}{\partial x^2} = -\frac{e}{\epsilon} \sum_i z_i n_{i0} \exp\left(\frac{-z_i e \psi}{kT}\right). \quad (10)$$

This relationship is the starting point of Debye-Hückel theory of electrolyte non-ideality, except that this relationship exists in a 3-D spherical coordinate system. This derivation implies that potentials associated with various charges are additive.

By expanding the exponential on the right hand side of Equation (10) into a power series and retaining only the first order terms of the equation, and by taking into account the electroneutrality, we have,

$$\frac{d^2\psi}{dx^2} = -\frac{e\psi^2}{\epsilon kT} \sum_i z_i^2 n_{i0} \quad (11)$$

Integrating,

$$\psi = \psi_0 \exp(-\kappa x) \quad (12)$$

Where,  $\kappa^2 = \frac{e^2 \sum_i z_i^2 n_{i0}}{\epsilon kT}$

A plot of  $\frac{\psi}{\psi_0}$  versus distance from surface according to the Debye-Hückel

Approximation would show an *exponential decrease* in potential from the surface of the microparticle. This variation of potential results in attraction or repulsion of colloidal particles in solution, and the effective distance of interaction, in terms of molecular distance, is called the “double layer”.

Equation (12) can be written for a spherical particle as

$$\psi = \frac{q}{4\pi\epsilon r} \exp(-\kappa r) \quad (13)$$

In the Equation (13) the potential is rewritten as a function of charge. The Debye-Hückel Approximations are strictly applicable only for low potentials. These equations take into consideration the effect of electrolyte concentrations and valence of the charges, and are consistent with more elaborate calculations.

Throughout the preceding discussion charged particle was treated as a point charge without volume, but in practice they do occupy a volume and we define a “stern-layer” (Figure 2.8, stern surface) which occurs at a distance  $\delta$  from the actual surface and is drawn through ions which are assumed to be adsorbed on the charged wall. Applying this definition to a particle migrating in an electric field, a layer of fluid occurs on the

particle surface that is immobilized and a surrounding layer on the particle occurs that moves at the same velocity as the particle due to surface shear (Figure 2.8). The exact distances of these layers are unknown but they are within a few molecular layers of the particle. It is however important to note that the surface of shear occurs well within the double layer.

Rather than identify the stern-surface we define the potential at the surface of shear to be zeta-potential represented by the Greek symbol ' $\zeta$ '. A representation of these magnitudes of potentials is shown in Figure 2.8. Simplistically  $\zeta$ -potential is surface potential at surface of shear and the surface of shear is the effective particle dimension as measured by the instrument.

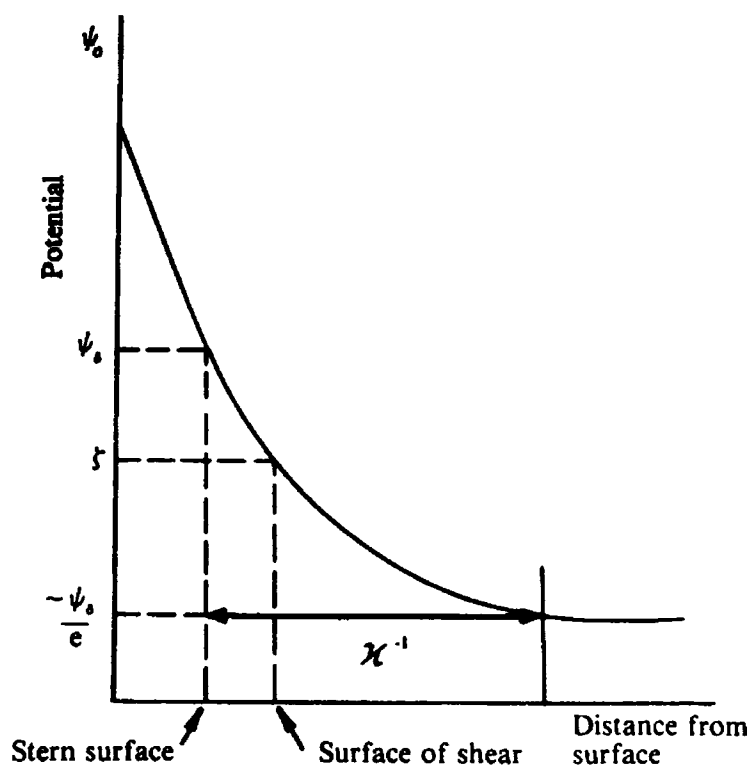


Figure 2.8. Relative magnitudes of potentials of interest.

Distances within the double layer are considered large or small, depending on their magnitude relative to  $\kappa^{-1}$ . In dilute solutions, where  $\kappa^{-1}$  is large, the surface of shear may be safely regarded as coinciding with the surface in units which are relative to double layer thickness. Therefore for small  $\kappa$  we can write Equation (13) as

$$\zeta = \frac{q}{4\pi\epsilon R} \exp(-\kappa R) \quad (14)$$

where,  $R$  is the actual radius of the particle.

Expanding the exponential we have,

$$\zeta \cong \frac{q}{4\pi\epsilon R} \frac{1}{\exp(\kappa R)} \cong \frac{q}{4\pi\epsilon R} \frac{1}{(1 + \kappa R)}. \quad (15)$$

For small values of  $\kappa R$  the above equation becomes

$$\zeta \cong \frac{q}{4\pi\epsilon R} \quad (16)$$

Taking into account the motion of a spherical particle in an electric field (Stoke's law to account for the drag on the particle), the velocity of the charged particle can be represented as

$$v = \frac{q\bar{E}}{6\pi\eta R}. \quad (17)$$

Also, the mobility is defined as velocity per unit field and  $u = \frac{v}{E}$ , where  $u$  is the electrophoretic mobility. Thus substitution of Equation (17) in (16) becomes

$$u = \frac{2\epsilon\zeta}{3\eta R}. \quad (18)$$

This equation is called the Hückel Equation.

This equation is valid for values where  $\kappa R$  less than 0.1, which means, that for particles of radius  $R=10^{-8}$  m the corresponding concentration is about 10  $\mu\text{M}$  of a monovalent electrolyte. The product  $\kappa R$  is represented in Figure 2.9 pictorially as the Hückel limit, establishing a range of values for  $\kappa$  and  $R$ .

This analysis assumes the particle to be a symmetrical rigid sphere with uniform surface charge distribution. Proteins or small protein complexes such as dimers hexamers are of the order of  $\sim 10$  nm in size, rarely have a symmetrical charge distribution, and are not rigid bodies. Furthermore, changes in the local environment strongly influence the structure of the molecules/molecular complexes. The  $\zeta$ -potential is related to surface potential and but is not surface potential itself. It is merely a derived value which changes with the surface potential. Thus, the interpretation of  $\zeta$ -potential as an absolute surface potential should be used with caution.

When the double-layer thickness is much smaller than the particle itself, i.e. particles with large values of  $\kappa R$ , the solution of Poisson Equation and drag on the surface of the particle yield an equation similar to Equation (18), which is

$$u = \frac{\varepsilon \zeta}{\eta R}. \quad (19)$$

This equation is called the Helmholtz-Smoluchowski Equation.

Unlike in Equation (18), Equation (19) requires no assumptions of the structure of the double layer. Only the Poisson Equation and bulk values of  $\eta$  (viscosity) and  $\varepsilon$  (dielectric constant) apply. This equation applies for  $\kappa R > 100$  or for particles with sizes typically  $\sim 500$  nm and above. The exact applications of the above equations are depicted in Figure 2.9, as the theoretical boundaries of colloidal science. However, practical experiments involving colloids involve particles with sizes up to 10  $\mu\text{m}$ .

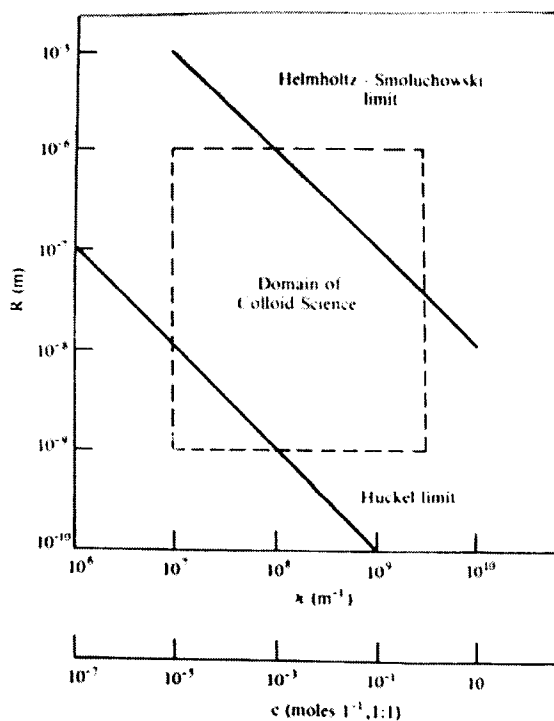


Figure 2.9. The domain within which most investigations of aqueous colloidal systems lie in terms of particle radii and 1:1 electrolyte concentration. The diagonal lines indicate the limits of the Hückel and the Helmholtz-Smoluchowski Equations.

Equation (19) applies to whole cell  $\zeta$ -potentials and large protein aggregates. However, the Equations (18) and (19) are the lower and upper limits of the domain of colloids (Figure 2.9) which we study. Too-large particles would make suspensions, (they will settle over a period of time) and too-small particles will make solutions (like ionic moieties). Larger particles such as silica, melamine formaldehyde microparticles, polystyrene latex microparticles, and insulin microparticles, all have applicability near the upper limit where the Helmholtz-Smoluchowski Equation applies. On most occasions we study suspensions using the same relations.

It may be argued that the absolute values of  $\zeta$ -potentials for biological samples obtained from the instrument are greatly inaccurate, first due to the assumptions involved in the theory and secondly due to the inaccuracies resulting from the solid theoretical background pertaining to such calculations. However, the  $\zeta$ -potential is used to study trends during LbL nanoassembly, and absolute values by themselves have little use. Thus under similar conditions we can safely assume the  $\zeta$ -potential to reflect the changes in surface potential of the microparticle in question.

Apart from surface charge characterization using  $\zeta$ -potential, colloidal particles with sizes over  $1\mu\text{m}$  can be visualized using optical techniques such as confocal microscopy. Fluorescently tagged polymers or nanoparticles aid in visualizing particles that are not natively fluorescent.

### **2.6.3 Confocal Microscopy**

Confocal microscope is an inverted compound microscope with laser optics, advanced electronics, and a software analysis system to study a sample under investigation. The primary advantage of confocal microscope is the laser light source. Unlike a regular microscope, chromatic aberrations are avoided by using a monochromatic light source from the laser; further, the effective resolution of the microscope is limited only by the wavelength of light used. Resolutions up to 190 nm can be achieved using a confocal microscope. The electronics and software included permit complex experiments like Fluorescence Recovery After Photobleaching (FRAP), which is illustrated in Figure 2.10 and has been employed in Chapter 4. The schematic of the model used is presented in Figure 2.10, which shows the bleach spot indicated by light grey color, and the region of interest indicated by the dark gray circle. The bleach spot is the area on the microscope slide where the laser intensity is maintained at maximum

level. The region of interest is the area where we measure fluorescence recovery; note that this region is inside the capsule. The development of the diffusion model used in Chapter 4 is described here.

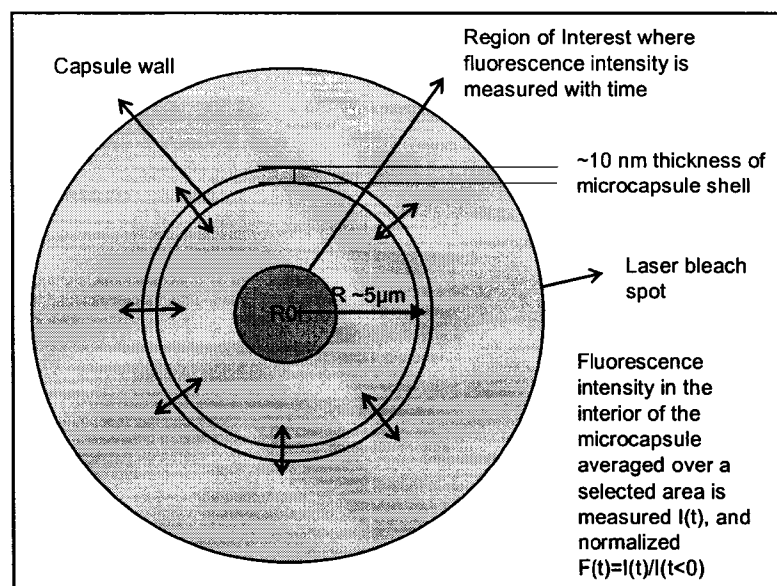


Figure 2.10. FRAP experimental schematic for estimation of diffusion coefficient of microcapsules.

Development of a working diffusion model for hollow polyelectrolyte capsules is based on the model for Fluorescence Recovery After Photobleaching (FRAP) developed by Axelrod et al. [68], in two-dimensional coordinates, and the use of the model to calculate diffusion coefficient, elaborated by Blonk et al. [69] is presented later.

A two-dimensional model is chosen because the diffusion coefficient across a thin membrane (capsule wall in Figure 2.10) is of interest in the current work.



The following assumptions are made for the model.

1. Diffusion of the species is effected primarily by the LbL assembly of the capsule.
2. In the lateral dimensions bulk diffusion is rapid and can be ignored for practical purposes, and the effective diffusion in the capsule interior is determined by the diffusion properties of the capsule walls.
3. Fluorescence intensity in the interior of the capsule (ROI Figure 2.10) at infinite time is equal to the fluorescence intensity prior to photobleaching

$$F(t)_{t=\infty} = F(t)_{t<0}.$$

4. For the current situation, as the microcapsules are isolated on a glass slide covered with a cover slip, only lateral diffusion is important, and a two-dimensional model may be used.
5. The immobile fraction is assumed to be absent.

Based on the two-dimensional model proposed by Axelrod et al. [68], the normalized fluorescence recovery curve can be written as follows:

$$F(t) = \sum_{n=0}^{\infty} \frac{(-\kappa)^n}{n!} \frac{1}{1+n \left[ 1 + \left( \frac{2t}{\tau_D} \right) \right]}. \quad (19)$$

Where,

$\tau_D$  is the two-dimensional characteristic diffusion time and is related to the diffusion coefficient

$D$  by the relation

$$\tau_D = \frac{\omega^2}{4D} \quad (20)$$

and  $\omega$  is the half-width of the Gaussian profile of the focused laser spot, it is usually determined at  $e^{-2}$  times the height of the profile.  $D$  (cm<sup>2</sup>/s) is defined by

$$D = \frac{kT}{6\eta r} \times 10^4, \quad (21)$$

where,  $k$  is Boltzmann's constant,  $T$  is the temperature (K),  $\eta$  is the viscosity (N.s/m<sup>2</sup>) of the medium and  $r$  is the effective radius (m) of the diffusing particles,  $\kappa$  is a bleach constant and depends on the sensitivity of the system for bleaching and is empirically related to the percentage of bleach by

$$\% \text{ bleach} = 100 \frac{\kappa - 1 + e^{-\kappa}}{\kappa}. \quad (22)$$

The fluorescence recovery when an immobile fraction is present, due to irreversible adsorption, is given by

$$F(t) = F(i) \{1 - R(1 - f(t))\}, \quad (23)$$

where  $F(i)$  is the intensity of the bleach spot before bleaching, and  $R$  is the mobile fraction defined by

$$R = \frac{F(\infty) - F(0)}{F(i) - F(0)}, \quad (24)$$

where  $F(\infty)$  is the normalized intensity of the bleached spot at infinite time after bleaching and  $F(0)$  is the normalized intensity just after bleaching.

However, for practical purposes the working model is designed as follows based on the schematic presented in Figure 2.10.

The value of  $\omega$  is determined experimentally to be 0.0000557, (Blonk et al.[69])

The bleach constant  $\kappa$  is calculated using the modified Equation (22) as

$$\frac{I_0}{I_{t<0}} = \frac{1 - e^{-\kappa}}{\kappa}, \quad (25)$$

where  $I_0$  is the fluorescence intensity of the bleach spot immediately after photobleaching, and  $I_{t<0}$  is the fluorescence intensity prior to photobleaching.

Normalized fluorescence intensity  $F(t)$  is obtained and the data is fitted to Equation (19) and  $\tau_D$  is estimated. Following which, an estimate for the diffusion coefficient is made using Equation (20).

#### **2.6.4 Thermogravimetric Analysis**

For a mixture of organic and inorganic samples or for inorganic samples containing thermally decomposable constituents, thermogravimetric analysis (TGA) provides a tool for quantitatively estimating the decomposable constituents. TGA relies on the principle of thermal decomposition of the material. The thermal decomposition or evaporation of solid products into gaseous form usually occurs at a temperature characteristic of that material. For example, during the decomposition of  $\text{CaCO}_3$ , it breaks down into  $\text{CaO}$  and  $\text{CO}_2$ . However, organic material may be thermally decomposed into numerous products depending on the length of the carbon chain and other radical groups present. Pictorially, the working of the thermogravimetric measurement is shown in Figure 2.11, where a sample is heated at the rate of  $5\text{ }^\circ\text{C}/\text{min}$  and the resulting changes in mass are recorded.

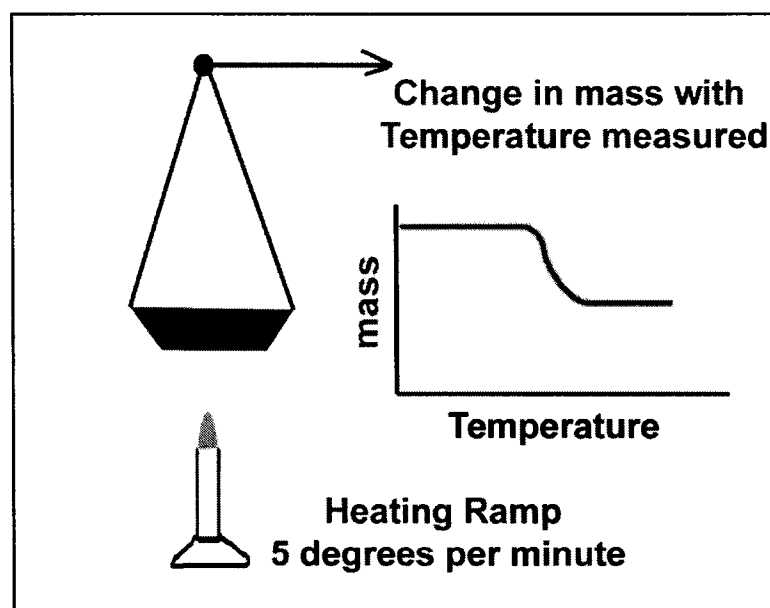


Figure 2.11. Principle of thermogravimetric analysis: a sample is heated at a fixed rate and mass changes are recorded with changes in temperature.

Thermogravimetric analysis can thus be used to estimate the thermal decomposition temperature of different materials with the same or different stoichiometric composition. It allows the determination of strength of covalent and other linkages in the material.

# **CHAPTER 3**

## **SURFACE MODIFICATION OF INSULIN MICRO- PARTICLES USING ELECTROSTATIC LAYER-BY-LAYER ASSEMBLY**

### **3.1 Introduction**

Due to the success of biotechnology development, proteins represent the fastest-growing segment of pharmaceutical products, but delivery of proteins in a controlled manner is a major challenge. Controlling the rate of release of the therapeutic agents from delivery devices offers prolonged therapeutic levels of the protein, improved pharmacokinetics and pharmaco-dynamics, and increased patient convenience and compliance. A variety of drug delivery approaches has been developed over the years to control release. Conventional methods include spray drying, spray freeze drying, milling, nondegradable and degradable polymeric systems, etc. The drawbacks of these methods are the use of organic solvents which are often incompatible with proteins, the complexity, and cost-ineffectiveness as discussed in great detail in the background material.

EPIC Therapeutics Inc. developed a simple, scalable water-based process of microsphere formation via controlled phase separation of macromolecules with water soluble polymers that generates microspheres PROMAXX<sup>®</sup> with a narrow size

distribution [70, 71]. The template PROMAXX<sup>®</sup> microparticle can consist of protein, peptide, nucleic acid, polymer, or low molecular weight compound. The aim of the current research is to apply (LbL) assembly of oppositely charged polyelectrolytes on PROMAXX<sup>®</sup> insulin microspheres as a continuation of the particle formation process to obtain sustained release and control of surface functional properties.

The initial fundamental research on LbL assembly was performed on planar substrates. However, the LbL process is not limited to coating on large surfaces. The nanofilms may be deposited on tiny (micro- or nano-) three-dimensional templates [48, 51, 72-74]. Functional nanocomposite films deposited on these colloidal carriers enhance biocatalytic reactions and allow controlled release of the encapsulated compound due to adjustable thickness of the capsule walls. The microparticles can be separated from polyelectrolytes after adsorption saturation, which is achieved via centrifugation or filtration. Latex, inorganic microparticles, and some drug microcrystals (1-5  $\mu\text{m}$  Furosemide, Ibuprofen, Indomethacin, and Dexamethasone particles) have been nanocoated with linear polyelectrolytes with 5-12 polycation/polyanion bilayers, which gives capsule wall thicknesses of 20-100 nm [54, 56, 75-78]. Release time for these drugs was increased from ca 1 min for bare crystals to 1-3 hours for 8-10 bilayer encapsulation. 10  $\mu\text{m}$  insulin microcrystals also were encapsulated in 15 polylysine/sodium alginate multilayers, providing 10 times longer dissolution as compared with bare crystals. However, with less than 10 polyelectrolyte bilayers the release rates of bare and coated insulin microcrystals were similar [79, 80]. The nano-organized shell around drug microparticles was considered in these works as an adjustable diffusion barrier, and specific interaction with microcores was not considered. In another approach,

interpolyelectrolyte complexation of drugs with polyelectrolytes to form microparticles spontaneously, was developed [81] but LbL assembly was not used.

In this work the combination of interpolyelectrolyte complex formation and organized multilayer shells are used to encapsulate 2  $\mu\text{m}$  diameter PROMAXX<sup>®</sup> insulin particles for controllable prolonged release. It was found that formation of 10-100 nm LbL multilayers on soft semi-soluble and permeable PROMAXX<sup>®</sup> insulin cores was insufficient to provide a significant physical barrier to slow the diffusion of insulin from the core into aqueous solution. Conditions for complexation of the outermost part of the insulin microparticles with the first polyelectrolyte layer were established, which played a critical role for sustained release, by decreasing the release rate of drug from the polyelectrolyte-complexed microparticle (Figure 3.1). Further polycation/polyanion multilayer assembly allowed fine adjustment of the insulin release profile (Figure 3.1). The odd polycation layers reinforced the microparticle complex, and even polyanion cores weakened the complex. The overall effect was a cumulative decrease in the release rate with increase in total number of odd polyelectrolyte layers.

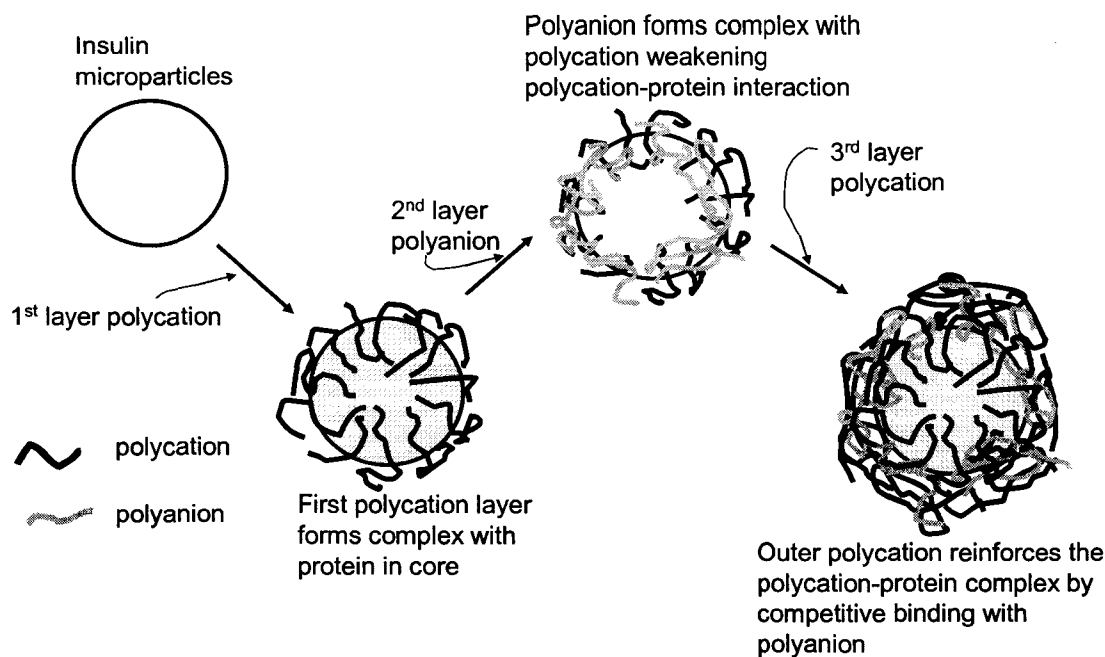


Figure 3.1. A schematic illustration of the assembly of polyelectrolyte layers on insulin PROMAXX<sup>®</sup> microspheres at pH 7.0.

### 3.2 Experimental Methods

#### 3.2.1 Materials

Chondroitin sulfate C sodium salt (ChS, from shark cartilage), poly-L-glutamic acid sodium salt (PGlu, MW 17000), poly-L-aspartic acid sodium salt (PAsp, MW 33400), poly-L-lysine hydrochloride (PLys, MW 22100), protamine sulfate (ProtS,) and poly-L-lysine hydrochloride fluorescein-labeled (PLys-FITC) were purchased from Sigma and used as received. Poly(sodium-4-styrene sulfonate) (PSS, MW 70000), carboxymethyl cellulose (CMC, MW 70000), poly(diallyldimethyl ammonium chloride) (PDDA, MW 200000), and polyallylamine hydrochloride (PAH, MW 70000) were purchased from Aldrich and used as received. Dextran sulfate sodium salt (DexS, MW



500000) was purchased from Fluka, and poly-l-arginine hydrochloride (PArg, MW 20000) from MP Biomedicals Inc.

PROMAXX<sup>®</sup> insulin microparticles (EPIC Therapeutics, Lot# 300X17) were used as cores. The microparticles were fabricated using EPIC's proprietary Controlled Phase Separation (CPS) technology and the resulting suspension was frozen and stored at -20°C until used. The LbL coating process was conducted in an aqueous solution composed of 16% polyethylene glycol MW 3350 kD (PEG 3350) and 0.7 % NaCl unless otherwise noted. The pH of this solution was adjusted to a desired value using either hydrochloric acid or sodium hydroxide.

### **3.2.2 Layer-by-Layer Coating of Insulin Microspheres with Multiple Polyelectrolyte Layers**

Before LbL coating, 20 mL aliquots of insulin microparticles were thawed at ambient temperature to melt previously frozen samples. The suspension of microparticles was then kept on ice (~2<sup>0</sup> C) during the entire procedure. Insulin microparticles with average diameter of 2 μm were separated from the supernatant by centrifugation at 2500 rpm (Eppendorf 5804R), and the buffer was replaced with an equal volume of fresh buffer that was used for the set of experiments. The following buffers were used: (a) 16 % PEG-0.7 % NaCl buffer with pH adjusted to a desirable value (5.8 or 7.0), (b) 16 % PEG-0.7 % NaCl, pH 7.0, containing 0.026 % ZnCl<sub>2</sub> to reduce solubility of insulin, and (c) 0.16 % PEG, 1.3x10<sup>-3</sup> % acetic acid 0.026 % ZnCl<sub>2</sub>, pH 7.0 buffer.

For deposition of the first polyelectrolyte layer, polyelectrolyte solution was added to insulin microparticles suspended in the 20 mL of buffer and thoroughly mixed. The final concentration of the polyelectrolyte in the supernatant solution was between

0.005 and 1.5 mg/mL. After 60 min adsorption of the first polyelectrolyte layer, the microparticles were separated from the supernatant using centrifugation; the supernatant was removed and the microparticles were re-suspended in fresh buffer. The centrifugation / re-suspension cycle was repeated twice to remove traces of unadsorbed polyelectrolyte. The second polyelectrolyte layer with the charge opposite to that of the first polyelectrolyte layer was assembled by repeating the procedure above. Multiple layers of polyelectrolytes were adsorbed by repeating the procedure.

### **3.2.3 Quartz Crystal Microbalance Measurements**

The quartz crystal microbalance (QCM) method was used to elaborate LbL assembly in the presence of PEG at different temperatures and estimate the thickness of the layers. A precursor film of (PAH/PSS)<sub>n</sub> films (n=2-4) was deposited on 9 MHz silver QCM resonators. Polyelectrolyte and protein layers were assembled from 1 mg/mL solutions of the substances in corresponding buffers. The time for deposition was 15 min or 1 hour per layer; the temperature was 2 °C (in melting ice). The QCM resonator was rinsed with DI water and dried in a stream of nitrogen after absorption of each layer. The frequency changes ( $\Delta F$ ) of the resonators was monitored using an universal counter (Agilent) with an attachment (USI-System, Japan) adapted for QCM resonators and translated into the thickness using the Sauerbrey Equation with the experimental scaling:  $\Delta t(\text{nm}) = -0.016\Delta F (\text{Hz})$  [52].

### **3.2.4 Microparticles Zeta- Potential Measurements**

Zeta-potential measurements of microparticles were taken using a Brookhaven ZetaPlus microelectrophoretic system. For  $\zeta$ -potential measurements, 40  $\mu\text{L}$  of the

sample under investigation was added to 2.0 ml of buffer, mixed, and the suspension was analyzed immediately. The temperature of the cell was equilibrated to 8 °C to avoid the dissolution of PROMAXX<sup>®</sup> insulin particles. In calculations of the  $\zeta$ -potentials using the Smoluchowski Equation, increased solvent viscosity due to the high (16 wt %) PEG concentration was taken into account.

### **3.2.5 Confocal Laser Scanning Microscopy**

Confocal images of PROMAXX<sup>®</sup> insulin microspheres were taken with a confocal laser scanning microscopy (Leica DMI RE2) equipped with 63x oil objective. Fluorescent labeling of ProtS and PLys with FITC were performed with the standard procedure [82, 83].

### **3.2.6 In Vitro Release Study**

Dissolution of insulin microspheres was studied by addition of 10 ml of the release buffer (10 mM Tris, 0.05% Brij 35, 0.9% NaCl, pH 7.4) into glass vials containing 3 mg equivalence of the insulin microspheres, and incubation at 37°C. At designated time intervals 400  $\mu$ L of the medium was transferred into a microfuge tube and centrifuged for 2 min at 13000 rpm, and 300  $\mu$ L of the resulting supernatant was removed and stored at -80°C until analyzed. The 300  $\mu$ L of fresh medium was added to the remaining portion of the collected sample, the pallet was reconstituted, and was transferred back to the corresponding *in vitro* release medium. The amount the released protein was estimated with the bicinchoninic acid (BCA) assay.

To determine protein content, a known amount of microspheres was suspended in 1.0 ml 0.01 N HCl. The medium was centrifuged at 13000 rpm for 5 minutes at 4°C. The

protein content in the supernatant was determined by BCA assay, using solutions of insulin in 0.01 N HCl to construct the calibration curve.

### **3.3 Results and Discussion**

#### **3.3.1 Electrostatic LbL Assembly in the Presence of PEG**

In earlier works on LbL assembly, experiments to determine the feasibility of LbL assembly of polyelectrolytes in the presence of high concentrations of other hydrophilic macromolecules had not been performed [47, 48, 74].

Therefore, first it had to be determined whether polyelectrolytes and proteins could be assembled in aqueous solutions containing up to 16 % PEG, which is necessary for insulin microparticles' stabilization. Figure 3.2(a) shows a linear step-by-step increase of film thicknesses for different polyelectrolyte films assembled in 16 % PEG-0.7 % NaCl, pH 5.8 and at room temperature. Stable growth of the films is observed for different polyelectrolyte combinations. The assembly of polyelectrolytes in the presence of PEG resulted in thicker films, compared with LbL films obtained in DI water without any polymer additives, and had a typical bilayer thickness of ca. 2-11 nm (Table 3.1).

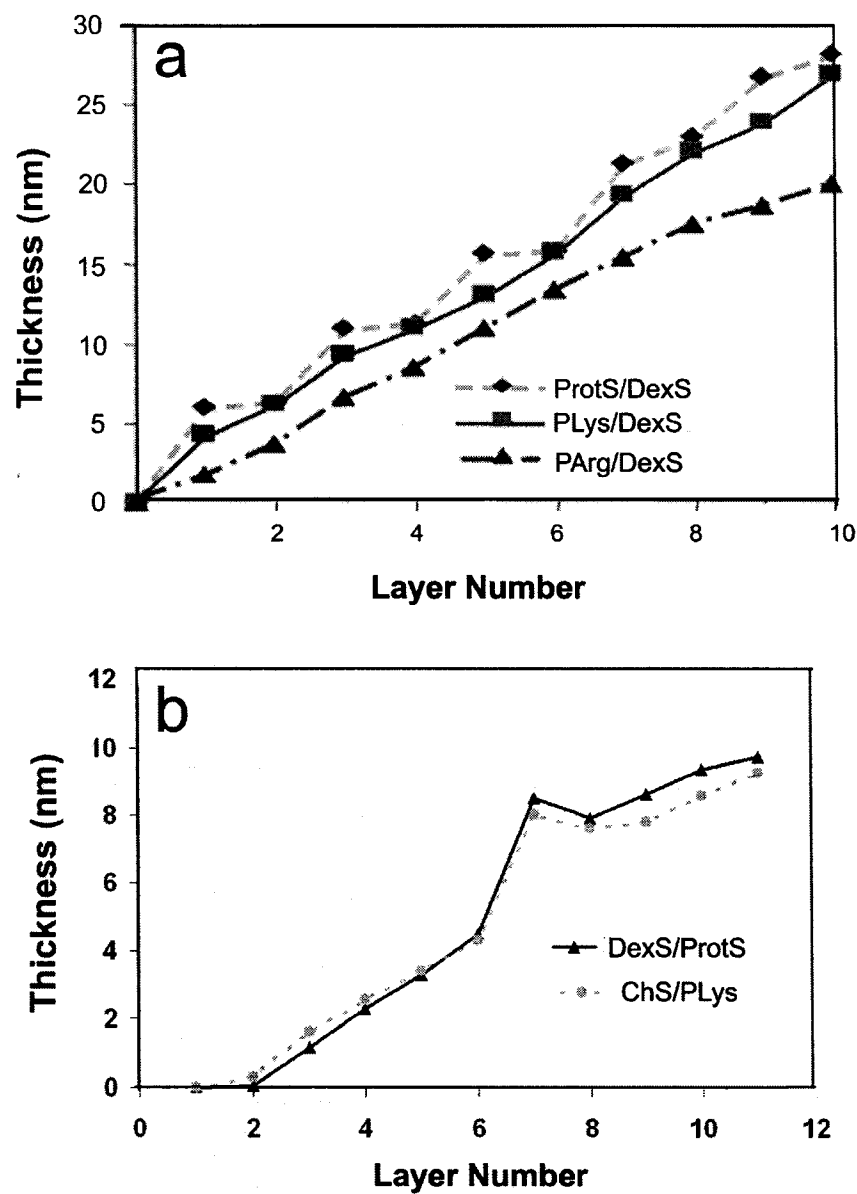


Figure 3.2. Quartz crystal microbalance data for assembly of different polyelectrolytes from 1 mg/mL solutions in 16 % PEG-0.7 % NaCl buffer, pH 5.8 at room temperature (a) and over ice (b). Experimental errors are  $\pm 0.5$  nm.

Table 3.1. Bilayer thickness (in nm) for polycation / polyanion assemblies in 16% PEG-0.7% NaCl, pH 5.8, room temperature, 15 min per layer.

| Polyanions   | Polycations |          |         |
|--------------|-------------|----------|---------|
|              | PLys        | PArg     | ProtS   |
| DexS         | 4.9±1.0     | 4.2±0.8  | 5.0±1.5 |
| ChS          | 6.3±2.0     | 11.3±3.9 | 5.4±1.4 |
| Alginic acid | 6.7±2.2     | 6.7±2.3  | 1.8±0.4 |

PEG is well known as a complexing and aggregating agent, which induces bulk coil conformation in polypeptide and DNA molecules [84]. Therefore, the presence of PEG can increase polyelectrolyte layer thickness.

Therefore it can be concluded that electrostatic LbL assembly of polyelectrolytes and proteins can be carried out in the presence of hydrophilic uncharged polymers. In related work, a competitive adsorption of polyelectrolytes from binary mixtures was recently reported [85, 86].

### **3.3.2 Influence of Temperature on LbL Assembly in the Presence of PEG**

To prevent undesirable dissolution of the microparticles, the LbL assembly was performed in the temperature range of a low 2-5 °C. The influence of low temperature on polyelectrolyte assembly in the presence of PEG was investigated for DexS and PLys combination using QCM. At 2° C, the assembly still occurs, but the bilayer thickness after 15 min deposition is much lower than that for the same combination at room temperature (0.6 nm vs 4.9 nm). The thickness of a polyelectrolyte bilayer was restored by increasing the adsorption time to one hour to achieve a thickness of 2.2 nm for a DexS/PLys bilayer. Similar results were obtained for other polycation / polyanion pairs.

All QCM resonators were initially coated with several PSS/PAH bilayers to create a uniformly charged surface and to mimic the surface of the microparticles under investigation (Figure 3.2(b)). The bilayer thickness for the films assembled in 16 % PEG-0.7 % NaCl buffer, pH 5.8 is between 1 and 5 nm depending on composition (Table 3.2).

Table 3.2. Bilayer thickness (in nm) for polycation / polyanion assemblies in 16% PEG-0.7% NaCl, pH 5.8, 2 °C, 60 min per layer.

| Polyanions | Polycations |         |         |           |          |
|------------|-------------|---------|---------|-----------|----------|
|            | PLys        | PArg    | ProtS   | Gelatin B | Chitosan |
| DexS       | 2.3±0.3     | 1.8±1.2 | 1.1±0.2 | 4.8±1.1   | 3.2±0.2  |
| ChS        | 1.4±0.3     | 3.2±0.4 | 1.5±0.2 | 1.8±0.4   | 2.7±0.5  |
| PAsp       | 1.3±0.1     | 5.1±0.5 | 1.3±0.2 |           |          |
| PGlu       | 4.3±0.7     | 3.7±0.5 | 1.0±0.1 |           |          |

It can be assumed that intermediate rinsing with DI water done after adsorption of each layer removes most of the hydrophilic PEG, making the final structure of the films close to that obtained in the absence of PEG. At the same time, as can be seen from Table 3.1 and Table 3.2, the experimental errors observed for different combinations are 10-15 %. This variation can be associated with trace amounts of PEG varying from layer to layer in the films due to minute differences in film rinsing.

In some of the QCM experimental series, to simulate conditions closer to deposition on insulin microcores, an insulin layer was additionally deposited on the top of the PAH/PSS precursor to simulate conditions closer to the assembly on insulin cores (Figure 3.2(b), seventh assembly step). The thickness of the insulin layer was  $4.5 \pm 1.0$  nm, which corresponds to adsorption of ~2 monolayers of insulin. As insulin is positive at pH 5.8, the insulin layer was followed by a polyanion layer. A slight decrease in film

thickness was observed for all films as the insulin layer was partially removed. Polyanions peel off some loosely attached insulin molecules and adsorb on the top of the films, since it was observed that the film thickness increases again with assembly of the next polycation layer. This behavior is common in protein/polyelectrolyte LbL assembly [52]. To conclude this section, the conditions desirable for coating of insulin microcores were determined as 2 °C and 60 min per layer deposition and are used hereafter.

### **3.3.3 Coating PROMAXX<sup>®</sup> Insulin-Microspheres with Polyelectrolytes**

Figure 3.3 shows the surface charge reversal of insulin microparticles after adsorption of single layers of different polyelectrolytes at 2 °C. Further, the results for assembly are described 1) at pH 5.8, below isoelectric point of insulin where PROMAXX<sup>®</sup>-microcores are positive, and 2) at pH 7, above its isoelectric point (apparent pI = 5.9) where PROMAXX<sup>®</sup> insulin microparticles are negative.



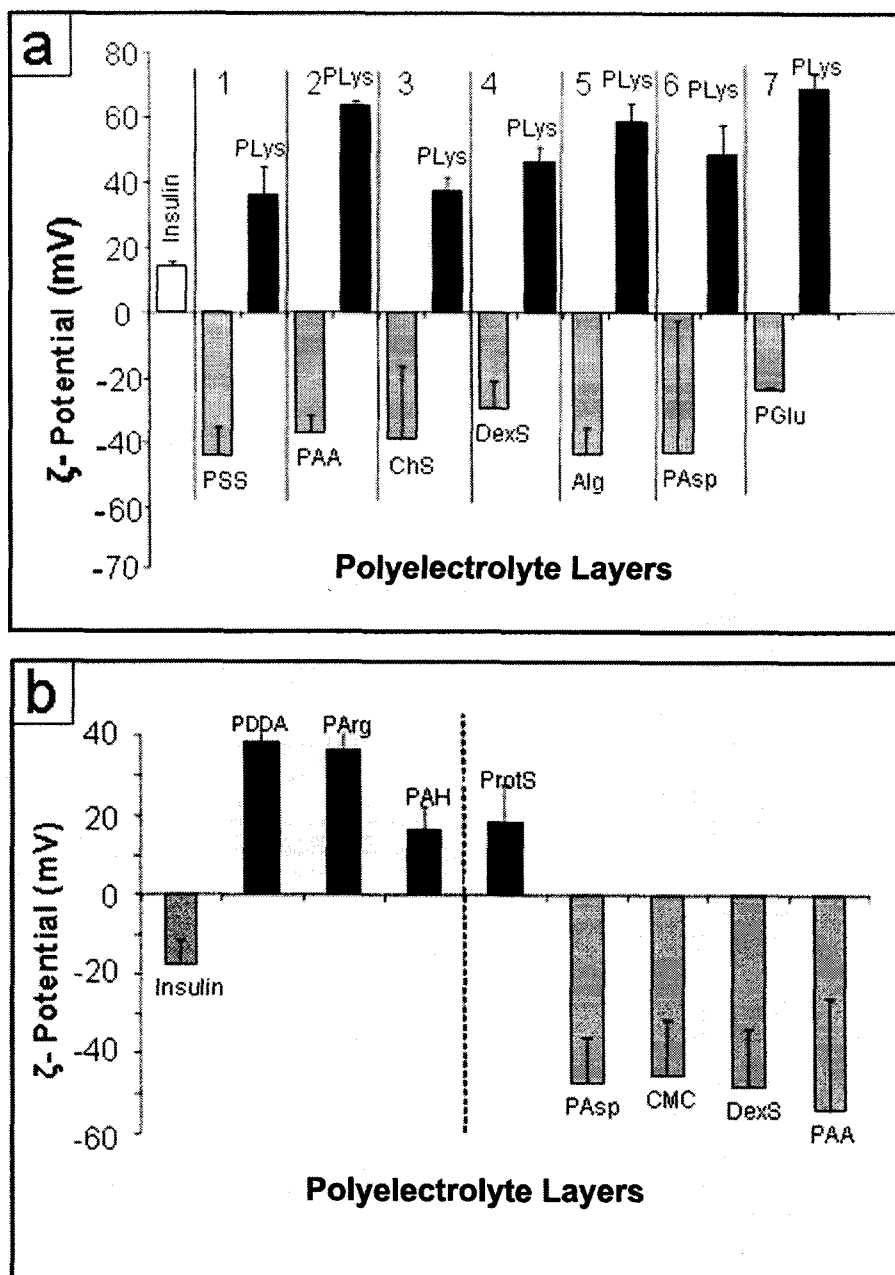


Figure 3.3. Surface charge of microparticles after deposition of different bilayers at pH 5.8 (a); and pH 7.0 (b).

### 3.3.3.1 pH 5.8, positive core

At pH 5.8, insulin microparticles are positively charged and negative polyelectrolytes as PSS, PAA, ChS, DexS, Alginate, PAsp were chosen to be

adsorbed as the first layer. After polyanion adsorption, the surface charge of microparticles changes to a negative value, indicating a successful deposition. Then a polycation, for example PLys, was adsorbed as the second layer and the surface charge of the microparticles reversed. Insulin microparticles coated with different polyanions as the first layer and PLys as the second layer show varying magnitudes of positive charge. This variability could result from the interaction of PLys with the polyanion layer, which affects the amount of adsorbed PLys, its structure, and ionization.

### **3.3.3.2 pH 7.0, negative core**

Figure 3.3(b) presents the results of coating insulin microparticles at pH 7.0, above the isoelectric point of insulin. At this pH, the microparticles were negative, and polycations were used as the first layer. After polycation adsorption, the charge of microparticles changes to a positive value (left side, Figure 3.3 (b)), indicating successful adsorption onto the microparticle surface. In the following step, a polyanion can be adsorbed as the next layer (right side, Figure 3.3(b)).

By alternating positively and negatively charged polyelectrolytes, a multiple coating consisting of 3-5 polyelectrolyte layers was formed on PROMAXX<sup>®</sup> insulin microspheres. Figure 3.4 shows monitoring of surface potential for some shell compositions that are potentially interesting for encapsulated PROMAXX<sup>®</sup> particles.

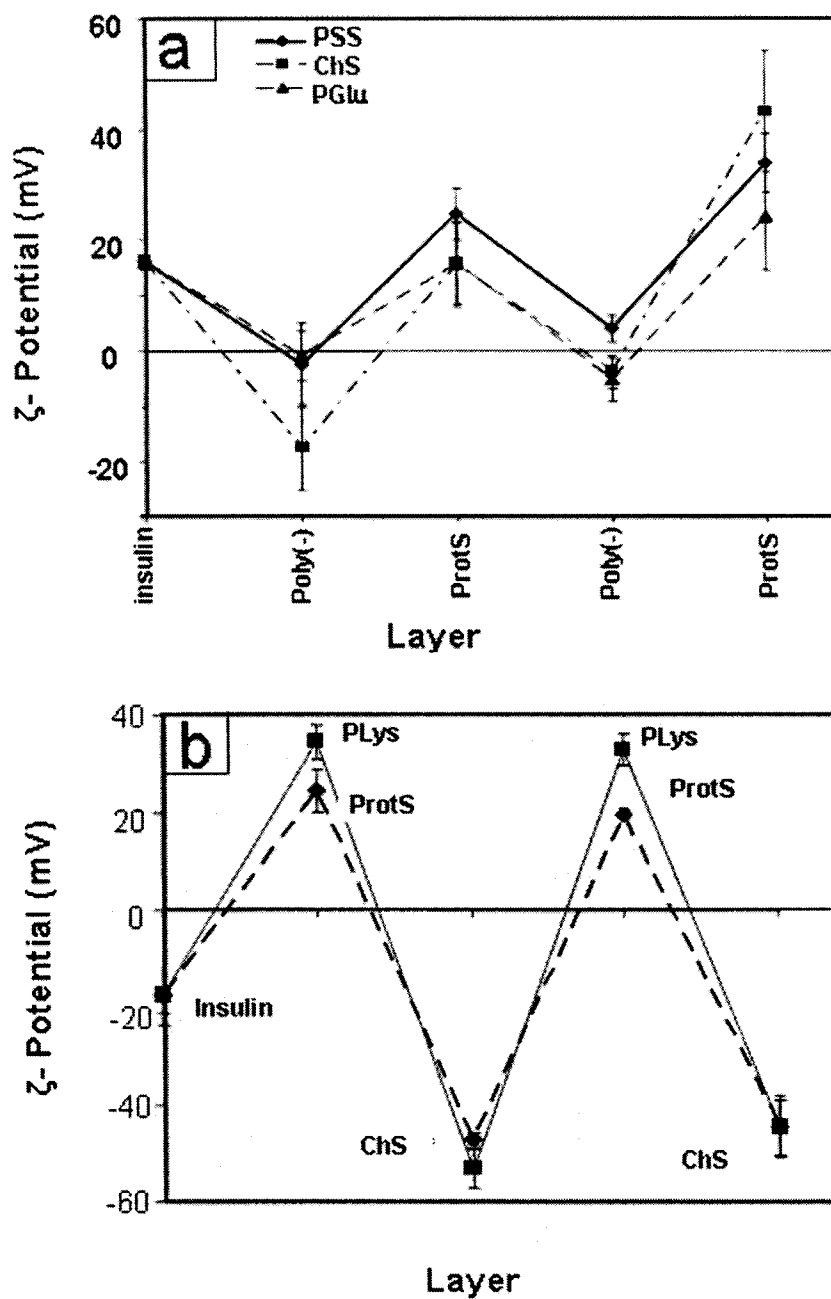


Figure 3.4. Surface charge alternation for insulin microparticles coated with multiple polyelectrolyte layers at, (a) pH 5.8 and (b) pH 7.0.

More than one pair of polycation and polyanion can be used to coat a microparticle, providing a complex shell composition. Such a complex architecture

increases the number of variants in designing shells with different properties and provides better control over microparticles' dissolution profile. Formation of multilayered coatings on the microparticles is complicated by insulin dissolution, which slowly occurs, even at low temperature. The amount of insulin remaining in the samples decreases after deposition of each layer. More than 50 % loss of insulin was found for a sample after completing the deposition procedure corresponding to 3-4 polyelectrolyte layers corresponding to 6-8 hrs of processing time. This loss makes assembly of the capsules with more than two polyelectrolyte bilayers undesirable because of low yield of the final product.

#### **3.3.4 Optimization of the Nanoencapsulation Conditions**

The dependence of  $\zeta$ -potential on total concentration of polyelectrolyte in the bulk is shown in Figure 3.5. With the 20 ml aliquots of insulin-microparticles in PEG buffer as basis, and a working volume of 20 ml in the PEG buffer, the concentration of the polyelectrolyte forming the outermost layer was varied in the range of 0-1.5 mg/ml. The plot with closed diamonds represents the  $\zeta$ -potential with a single layer of ProtS. The other plots represent the effect ChS (open circle) and CMC (closed triangle) in Figure 3.5, after a ProtS layer. ProtS as a third layer (closed square) is adsorbed after sequential assembly of ProtS and CMC.

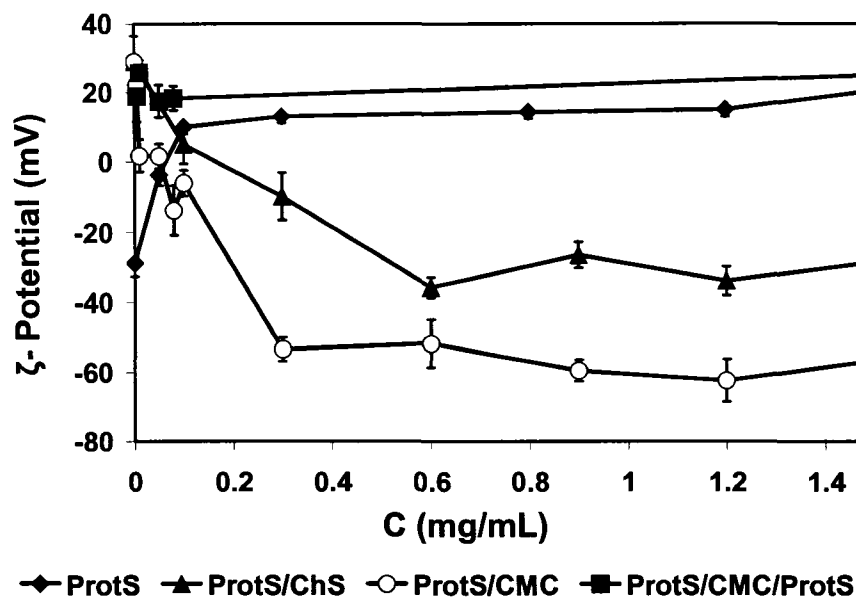


Figure 3.5.  $\zeta$ -potential of microparticles after LbL assembly at pH 7.0 on insulin microparticles in solutions with different concentrations. Closed diamonds represent ProtS. Open circles and closed triangles represent ChS and CMC respectively, on particles that were coated with ProtS at 1.5mg/ml. Closed squares represent particles that were first coated with ProtS at 1.5mg/ml, followed by CMC at 1.5mg/ml and finally a second layer of ProtS.

### 3.3.4.1 pH 7.0, negative core

A complete charge reversal for cationic ProtS adsorption on negative microcores (Figure 3.5) is observed only for solutions with concentrations higher than 0.3 mg/mL. Lower concentrations of ProtS are not sufficient for recharging of the microparticles' surface. This observation is different from those made previously for LbL assembly in aqueous solutions in the absence of PEG, where a polyelectrolyte concentration as low as 0.001 mg/mL was enough to form a saturated polyelectrolyte layer [45, 47]. A similar dependence was found for adsorption of the second polyanion layer (Figure 3.5).

### **3.3.4.2 pH 5.8, positive core**

The concentration needed for complete charge reversal in the case of anionic CMC and ChS is also elevated. For CMC, the minimal concentration level is around 0.1 mg/mL and for ChS it is 0.3 mg/mL.

In both cases, the degree of ionization of polymer functional groups and the charge density on the polymer chains determine the polyelectrolyte concentration needed. Competition between adsorption of PEG and polyelectrolytes could probably explain the increased concentration of polyelectrolytes needed for the LbL assembly in 16 % PEG as compared with aqueous solutions. Besides, it may indicate that the amount of insulin interacting with polyelectrolytes is not limited by the protein molecules located on the surface. Taking into account the properties of microparticles, permeation of polyelectrolytes into the microparticle interior and formation of complexes deeper within insulin microsphere matrix can be expected. The permeation of polyelectrolytes into the microparticles could increase the polyelectrolyte concentration needed to cause charge reversal of the microparticles.

### **3.3.5 Polyelectrolyte Interaction with Microparticles**

#### **3.3.5.1 At pH 7.0**

The interaction of polyelectrolytes with microparticles can be visualized using confocal microscopy using fluorescently labeled polyelectrolytes. Figure 3.6 (a) shows a confocal fluorescence image of insulin microparticles covered with one layer of FITC-labeled ProtS at pH 7.0 when core particles are negative. One can see that FITC-ProtS fluorescence emanating from a ring around the microparticle. The interior of microparticles is also partially fluorescent and the fluorescence intensity profile (Figure

3.6 (a)) shows that intensity of interior is of about 20 % of that of the walls indicating that some amount of ProtS-FITC forms complex with the insulin in the core matrix.

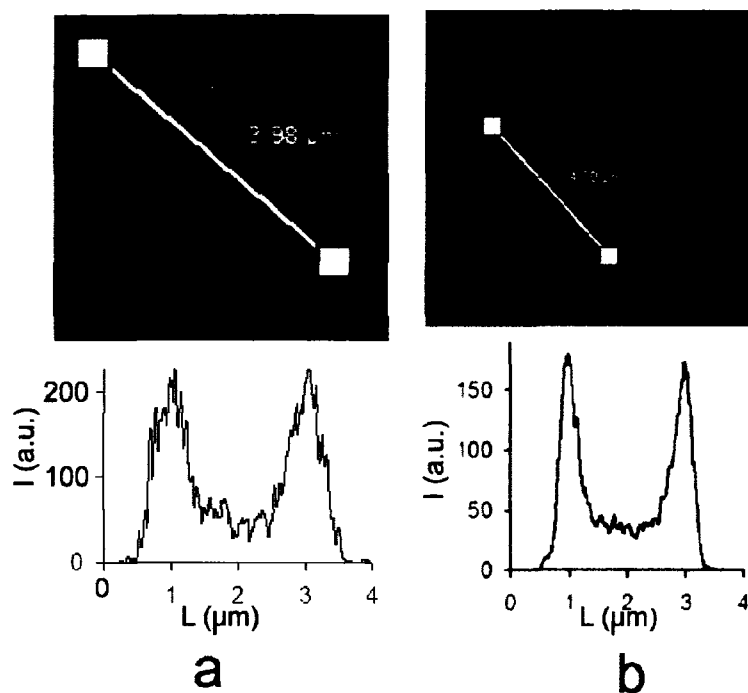


Figure 3.6. Confocal images of insulin microparticles coated with, a) FITC-ProtS layer in 16 % PEG-0.7 % NaCl, pH 7.0; and (b) PSS/FITC-PLys at pH 5.8.

### 3.3.5.2 At pH 5.8

At this pH microparticles are positive, and negative PSS was used as the first layer, followed by FITC-labeled polycation, PLys. Again, narrow fluorescence rings occur around the microparticles in the confocal microscopy image (Figure 3.6 b). We conclude that the fluorescently labeled polyelectrolyte is attached to the microparticle surface, but some fluorescence in the microparticle interior was also observed.

### 3.3.6 Modification of Microparticle Solubility

Unmodified insulin microparticles dissolve rapidly in a physiological solution. A large shift of pH from 5.8 (pH of the insulin suspension) to 7.4 (dissolution pH) with

simultaneous increase in temperature from 2 to 37°C makes the dissolution of insulin virtually instant. Therefore, we studied encapsulation at lower pH 5.8 and at higher pH 7.0.

### 3.3.6.1 pH 5.8, positive core

This pH is close to the apparent isoelectric point of insulin in the 16% PEG, 0.7% NaCl buffer. Polyanions were adsorbed as the first capsule layer. In spite of alternation of surface charge at these conditions, dissolution tests did not show significant reduction in release rate with the deposition of different assemblies of charged polyelectrolytes (Figure 3.7).

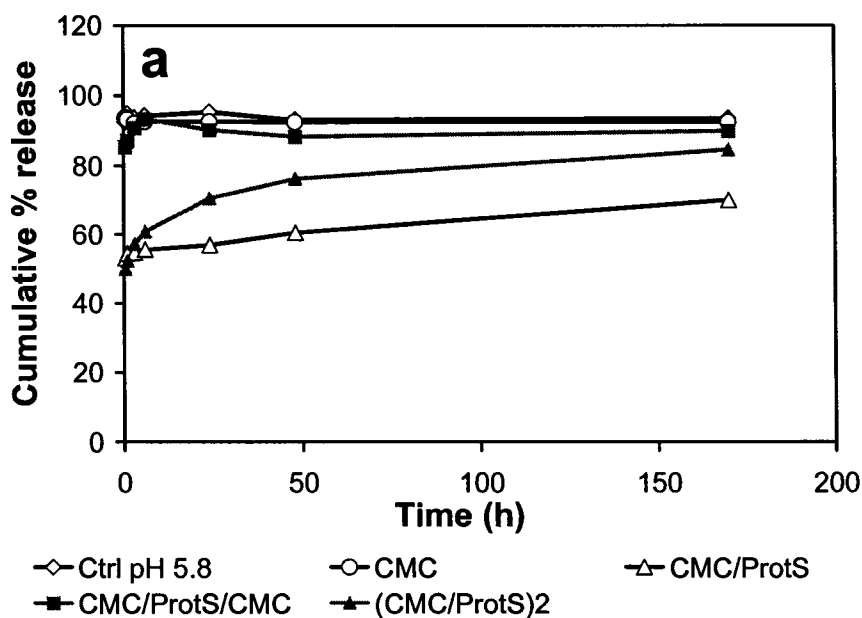


Figure 3.7. Cumulative *in vitro* release of insulin from microparticles coated with CMC and ProtS up to two bilayers at pH 5.8. The control is uncoated microparticles suspended in PEG buffer at pH 5.8.

Microparticles coated with a single layer of polyanion show solubility similar to that of an unmodified sample. At the same time, the next polycation layer decreases the



amount of insulin released to ~60 %. At this pH the solubility of insulin microparticles coated with a polycation layer as the outermost layer is somewhat lower than that of microparticles with a negative outermost layer, but this dependence is not pronounced.

### 3.3.6.2 pH 7.0 negative core

At this pH, insulin microparticles are negative and different polycations were used to form the first layer (Figure 3.8).

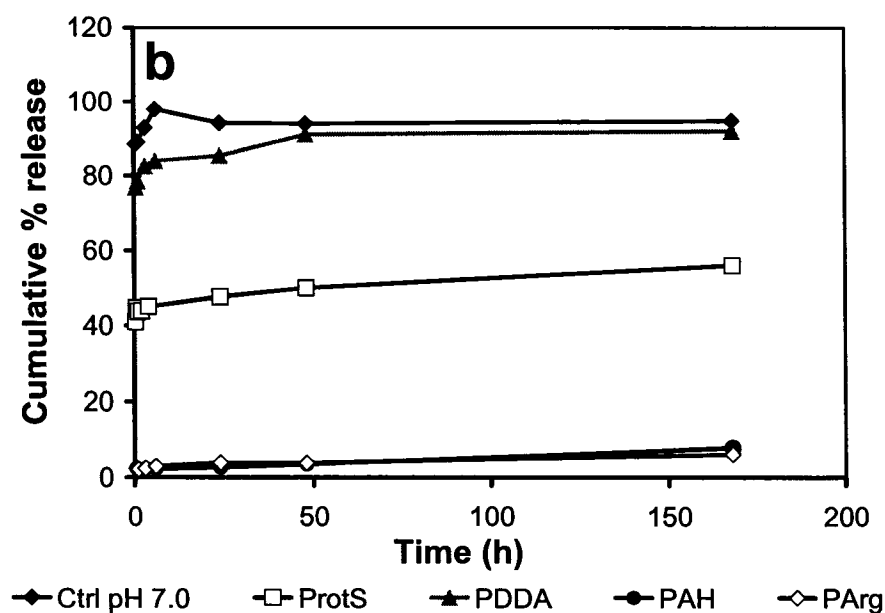


Figure 3.8. Cumulative *in vitro* release of insulin from microparticles coated with single layer of polycation at pH 7.0. The control is uncoated insulin microparticles.

For such modified microparticles the initial release is still rapid. Insulin concentration in solution reaches saturation after 30 min. However, in many cases, the release level is much lower than 100%, which implies that most of the insulin is fixed inside the microparticles due to complex formation with polyelectrolytes. It is known that a single polyelectrolyte layer does not form a diffusion barrier on the surface [48, 74].

Polycations with charged flexible side chains, such as PAH, PArg, and PLys, slow down the release to a larger degree than PDDA or chitosan having the charged groups on the main polymer chain. The action of ProtS can be attributed to its chemical structure, which, predominantly consists of Arg and Lys residues. A polyanion layer deposited on top of the polycation changes solubility of microparticles, increasing it up to 80-100% (Figure 3.9).

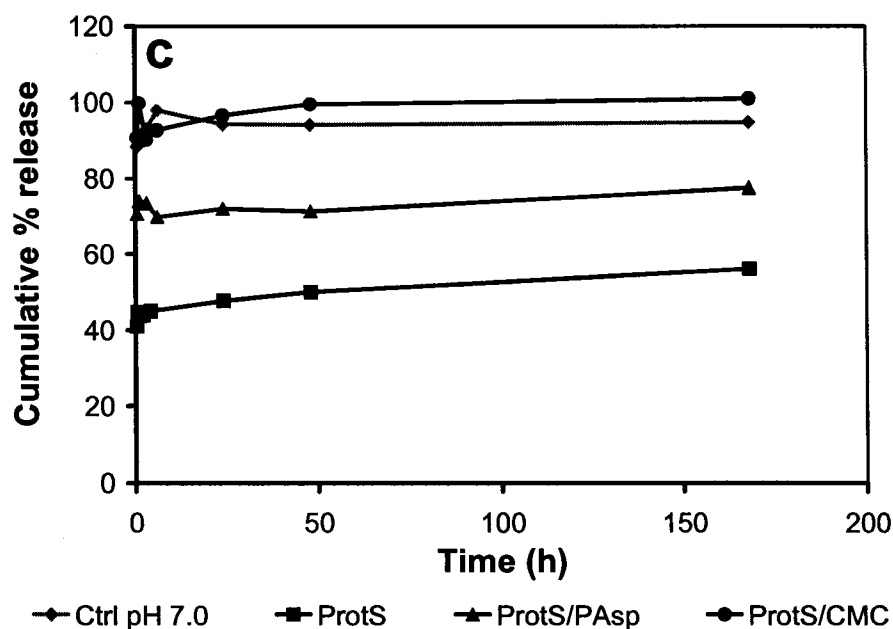


Figure 3.9. Cumulative in vitro release of insulin from microparticles coated with ProtS as the first layer and subsequent layers of polyanions- PAsp and CMC at pH 7.0. The control represents uncoated microparticles.

The effect of different polyanions is not as pronounced as the action of the first polycation layer. If a polycation is adsorbed as a third layer, the solubility of the microparticles decreases again. Coating of insulin cores at pH 7.0 (when the core is negative) with a polycation fixes the insulin in the core; addition of a polyanion relaxes

the structure and allows for complete release. The third layer of polycation again strengthens the shell-core complex. The QCM studies demonstrated that there are no specific features of polycation/polyanion multilayers assembled on a solid support. Therefore, formation of interpolyelectrolyte, and insulin-polyelectrolyte complexes in the microcore are responsible for such release profile. The dissolution properties of microparticles follow the same trend for all investigated polyelectrolyte combinations investigated.

Insulin microparticles can be coated by LbL in the buffers containing  $Zn^{2+}$  ions, which have an important influence on the synthesis and action of insulin in body [87]. Zinc decreases general solubility of insulin but does not change the general influence of polyelectrolytes on microparticle dissolution. At pH 7.0, the effect of polycation and polyanion layers deposited on the microparticle surface on dissolution of microparticles is similar to that in obtained without  $Zn^{2+}$  ions.

Therefore, the dissolution properties of insulin microparticles can be controlled by alternating polyelectrolyte layers on microparticles' surface. If coating pH and dissolution pH are on the same side of the isoelectric point (e.g., test pH 7.4 and coating pH 7.0 for insulin with pI 5.9), a polymer with opposite charge (a polycation above isoelectric point and a polyanion below it) decreases dissolution of the microparticles due to formation of electrostatically bound inter-polyelectrolyte complex between these macromolecules. The second polyelectrolyte layer competes with insulin for the previously adsorbed polyelectrolyte and thus weakens its interaction with the protein. The concept of a diffusion barrier formed by polyelectrolyte multilayers is less applicable for thin coatings consisting of 3-4 polyelectrolyte layers.

### 3.3.7 Effect of Polyion Concentration on Release of Insulin from Microparticles

It has been shown that surface properties of microparticles can be changed by varying polyelectrolyte concentration in coating solutions. The influence of concentration on microparticle dissolution is shown in Figure 3.10.

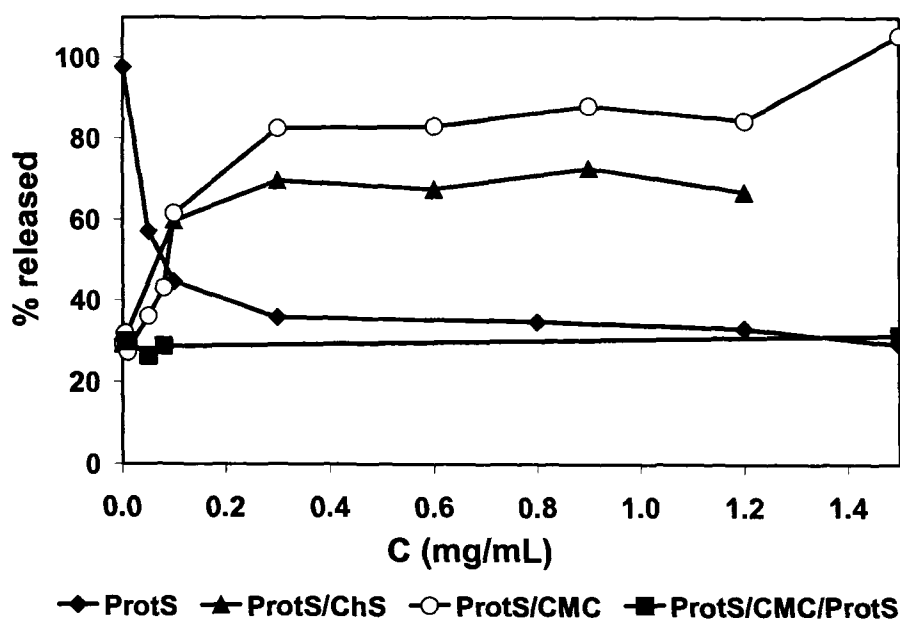


Figure 3.10. Concentration dependence of outermost polyelectrolyte layer on insulin release *in vitro* after 48 hours from insulin microparticles coated with different polyelectrolyte concentrations in 16 % PEG-0.7 % NaCl pH 7.0.

For a single ProtS layer, the dissolution level reaches a plateau at around 0.3 mg/mL. The relationship between dissolution and concentration parallels the relationship between  $\zeta$ -potential and concentration in Figure 3.5. As soon as the polyelectrolyte concentration is enough for complete charge reversal of microparticles' surface, the dissolution of the microparticles reaches a saturation level and depends only slightly on

further increase in concentration. A similar situation is observed for the second layer. For CMC or ChS at a concentration lower than 0.3 mg/mL, percent release is proportional to the amount of polyelectrolyte in the supernatant and almost reaches a maximum at 0.5 mg/mL. The deposition of the third layer, ProtS from a 1.5 mg/mL solution, brings the degree of dissolution back to a minimum. Varying supernatant concentrations during adsorption process helps to control insulin release from the microparticles.

The yield of the final product relative to the initial amount of protein used is an important parameter in developing sustained release drug formulations. The total insulin amount in the samples decreases with addition of new polyelectrolyte layers due to the losses during coating. Most of the losses occur when the samples are coated with a polyanion layer. Therefore, to avoid the waste of insulin from PROMAXX<sup>®</sup> microparticles, the conditions favoring low dissolution must be employed during LbL assembly. At pH 7.0, elevated polycation concentrations and lower polyanion concentrations are optimal.

### **3.4 Conclusions**

Nanoorganized encapsulation of protein microcores in the presence of high concentration of neutral polymers (PEG) was elaborated with LbL assembly. Uncoated insulin PROMAXX<sup>®</sup> microparticles formed by controlled phase separation from hydrophilic compounds dissolve rapidly if PEG concentration is decreased. LbL encapsulation extended insulin release time from PROMAX<sup>®</sup>. After the first layer of oppositely charged polymer is formed over the insulin core, the microparticle is stabilized and new polyelectrolyte layers can be added. Balancing strong interaction of the first polyelectrolyte layer with the protein microcore, and easing this interaction by depositing

the second oppositely charge polyelectrolyte (polyanion/polycation for positive cores at pH 5.8, and polycation/polyanion for negative cores at pH 7.0) allowed us to control complexation of the encapsulated proteins and to achieve a sustained release of insulin. The release profile was fine tuned by adding the third and fourth polyelectrolyte layer.

Therefore, the general idea of the controllable complex formation is as follows: adsorption of the first polyelectrolyte layer results in strong complex formation and slow-release. An addition of the second, oppositely charged polyelectrolyte layer, results in relaxed complex and quicker release. The third oppositely charged layer again gives slower release, and so on. Simple increase in thickness of the capsule walls in the range of 5-10 bilayers (30-60 nm) does not slow insulin release from the microparticles. With this, we converted the concept formulated in a Max Planck Institute's research group [48, 72, 73, 75, 76] where a LbL multilayer was considered as a tight diffusion barrier with adjustable thickness in the range of 5-12 bilayers, to the new approach where the main role in the controlled release from protein micro aggregates is the adjustable interpolyelectrolyte complex formation controlled by alternate polycation / polyanion coating of 2-3 monolayers.

In this chapter it was shown that a polyelectrolyte-complex on the outermost protein layer of the drug microparticle controls of release properties of the drug. In the next chapter we will see an alternate method for control of diffusion of small hydrophilic molecules from hollow polyelectrolyte microcapsules.

## CHAPTER 4

### LAYER-BY-LAYER ASSEMBLY USING PHOSPHOLIPIDS AS A DIFFUSION BARRIER

#### 4.1 Introduction

Conventional liposomal drug delivery is a well established method for *in vivo* delivery of pharmaceutical compounds with focus on injectable delivery forms. However, choice of materials for liposomal shells is limited. One way to create precise control with liposomal delivery methods would be to use phospholipids with the LbL technique to blend the biocompatibility of liposomal delivery with the versatility of LbL technique for making thin films and hollow shells. LbL assembly of amphiphilic molecules and polyelectrolytes can yield biomimetic systems for various applications[48, 88, 89]. The assembly of lipid bilayer membranes alternated with polyelectrolytes has been demonstrated on solid supports [3, 90, 91]. The polyelectrolyte/lipid architecture formed as microcapsules can have some advantages over liposomes due to better structural support and control over size of microcapsules [3, 91].

A lipid membrane onto solid or polymer-precoated templates can be created by direct vesicle fusion [3, 92-95] and the Langmuir-Blodgett technique [90, 92-96]. In both cases electrostatic forces play an important role in film formation. By vesicles (liposome)

adsorption, a uniform lipid bilayer forms rapidly, within 5 min after addition of solution to substrate, and covers more than 95% of the surface [92-96]. The almost perfect bilayer coverage was shown on negatively charged silica for neutral zwitterionic lipids and their mixtures with low concentration of negatively charged lipids. A uniform bilayer was also shown for lipid on mica and polyethylenimine-supported surfaces [92-96]. In some cases adsorption of more than one lipid bilayer on polycation coated surfaces was deduced from the thickness of the obtained films [3, 91].

Here, we report results of direct coating of polyelectrolyte microcapsules with lipid layers of different composition, and the first quantification of its influence on capsule permeability using the fluorescence recovery after photobleaching (FRAP) technique. The polyelectrolyte/lipid microcapsules, with controllable permeability, is of interest for drug delivery applications.

## **4.2 Experimental**

### **4.2.1 Materials**

The lipids— 1,2-dipalmitoyl-*sn*-glycero-3-phosphatidylcholine (DPPC), 1,2-dipalmitoyl-*sn*-glycero-3-phosphate (DPPA), L- $\alpha$ -phosphatidylglycerol (PG), L- $\alpha$ -phosphatidylcholine (PC) were purchased from Avanti Polar Lipids, polyethyleneimine (PEI MW 30,000), polyallylamine hydrochloride (PAH, MW 70,000), poly(dimethyl diallylamide hydrochloride) (PDDA, MW 100-200,000), polystyrenesulfonate (PSS MW 70,000), fluorescein isothiocyanate(FITC) labeled Dextran (FD, MW 4000) and chloroform were purchased from Sigma and chitosan was obtained from Wako Fine Chemicals Japan. Polymethacrylate (PMA, 3 $\mu$ m) were obtained from Fluka, manganese



carbonate microparticles were synthesized in the lab with the procedure elaborated by Shchukin et al. [77].

#### **4.2.2 Preparation of Unilamellar Liposomes**

Unilamellar vesicles of DPPC containing 5, 10, 17, 20 % (w/w) of DPPA and those of PC with 10, 20% (w/w) of PG were prepared by mixing the reagents in chloroform followed by solvent evaporation. The lipid cake was hydrated using Deionized (DI) water to obtain a concentration of 1 mg/mL solution of liposomes in DI water, and the mixture was subjected to ultrasonication, followed by extruding the liposomes using a 0.2  $\mu\text{m}$  nylon filter to obtain unilamellar liposomes.

#### **4.2.3 Preparation of Polyelectrolyte Solutions**

PEI, PAH, PDDA, and PSS were prepared as a 2 mg/mL solution in DI water at pH 6.5 and used without further purification. Chitosan is sparingly soluble at normal pH, so it was dissolved in 0.1 N HCl, and the pH of the solution was adjusted to pH 6.5 with concentrated NaOH prior to use.

#### **4.2.4 Assembly on Quartz Crystal Microbalance**

Negatively charged lipid layers were deposited from 1 mg/mL suspensions in alternation with PEI, PAH, PDDA, and chitosan on silver QCM resonators [46]. The resonators were coated with three PAH/PSS bilayers as precursor layers. Frequency change of the resonators was measured only after deposition of polyelectrolyte layers to prevent rearrangement of lipid bilayers due to drying.

#### **4.2.5 LbL Assembly on PMA Microparticles for $\zeta$ -Potential Studies**

For each set of polymers 10  $\mu$ l PMA microparticles were taken in a microcentrifuge tube and 1 mL of 2 mg/mL polyelectrolyte or 1 mg/mL of phospholipid solution was added and the particles were allowed to stand for 15 minutes to complete the adsorption step. Following the adsorption step, the microparticles were centrifuged at 4000 rpm for 10 minutes and the supernatant discarded to remove excess of material in solution. The pellet was resuspended in 2 mL DI water and the procedure repeated three times in all to remove excess polyelectrolyte/ lipid in the solution phase. After, rinsing the particles three times, surface charge ( $\zeta$ -potential) measurements were taken to check for alternation of surface charge.

#### **4.2.6 Phospholipid Coatings on Hollow PAH/PSS Microcapsules and Measurement of Diffusion Coefficient of the Capsule Wall**

For capsule preparation, 0.2 mL of 3 mg/mL PAH and PSS solutions in 0.5 M NaCl at pH 6.5 was added alternately to 15 mL of a suspension containing 25 mg of  $\text{MnCO}_3$  cores with a mean diameter of  $5.5 \pm 0.3$  nm (SEM microscopy). After 15 min adsorption of each layer, the particles were rinsed with deionized water three times. The cores were dissolved with 0.1 M HCl. The traces of  $\text{Mn}^{2+}$  were removed by washing with a 0.1 M ethylenediaminetetraacetic acid solution and deionized water. The empty capsules, after dissolution of the inner cores, can be slightly swollen or shrunken depending on the media they are in and the presence of other substances.

The operation sequence proposed by Moya et al. [3, 91] was employed to coat capsules with a lipid bilayer for FRAP experiments. The hollow (PSS/PAH)<sub>5</sub> capsules with an outermost PAH layer were suspended in a 10 μM solution of FITC-dextran of MW 4300 for 2 h to enable uniform distribution of the dyed polymer throughout the interior of the capsules and surrounding solution. This step was followed by the addition of lipid vesicles to form the outermost layer on the polyelectrolyte capsules. The capsules were then rinsed with FITC-dextran solution in order to remove any unabsorbed liposomes from the mixture. The final sample for FRAP experiments was a suspension of capsules coated with a lipid layer in a solution of FITC-dextran. Single capsules were isolated under a Leica confocal laser scanning microscope, photobleached, and the fluorescence recovery after photobleaching was monitored [97].

The diffusion in the individual capsules was studied by using a molecular diffusion model based on fluorescence recovery developed by Axelrod and co-workers [68, 69] as described in Chapter 2.

### **4.3 Results and Discussion**

#### **4.3.1 Quartz Crystal Microbalance Study of Lipid- Polyelectrolyte Multilayers**

Table 4.1 summarizes the results of polyelectrolyte-lipid LbL coatings on QCM resonators. The total thickness of the assembled films was less than 50 nm, indicating that the Sauerbrey Equation is valid [98].

Available data [3, 90-96], indicate that the prepared films consist of lipid bilayers sandwiched between two polycation layers. Deposition of multiple bilayers of a surfactant alternated with polyvinyl sulfate by the LbL method was previously reported

[90]. The mean thicknesses for three consecutive (lipid bilayer / polyelectrolyte) layers for different compositions are shown in Table 4.1. The thickness of a lipid bilayer/polycation layer is in the range of 2-7 nm.

In most cases, assembly is stable when the concentration of a charged lipid in the mixtures is 20%. The obtained (lipid bilayer/polyelectrolyte) bilayer thickness is in good agreement with the reported values for DPPC bilayer[3, 91-96, 99, 100]. The total thickness of a DPPC bilayer is 4.6 - 5.0 nm (including a 3.4 - 3.7 nm hydrophobic layer) in gel state and 3.7 – 4.5 nm (2.6-3.0 nm for hydrophobic layer) in fluid state.

Table 4.1. Thickness of lipid/polyelectrolyte bilayers.

| <b>Bilayer composition<sup>a</sup></b> | <b>Freq. shift<sup>b</sup>/<br/>Hz</b> | <b>Thickness<sup>c</sup>/<br/>nm</b> |
|--|--|--------------------------------------|
| DPPA-DPPC 5%(w/w)/PEI                  | 166 ± 51                               | 2.65 ± 0.82                          |
| DPPA-DPPC 10%(w/w)/PEI                 | 133 ± 47                               | 2.12 ± 0.75                          |
| DPPA-DPPC 17%(w/w)/PEI                 | 409 ± 23                               | 6.54 ± 0.37                          |
| DPPA-DPPC 20%(w/w)/PEI                 | 284 ± 27                               | 4.55 ± 0.43                          |
| DPPA-DPPC 5%(w/w)/PAH                  | 366 ± 39                               | 5.86 ± 0.62                          |
| DPPA-DPPC 10%(w/w)/PAH                 | 190 ± 40                               | 3.05 ± 0.64                          |
| DPPA-DPPC 17%(w/w)/PAH                 | 199 ± 39                               | 3.18 ± 0.62                          |
| DPPA-DPPC 20%(w/w)/PAH                 | 161 ± 18                               | 2.58 ± 0.29                          |
| DPPA-DPPC 5%(w/w)/PDDA                 | 111 ± 10                               | 1.78 ± 0.16                          |
| DPPA-DPPC 10%(w/w)/PDDA                | 491 ± 10                               | 7.85 ± 1.62                          |
| DPPA-DPPC 17%(w/w)/PDDA                | 327 ± 10                               | 5.23 ± 1.60                          |
| DPPA-DPPC 20%(w/w)/PDDA                | 273 ± 42                               | 4.37 ± 0.67                          |
| PG-PC 10%(w/w)/Chitosan                | 339 ± 65                               | 5.42 ± 1.05                          |
| PG-PC 20%(w/w)/Chitosan                | 307 ± 25                               | 4.91 ± 0.38                          |

<sup>a</sup> The percentages indicate total weight percent of charged lipid components in a mixture.  
<sup>b</sup> The average of two independent experiments.  
<sup>c</sup> The frequency shift of the QCM resonators was converted into thickness using the experimental equation  $\Delta d \text{ (nm)} = -0.016 \Delta F \text{ (Hz)}$ .

Admixture of another lipid (surfactant, hydrocarbon etc.) into a lipid bilayer can dramatically change mean transition temperature of the mixture [101, 102], and therefore,

influence lipid bilayer thickness. In addition, oppositely charged substances can be incorporated between lipid heads into hydrophilic layers slightly increasing their thickness and decreasing hydrophobic thickness, the effect more pronounced for the mixtures with charged lipids [103]. However, in the case of the mixtures with low concentration of charged lipid (5-10% w/w DPPA), formation of incomplete lipid bilayer (or polyelectrolyte layer on the top of lipid bilayer) because of absence of electrostatic charge is possible. In the case of strong polycation PDDA, the formation of thicker layers can be explained by deposition of more than one DPPC-DPPS bilayer on the top of the polycation layer to compensate its high positive charge.

The assembly of PG-PC vesicles in alternation with cationic chitosan shows a bilayer thickness of ~5 nm. The last architecture is of considerable importance since chitosan is a non-toxic, natural, biocompatible polymer with antimicrobial properties, which makes this architecture suitable for *in vivo* applications [104].

#### **4.3.2 Analysis of $\zeta$ -Potential Measurements**

For microparticles and microcapsule coatings we chose conditions giving a stable assembly and providing a 4-5 nm thick bilayer, which is consistent with the length of two lipid molecules [3, 90-96, 99, 105]. The lipid mixtures with 20% w/w charged lipid were used hereafter. Lipid layers in alternation with polyelectrolytes were assembled on 3  $\mu\text{m}$  polymethacrylate microspheres (PMA) precoated with two PAH/PSS bilayers, and changes in surface charge ( $\zeta$ -potential) of the microparticles were measured after each adsorption step. The detailed procedure can be found elsewhere [106]. The latex particles were used in this series of experiments to avoid interference of lipids with multivalent ions, which can precipitate lipids [107]. The  $\zeta$ -potential values (Figure 4.1) show

complete charge reversal with synthetic polyelectrolytes such as PDDA, PEI, and PAH, and the assembly with PAH shows most consistent alternation of surface charge. For assembly of chitosan and PG-PC, a shift in the magnitude of the positive charge was found, but not complete charge reversal, probably because of perturbation of lipid bilayers by chitosan [108].

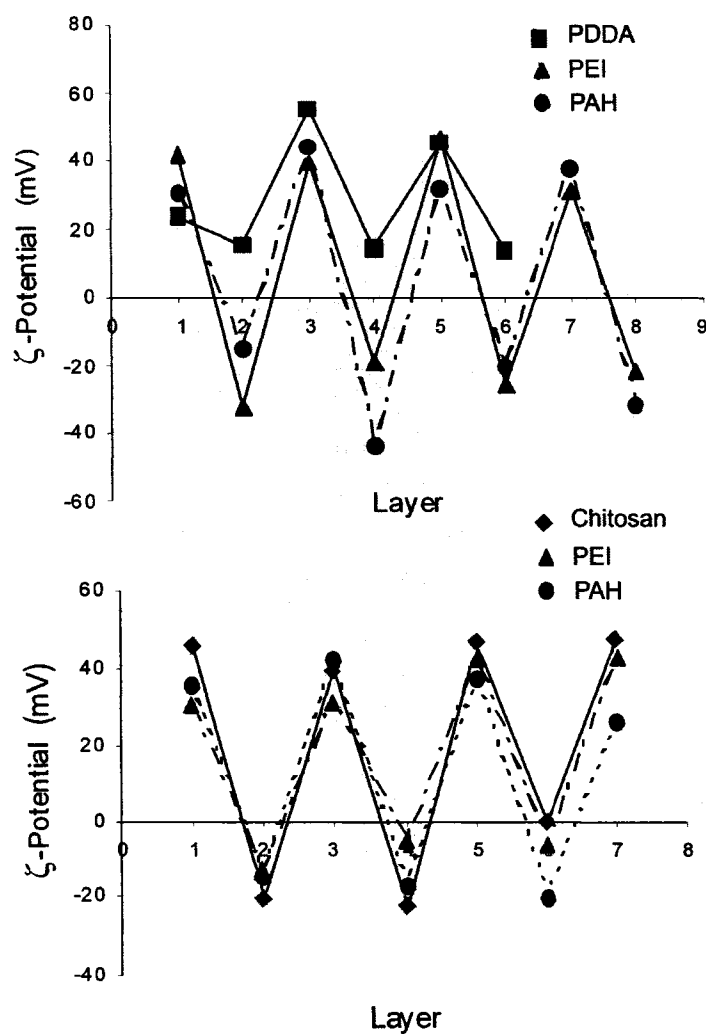


Figure 4.1.  $\zeta$ -Potential analysis of polyelectrolyte/lipid assemblies on PMA/(PAH/PSS)<sub>2</sub> microparticles, the first layer corresponding to respective polycation (Top): lipid – DPPA-DPPC 20% w/w with polyelectrolytes. (Bottom): lipid – PG-PC 20% w/w with polyelectrolytes.

### **4.3.3 Diffusion Properties of Lipid Coated Hollow Polyelectrolyte Microcapsules**

The possibility of capsule coating with lipid bilayers was confirmed by deposition of a DPPC–17% w/w DPPA mixture with 3% admixture of 1,2-dioleoyl-sn-glycero-3-phosphoethanolamine-N-(carboxyfluorescein) on the top of the hollow capsules (Figure 4.2).

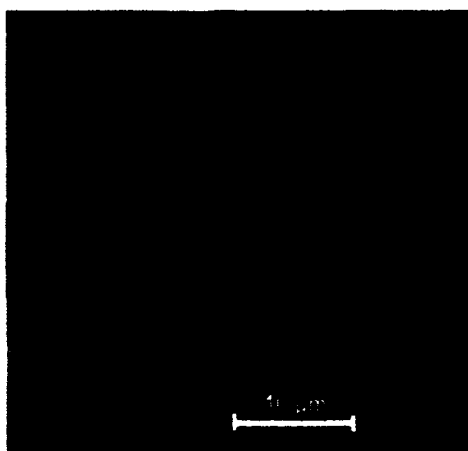


Figure 4.2. Lipid coating on (PAH/PSS)<sub>5</sub> to show lipid coating on microcapsules.

The FRAP model used to study the fluorescence recovery is described in Section 2.6.3 where the two-dimensional model discussed has been used in these experiments. Although, a three-dimensional model is recommended for volume diffusion, for diffusion through a thin membrane, such as the microcapsule wall in our experiments a two-dimensional model is a reasonable and sufficient. In the FRAP model under investigation, the diffusion of FITC-Dextran from the bulk to the interior of the capsule causes an increase in fluorescence intensity in the capsule interior. The fluorescence intensity is normalized over a given area in the interior of the capsule designated as region of interest (ROI in Figure 2.10). The fluorescence recovery after photobleaching is in the interior of

the hollow (PAH/PSS)<sub>5</sub> capsules with and without lipid coating is presented in Figure 4.3.

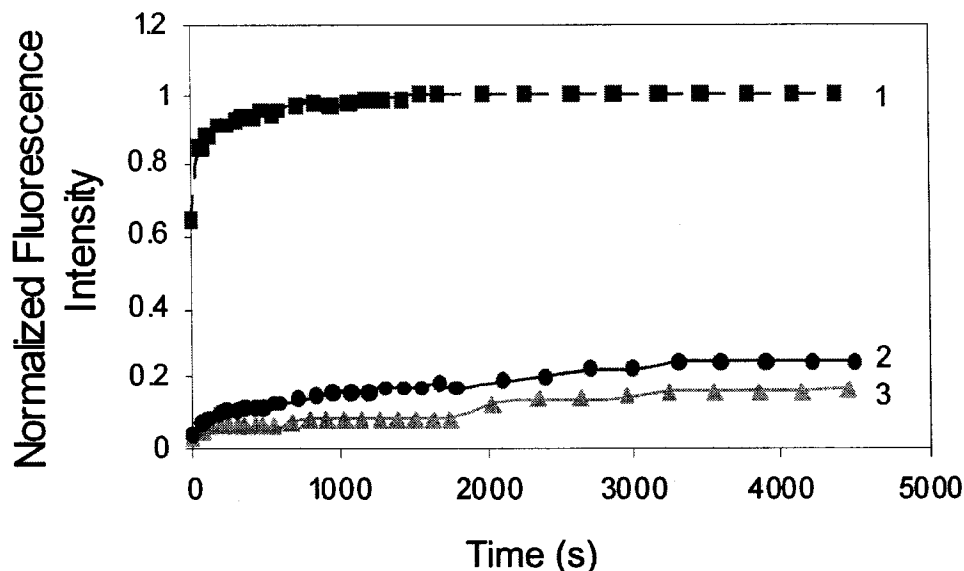


Figure 4.3. Fluorescence recovery of (PSS/PAH)<sub>5</sub> capsules coated with different lipid mixtures: (1) uncoated, (2) PG-PC 20% coated, (3) DPPA-DPPC 20% coated. The intensities of capsule interior are shown relatively that of surrounding solution.

As anticipated, the results indicate slower fluorescence recovery for lipid coated capsules than for uncoated ones (Figure 4.3). Images in the process of photobleaching are presented in Figure 4.4, where (Figure 4.4 A) represents the control which is uncoated (PAH/PSS)<sub>5</sub> capsule, where progressively the fluorescence intensity in the interior of the capsule increases over a period of 16 minutes. However in the lipid-coated capsules (Figure 4.4 A and B) there is no increase in fluorescence intensity even after 75 minutes.



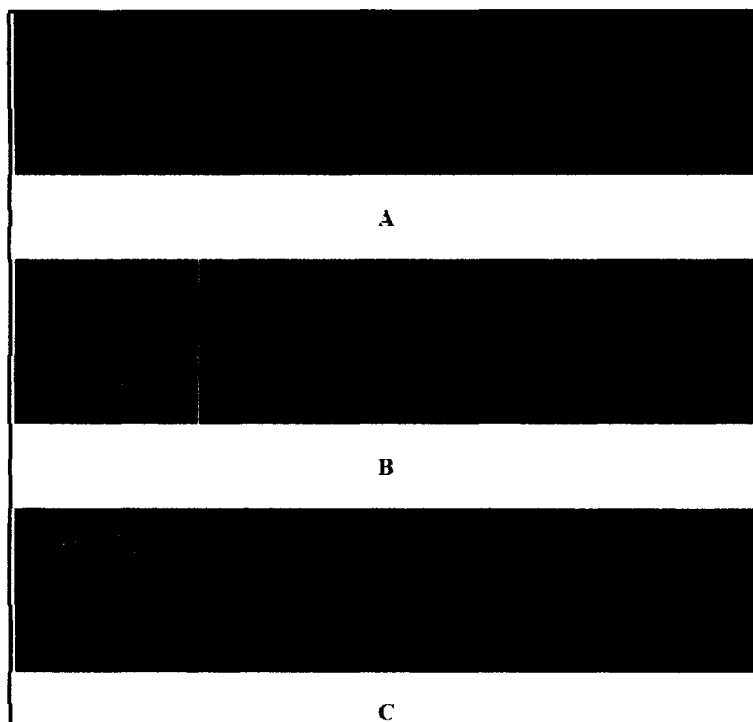


Figure 4.4. Fluorescence recovery after photobleaching for different capsules in a 10  $\mu\text{M}$  solution of FITC-dextran of MW 4300: a) an uncoated (PSS/PAH)<sub>5</sub> capsule, b) a capsule coated with one bilayer of PG-PC (20 % w/w) and c) a capsule coated with one bilayer of DPPA- DPPC (20% w/w).

The diffusion properties are a representation of about 70% of the population. FITC fluorescence recovery in lipid-coated capsules was slower than that in uncoated ones indicating that the deposited lipid bilayer reduced the diffusion coefficient through the polyelectrolyte walls drastically for low molecular substances. The diffusion coefficient of FITC-dextran of MW 4300 into polyelectrolyte microcapsules was evaluated on the basis of a fluorescence recovery model proposed by Axelrod and co-workers [68]. For uncoated (PSS/PAH)<sub>5</sub> capsules, the coefficient is  $(7.1 \pm 2.1) \times 10^{-12} \text{ cm}^2/\text{s}$ . For lipid coated capsules it is  $(1.4 \pm 0.3) \times 10^{-13} \text{ cm}^2/\text{s}$  (DPPA/DPPC-coated), and  $(1.5 \pm 0.4) \times 10^{-13} \text{ cm}^2/\text{s}$  (PG-PC-coated). These results indicate nearly two orders of

magnitude difference in the diffusion coefficient for FITC-dextran of MW 4300 between lipid-coated and uncoated microcapsules.

The diffusion coefficients for FITC-dextran with a MW 4300 estimated from this study into uncoated and lipid coated capsules are higher than those compared with previously reported data [2, 3, 97]. It is possible that the different core type used for capsule preparation in this study is the cause of the higher diffusion coefficient. Previous studies on lipid-modified capsules were based on melamine formaldehyde microparticles and blood cells as soluble cores; however, recent evidence indicates incomplete dissolution of such cores, which could lead to residue in the capsules and polyelectrolyte capsule swelling [109]. Various diffusion models used for evaluation of diffusion coefficients can also introduce variability into results.

#### **4.4 Conclusions**

In summary, the multilayer architecture of lipid/polyelectrolyte capsules has been reported. The lipid coating introduced directly on polyelectrolyte microcapsule surface significantly reduces the permeability of the capsule walls. The size, wall composition, and diffusion properties of the microcapsules are closer to biological cell wall structure than many other model systems. These lipid/polyelectrolyte microcapsules can be a further development of traditional liposome delivery system technologies.

In the previous two chapters we have discussed the use of LbL assembly for diffusion control properties that can be applied to delivery of hydrophilic drugs. In the next chapter we will demonstrate an alternate method for delivery of hydrophobic drugs, through entrapment of phospholipids in mineral  $\text{CaCO}_3$  microparticles

**CHAPTER 5**

**COMPOSITE PHOSPHOLIPID - CALCIUM  
CARBONATE MICROPARTICLES:  
CO-ENTRAPMENT OF ANIONIC  
PHOSPHOLIPIDS AND  
HYDROPHOBIC  
MOLECULES**

**5.1 Introduction**

Calcium is the most abundant mineral in the human body. It is a component of bones and teeth and is also required for blood clotting, transmission of signals in nerve cells, and muscle contraction. The importance of calcium for preventing osteoporosis is probably its most well-known role. Most calcium supplements contain calcium carbonate, which is also one of the principal components of many biomineralization schemes occurring in nature, primarily involving a hierarchical organization of proteins and calcium salts [110]. The control of crystal morphologies of calcium carbonate is important for biomineralization reactions. The effect of various organic additives and template mediated reactions on calcium carbonate crystal morphologies has been studied [111-117]. Biomineralization in phosphatidylcholine vesicles by a diffusion-mediated process has been reported as a model system for biomineralization [111, 118].

Most of the research has been centered on elucidating particle formation and understanding the kinetics and mechanisms of crystallization [119-124]. Recently, Sukhrukov et al. [53] showed that porous calcium carbonate microparticles can be synthesized by directly mixing  $\text{Ca}^{2+}$  and  $\text{CO}_3^{2-}$  salts, which can be used as a template for polyelectrolyte LbL assembly. Here we report the synthesis of calcium carbonate microparticles of a highly porous nature, having phospholipid molecules entrapped in the porous structure, resulting in an organic/inorganic complex matrix. The microparticles can be used to load hydrophobic molecules in an inorganic core with potential applications in medicine and industry. The calcium carbonate microparticles synthesized in this work also show a prospect for air based nasal drug delivery systems. A surface-mediated reaction for the preparation of the mesoporous calcium carbonate microparticles is proposed. The resulting microparticles have phospholipids entrapped in the mineral matrix of  $\text{CaCO}_3$  with the hydrophobic material localized in the hydrophobic regions of the phospholipids vesicles (Figure 5.1). Moreover, this scheme can be extended to the entrapment of surface active macromolecules, including proteins, and peptide drugs.

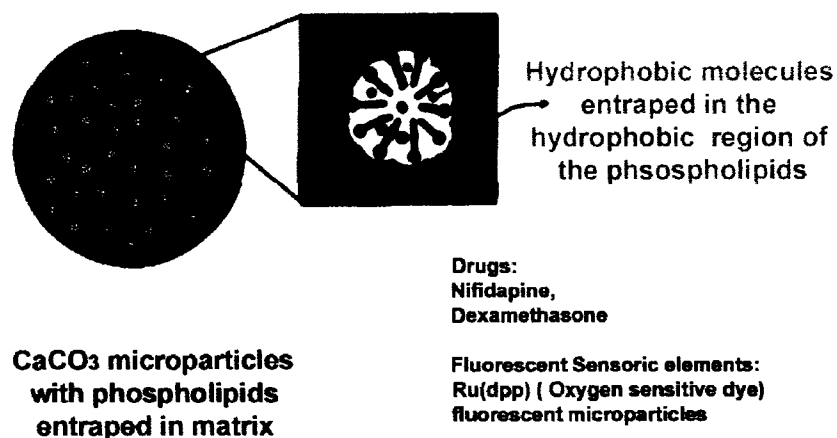


Figure 5.1. Scheme for entrapment of hydrophobic drugs in mineral matrix. The hydrophobic molecules are localized in the hydrophobic tail regions of the phospholipids molecules. The hydrophilic head interacts with the mineral matrix.

These microparticles are amenable to LbL assembly for surface modification to make the surface of the microparticles biocompatible; the particles can also be used as templates for preparing hollow polyelectrolyte microcapsules by various approaches [125]. The presence of phospholipids in the calcium carbonate matrix also facilitates entrapment of small hydrophobic molecules in conjugation with other bioactive molecules.

## 5.2 Experimental

### 5.2.1 Materials.

The lipids— 1,2-dipalmitoyl-*sn*-glycero-3-phosphate (DPPA), 1,2-distearoyl-*sn*-glycero-3[phospho-*rac*-(1-glycerol)](sodium salt) (DSPG), 1,2-dipalmitoyl-*sn*-glycero-3-phosphatidylcholine (DPPC) and 1,2-dioleoyl-*sn*-glycero-3-phosphoethanolamine-*N*-(carboxyfluorescein) (FITC-EA) were purchased from Avanti Polar Lipids. Calcium Chloride (CaCl<sub>2</sub>), and ammonium bicarbonate (NH<sub>4</sub>HCO<sub>3</sub>) were purchased from Sigma

and Fluka respectively. Tris(4,7-diphenyl-1,10-phenanthroline)ruthenium(II) dichloride complex ( $[\text{Ru}(\text{dpp})_3]\text{Cl}_2$ ) was purchased from Fluka.

### **5.2.2 Preparation of Calcium Carbonate Particles Incorporating Phospholipids in the Matrix**

To prepare calcium carbonate microparticles incorporating phospholipids in the matrix, liposomes of DPPA (1,2-dipalmitoyl-sn-glycero-3-phosphate), DSPG (1,2-distearoyl-sn-glycero-3[phospho-rac-(1-glycerol)])(sodium salt), and DPPA 20% (w/w)-DPPC (1, 2- dipalmitoyl -sn-glycero-3-phosphocholine) mixtures were prepared in DI water using standard protocol described in the previous chapter. Two mL of 1 mg/mL phospholipid liposomes were first treated with (0.01 to 0.15 M)  $\text{Ca}^{2+}$  ions ( $\text{CaCl}_2$ ) for 10 minutes with slow stirring to form cochleates [126, 127]. The cochleates were dispersed by sonication followed by immediate addition of 0.375 M  $\text{NH}_4\text{HCO}_3$  with different volume ratios and in large excess of the stoichiometric reaction requirement. After 15 minutes of reaction, the products were centrifuged and rinsed in DI water three times followed by rinsing in a 1:1 methanol:chloroform mixture three times to remove any free ions and phospholipids. The samples were then dried under a stream of nitrogen.

### **5.2.3 Preparation of Calcium Carbonate Microparticles Without Phospholipids in the Matrix**

Pure calcium carbonate microparticles were prepared by mixing equal volumes of  $\text{CaCl}_2$  and  $\text{NH}_4\text{HCO}_3$  in a constant volume reactor, at ambient conditions, with uniform stirring. Following a 15 minute reaction, the reaction products were centrifuged, rinsed in deionized water (DI water), and dried under a stream of dry nitrogen.

#### **5.2.4 Preparation of Calcium Carbonate Microparticles with Hydrophobic Molecule Entrapped in the Matirix**

During the preparation of liposomes, as indicated in Section 5.2.1, the hydrophobic molecule or fluorescent phospholipid is added to the chloroform mixture during cake formation and the liposomes consequently formed incorporate the hydrophobic molecules in their fatty side chains. The rest of the procedure remains the same.

### **5.3 Results and Discussion**

#### **5.3.1 Characterization of Morphology and Microstructure**

To study the morphology and microstructure of the CaCO<sub>3</sub> microparticles, the samples obtained were visualized using Scanning Electron Microscopy (SEM, Gemini, Leo 1550). The crystal structure of the CaCO<sub>3</sub> microparticles synthesized in the presence and absence of anionic phospholipids were also characterized using X-ray diffraction (Philips Cu  $\kappa\alpha$  radiation). In the absence of any additives, the reaction of Ca<sup>2+</sup> and HCO<sup>3-</sup> yields particles with diameters in the range of 10±5  $\mu\text{m}$ . The SEM images in Figure 5.2(a) and the powder X-ray diffraction pattern in Figure 5.3 indicates calcite polymorph as the predominant form

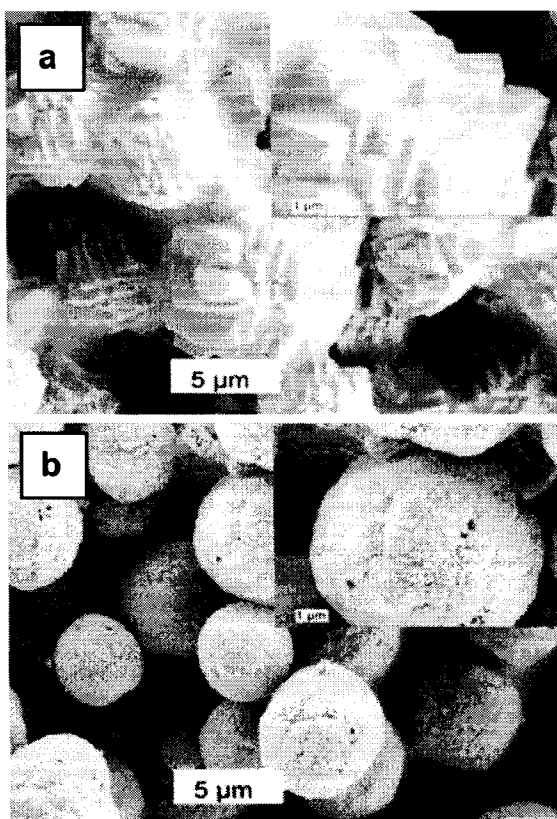


Figure 5.2. Representative SEM images of calcite microcrystals prepared by reaction of 1 mL 0.01 M  $\text{CaCl}_2$  + 1 mL 0.375M  $\text{NH}_4\text{HCO}_3$  + 2 mL of DI water (a). Porous  $\text{CaCO}_3$  microparticles by first reacting 2 mL of 1 mg/mL DPPA + 1 mL 0.01 M  $\text{CaCl}_2$  + (after 10 min) 1 mL of  $\text{NH}_4\text{HCO}_3$  (b), these microparticles contain 3%(w/w) phospholipids in matrix.

The shape of the calcite crystals depends on the rate of mixing of lipids during reaction. No-stirring results in wide size distributions of particles with fewer crystal faces, whereas vigorous stirring yields narrower size distributions with multifaceted particles (Figure 5.2(a)). Under identical conditions used for preparation of calcite microparticles described above, the presence of phospholipids in the reaction-mixture results in particles that are porous in nature and have no crystalline edges Figure 5.2(b). The size distributions of these microparticles are in a range of  $5 \pm 2 \mu\text{m}$ .



The powder X-ray diffraction pattern of calcium carbonate microparticles synthesized in the presence and absence of DPPA was used to determine the polymorphs present in the synthesized mixture. The X-ray diffraction patterns indicate that in the absence of phospholipids the resulting calcium carbonate microparticles are predominantly calcite (Figure 5.3 (top)). In the presence of DPPA the resulting microparticles are predominantly vaterite polymorph (Figure 5.3). It is well known that the vaterite polymorph is thermodynamically less stable than calcite. The occurrence of less stable vaterite polymorph in the presence of DPPA, strongly suggests to the involvement of phospholipids surface in altering the nucleation and crystallization of  $\text{CaCO}_3$ . However, traces of calcite peaks are also seen (less than 2% by volume), which can be attributed to the phase transformation of the microparticles or some nucleation occurring in aqueous phase as opposed to phospholipid surface.

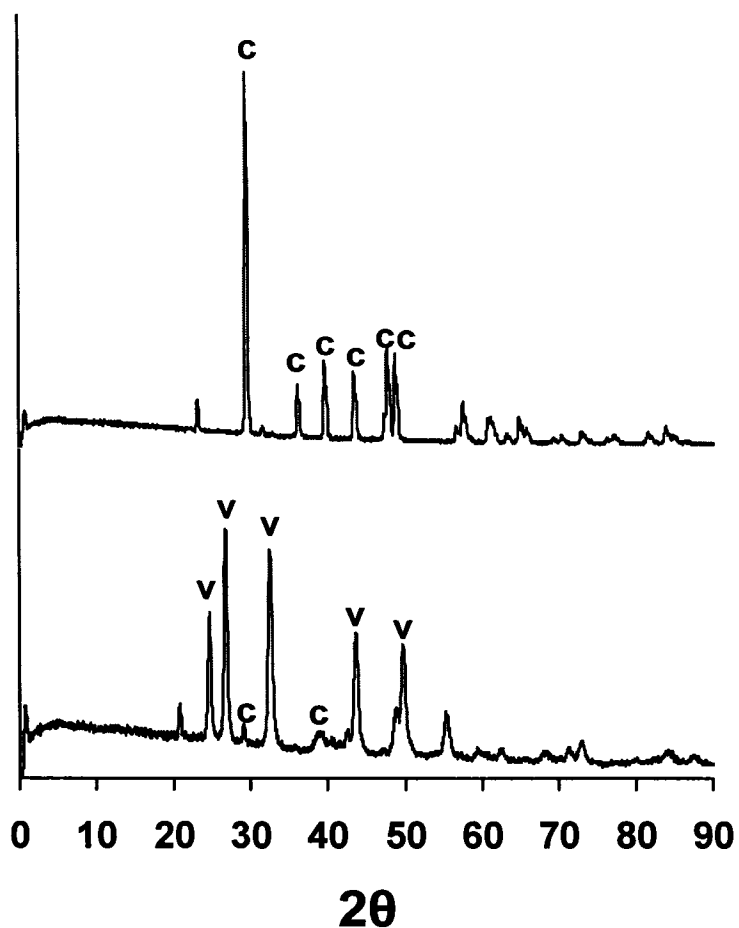


Figure 5.3. X-ray diffraction pattern of calcium carbonate microparticles. The top graph shows the X-ray diffraction pattern of calcite with the principal peaks highlighted [117]. The bottom graph shows the X-ray diffraction pattern of calcium carbonate microparticles synthesized in the presence of DPPA (V-vaterite, C-calcite).

### **5.3.2 Effect of Molar Ratio of Reactants**

The size of the particles depends on the initial concentration of reactants. The influence of molar ratio of reactants on the mean size of microparticles gives an insight into this aspect. The weighted mean of the microparticles is plotted as a function of molar ratio of bicarbonate and calcium (Figure 5.4) indicates a nonlinear decrease with increasing concentration.

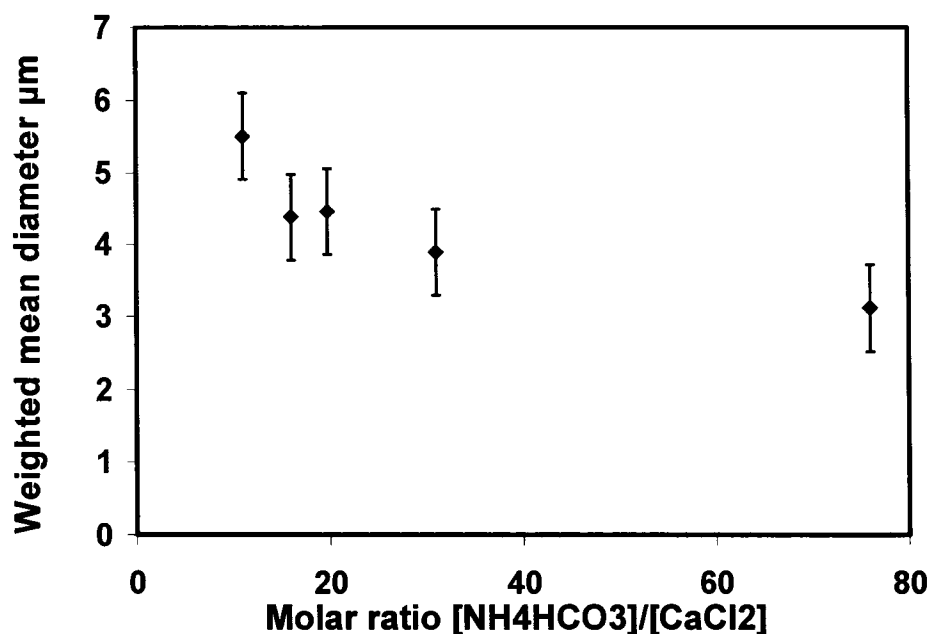


Figure 5.4. Effect of the ratio of  $\text{Ca}^{2+}$  to  $\text{HCO}_3^-$  ions on the size of calcium carbonate microparticles based on 0.375 M concentration of  $\text{NH}_4\text{HCO}_3$  in total volume, with DPPA concentration constant at 0.2 mg/mL.

The mean diameter of the microparticles decreases with decreasing  $\text{CaCl}_2$  concentration. Higher molar ratio of  $\text{CaCl}_2$ , relative to phospholipids, results in a non-homogeneous distribution of phospholipids in the  $\text{CaCO}_3$  matrix that occasionally results in rhombohedral  $\text{CaCO}_3$  calcite in the final product. This observation can also be correlated to the fact that with lower phospholipid concentrations or non-uniform stirring of the reaction mixture, nucleation may begin in the aqueous phase as opposed to on the phospholipid surface and yield a mixture of porous  $\text{CaCO}_3$  microparticles as well as calcite crystals.

The results indicate that a higher concentration of phospholipids to  $\text{Ca}^{2+}$  results in a narrow size distribution of the resulting microparticles. In the presence of excess phospholipids, most of the calcium ions are bound to the phospholipid surfaces, which

results in fewer reaction centers in the media. The nucleation occurs on phospholipid surfaces or begins in solution and propagates on the phospholipid surface resulting in a predominantly phospholipid surface mediated reaction. To verify this hypothesis, 5%(w/w) of 1,2-dioleoyl-sn-glycero-3-phosphoethanolamine-N-(carboxyfluorescein) (FITC-EA) was admixed with DPPA and used to prepare the microparticles. The resulting microparticles were visualized using a confocal laser scanning microscope (CLSM, DMI-RE2). Figure 5.5(a) shows the confocal microscopy image of calcium carbonate microparticles prepared in the presence of phospholipids admixed with FITC-EA, which fluoresces green, and Figure 5.5(b) shows calcium carbonate microparticles entrapped with  $[\text{Ru}(\text{dpp})_3]^{2+}$  which fluoresces red; it will be discussed in Section 5.3.5. The distribution of fluorescence was uniform in the calcium carbonate matrices prepared in the presence of excess phospholipids (Figure 5.5(a)) compared with microparticles prepared in a phospholipid deficient reaction mixture (Figure 5.5(a) (inset)). The images also illustrate that the distribution of phospholipids in the matrix is uniform and lends support to the postulated phospholipid surface mediated reaction of calcium and carbonate ions.

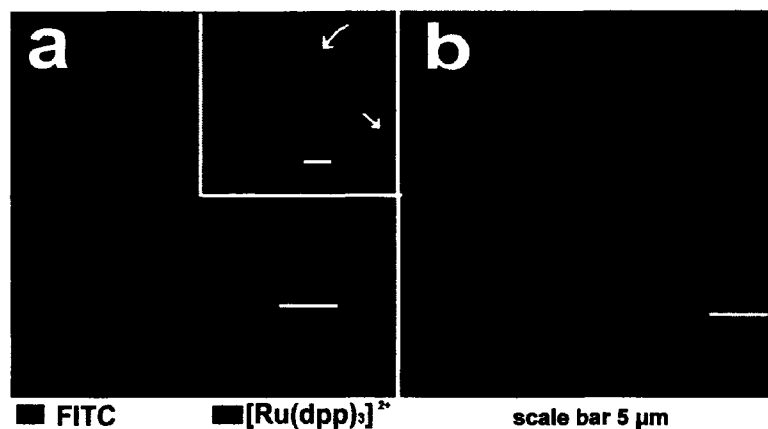


Figure 5.5. CLSM image of cross-section of (a) calcium carbonate microparticles incorporating FITC-EA; in phospholipid deficient medium the non-uniform distribution of phospholipids in the matrix is observed (inset) and (b) prepared by reaction of  $\text{CaCl}_2$  and  $\text{NH}_4\text{HCO}_3$  in the presence of (DPPA 20%(w/w) -DPPC mixture containing  $[\text{Ru}(\text{dpp})_3]^{2+}$  which is a hydrophobic molecule localized in the hydrophobic region of fatty acid side chain.

### **5.3.3 Thermogravimetric Analysis of Calcium Carbonate Microparticles Prepared by Different Methods**

Thermogravimetric analysis of calcium carbonate microparticles was used to determine the temperature at which different volatile species desorb from a sample. Figure 5.6 shows the changes in weight with temperature, the temperature of the sample crucible was increased at the rate of  $5^\circ\text{C}$  per minute. The x-axis shows the changes temperature and the y-axis is the normalized weight of the sample.

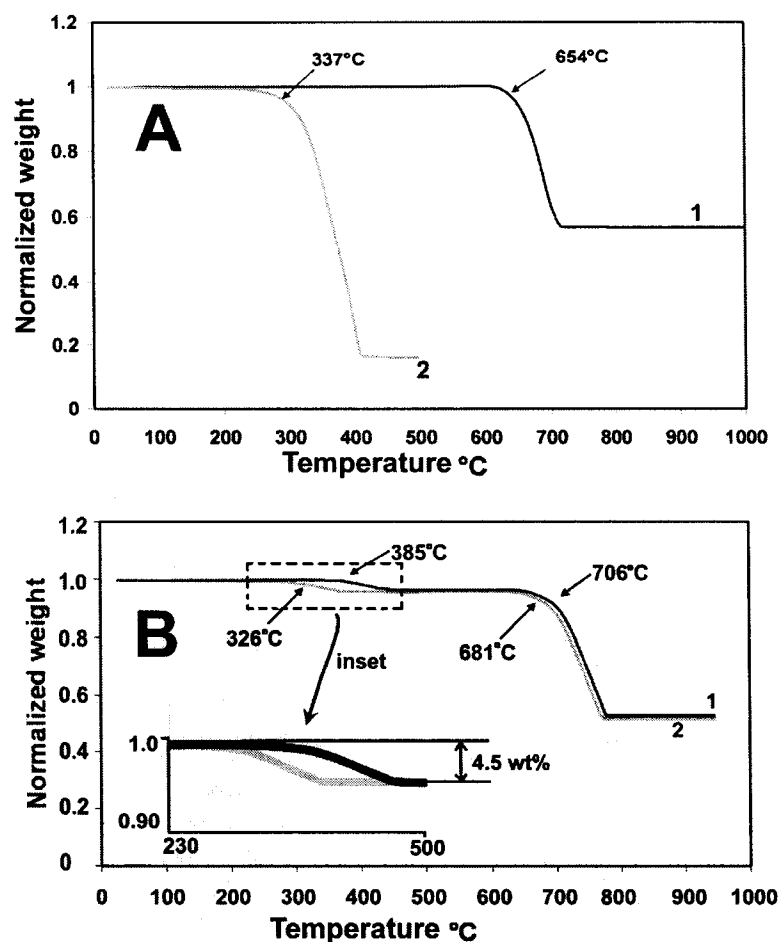


Figure 5.6. Thermogravimetric analysis of (A) calcite and DPPA and (B) calcium carbonate microparticles prepared in the presence of DPPA, the change in weight is shown as percentage total weight (inset) (1) and mixture of calcite and DPPA (2). The temperature was increased at 5°C/minute.

Thermogravimetric analysis of the calcium carbonate microparticles prepared in the presence of DPPA indicated that the DPPA in the calcium carbonate matrix desorbed at higher temperatures ( $385 \pm 6$  °C), compared with either pure DPPA ( $337 \pm 6$  °C) or a physical mixture of phospholipid with calcite microparticles ( $326 \pm 6$  °C) (Figure 5.6). The desorption of carbon dioxide from calcium carbonate also occurs at higher temperature ( $706 \pm 6$  °C) compared with pure calcite ( $654 \pm 6$  °C) or a physical mixture of calcite and

DPPA ( $681 \pm 6$  °C). The higher temperature of desorption can be attributed to a strong calcium carbonate phospholipid interaction. The microparticles contain  $\sim 2.5$ -5 % by wt. of phospholipids in the matrix.  $\text{Ca}^{2+}$  ions interact with anionic phospholipids (phosphatidic acid, phosphatidyl serine) to form a co-ordinate complex such that each  $\text{Ca}^{2+}$  ion demonstrates four, and in some cases six, coordination valencies that bonds with phosphate groups of phospholipids or with other molecules like water [126, 127]. Lamellar amphiphile-calciumhydroxyapatite structures have been extensively studied, which also suggest existence of such calcium ion-phospholipid coordination[65, 66, 128]. The results strongly suggest that this theory could be extended to the carbonated calcium ions in our system. Another contributing factor to the delayed desorption could be the strong Van der Waals and hydrophobic interactions between the phospholipid vesicles and the mesoporous matrix of the calcium carbonate. The negative-charged phospholipid vesicle structure prevents  $\text{HCO}_3^-$  ion penetration into the interior of the vesicle, thus limiting the calcification occurring only on the surface of that structure; this could lead to nanometer sized voids explaining the porous nature of the calcium carbonate microparticles synthesized.

#### **5.3.4 Long-Term Stability of the Calcium Carbonate Microparticles**

The stability of porous calcium carbonate microparticles in DI water was studied using particles incorporating phospholipids (FITC-EA, DPPA, and DPPC mixture) with confocal microscopy (Leica DMI RE2). Over a period of one to three weeks, the veterite microparticles recrystallized to calcite. The first signs of recrystallization were observed after one week of storage in an aqueous solution and progressed for 3-4 weeks, after which nearly 90% of the microparticles had recrystallized and the phospholipids were

excluded from the matrix. However, when the particles are dried after preparation using a methanol:chloroform mixture, the particle morphology remains unchanged over 3-4 months.

### **5.3.5 Incorporation of Hydrophobic Molecules in Calcium Carbonate Matrix to Simulate a Model Drug**

To study the possibility to incorporate hydrophobic molecules, a model fluorophore, tris(4,7-diphenyl-1,10-phenanthroline)ruthenium(II) dichloride complex ( $[\text{Ru}(\text{dpp})_3]\text{Cl}_2$ ), was incorporated in the phospholipid vesicles and the resulting microparticles studied using CLSM (Figure 5.5(b)).  $[\text{Ru}(\text{dpp})_3]^{2+}$  is insoluble in DI water, but readily localizes in the hydrophobic region of the phospholipid bilayer. The distribution of the dye is uniform in the matrix of the calcium carbonate. Figure 5.5(b) shows that the distribution of the hydrophobic molecule  $[\text{Ru}(\text{dpp})_3]^{2+}$  is as uniform as the distribution of the amphiphile itself. This result is important from a pharmaceutical standpoint, since it demonstrates the possibility that these microparticles can be used as carriers for hydrophobic drug molecules. Preliminary trials showed feasibility to entrap the drugs nifedipine and dexamethasone in the calcium carbonate matrix. However further investigation is necessary to draw conclusions.

## **5.4 Conclusion**

Anionic phospholipid (phosphatidic acid, phosphor glycerol) mediated synthesis of calcium carbonate microparticles from  $\text{Ca}^{2+}$  and  $\text{HCO}_3^-$  salts yields a composite organic/inorganic matrix. The inorganic matrix is predominantly the veterite polymorph of calcium carbonate. The microparticles contain ~ 2.5-5 % by wt. of phospholipids in the matrix. The phospholipids show stable entrapment in the calcium carbonate matrix



with strong interactions with the matrix. Such architecture is conducive to the entrapment of small hydrophobic molecules and other bioactive substances in an inorganic matrix.

## CHAPTER 6

### CONCLUSIONS AND FUTURE WORK

#### 6.1 Conclusions

In this dissertation the author has demonstrated that LbL self-assembly can be applied to encapsulate peptide microparticles in the presence of high concentrations of uncharged polymers such as PEG. Two different approaches have been used for entrapment, which rely on the isoelectric point of the peptide. With insulin as a model drug, with an isoelectric point  $\sim 5.9$ , formulations were prepared at pH 5.8 and at neutral pH 7.0. Both pH values are relevant for pharmaceutical formulations, which are typically prepared in the range of pH 4.0 to 8.0. Human insulin is unstable in acidic pH because of deamidation of the Asparagine (Asn) residue located at A21, leading to long term storage instability. However, acidic pH insulin formulations dissociate at a faster rate compared with neutral pH formulations. At pH 5.8 the insulin microparticles behave like a positive core and LbL assembly was achieved using a polyanion as the first layer. The LbL thin films form complex with the outermost layer of insulin molecules, imparting some degree of structural integrity to the microparticle in storage. Available literature [8] strongly suggests that the structural integrity prevents the release of insulin in storage at pH 5.8, thus limiting the adverse effects of dilution of insulin. The adverse effects which could

induce loss of therapeutic value of insulin include— polymerization, chemical modification, adsorption to storage vessel wall, fibril growth and crystallization. At pH 7.0 PROMAXX<sup>®</sup> insulin microparticles behave as a negative core and the LbL assembly was performed using a polycation as the first layer. It was observed that differential number of layers enables differential control of drug. This effect was most pronounced in ProtS/CMC combination. This is interesting from the point that the adsorbed layers are nanometers thick and the influence of a single outermost layer can be significant. However, there is significant penetration of polyelectrolyte inside the insulin core, thus forming stable complex in storage. This complex formation imparts similar benefits as stated above for pH 5.8.

The study involving complex formation established the amount of polyelectrolyte required for complete complex formation. This information is useful for process scaleup and can be efficiently employed on a larger scale to avoid the rinsing steps that were performed in the experiments described in this work. The absence of rinsing would consequently lead to a reduction in the amount of materials used, providing significant cost benefits. Further, this information alone can be used to create formulations with release properties entirely regulated by the amount of polyelectrolyte added. The experimental results relating different polyelectrolytes and corresponding release kinetics can be used as a library for polyelectrolyte-insulin complex reversibility, thus aiding better material selection in the future. Such a library also provides information for better understanding insulin-polyelectrolyte complexes and designing a mathematical model for a specific material, which in turn would lead to the development of an *in vivo* model. The work presented in Chapter 3 leads us to a general idea which applies to all LbL

assemblies on protein cores, in that when a negatively charged protein interacts alternatively with a cationic and anionic polyelectrolyte, the relative affinity of the inter-polyelectrolyte interaction may dictate the overall strength of protein-polyelectrolyte(s) complex. Converse is true for a positively charged protein core.

The insulin coating with LbL was performed mostly with the use of biologically derived polyelectrolytes, with occasional use of synthetic polyelectrolytes to relate with existing knowledge on LbL. Consequently, the experiments were designed to identify the polyelectrolytes which yielded the desired results, and investigate them further. It was demonstrated that different polyelectrolytes can be used as the outermost coating, thus imparting desired surface charge at any pH value. This work also suggests that the use of pegylated polyelectrolytes as the outermost layer of the LbL assembly on insulin microparticles results in a PEG-terminated outer coating, which has been known to be completely biocompatible.

The use of phospholipids in LbL assembly was treated as a separate chapter, because establishing proof of concept was essential prior to use in drug formulation. Phospholipids were used because they are inherently biocompatible in nature and are used in existing drug formulations. However, the work presented in this dissertation established the right concentration of charged anionic and zwitterionic lipids for use in LbL. Further, as an extension of work by Moya et al.[3], who demonstrated the feasibility to make a single lipid bilayer structure, this work presents the prospect of using multilayer lipid-polyelectrolyte constructs. Differing from earlier works, which enable the coating of solid colloidal particles, this work establishes the coating on hollow polyelectrolyte multilayer capsules. Moreover, the author has provided the first of its kind

comparison of diffusion properties of hollow polyelectrolyte capsules and lipid coated polyelectrolyte capsules. Conventional LbL assembly does not use phospholipids as a component of the thin films, and relies primarily on the number of layers of polyelectrolyte to regulate the diffusion of substances from microcapsules. Increasing number of layers incurs a great deal of time and materials cost. The use of phospholipids could significantly reduce these, and the work presented in this dissertation is a significant achievement in terms of establishing the usefulness of lipid polyelectrolyte multilayers. The choice of FITC-Dextran MW4300 is guided by its molecular weight, which is close to the molecular weight of insulin. The use of a diffusion technique used to load hollow polyelectrolyte shells could potentially be used to load hollow polyelectrolyte multilayer capsules, followed by outermost lipid coating could be used to design a slow-release formulation. Alternatively, the use of insulin cores or crystals coated with LbL multilayers followed by an outermost lipid coat can also be envisaged.

The size, wall composition, and diffusion properties of the lipid/polyelectrolyte microcapsules developed in this work are closer to biological cell wall structure than many other model systems. These lipid/polyelectrolyte microcapsules can be treated as a further development of traditional liposome delivery system technologies. This work could be beneficially exploited by reinforcing liposomal technology with the use of electrostatic layer-by-layer technology, thus enhancing the existing liposomal technology for drug delivery.

Extending the particulate delivery technology the incorporation of hydrophobic and surface active molecules in an inorganic core is a new dimension in drug delivery. The novelty of the method lies in the use of anionic phospholipids (phosphatidic acid,

phosphoglycerol)-mediated synthesis of calcium carbonate microparticles from  $\text{Ca}^{2+}$  and  $\text{HCO}_3^-$  salts yields a composite organic/inorganic matrix. The inorganic matrix is predominantly the vaterite polymorph of calcium carbonate. The microparticles contain ~ 2.5-5 % by wt of phospholipids in the matrix. The phospholipids show stable entrapment in the calcium carbonate matrix and strong interactions with the matrix. Such architecture is conducive to the entrapment of small hydrophobic molecules and other bioactive substances in an inorganic matrix. Surprisingly, a large number of macromolecules are surface active in that they show a tendency to selectively partition at an interface. The development of calcium carbonate microparticles entrapping phospholipids is based on the surface active properties of phospholipids. It can be inferred that, this technique of entrapping material can be extended to insulin, and similar peptide drugs which are amphoteric in nature. Further phospholipids can be used advantageously to boost the drug loading in the calcium carbonate matrix because existing literature on material loading into calcium carbonate microparticles suggests a loading of less than 1% in most cases.

## **6.2 Future work**

The insulin reformulation with LbL was designed with biocompatible, biodegradable polymers. The choice of materials was guided by its biological source, and inherent capacity of biological organisms to degrade the materials, or the presence of pathways for removal of the material. Although the word *biocompatibility* is used liberally to describe a whole set of biologically derived polymers, *in vivo* testing is essential in establishing the true behavior of the material for a given mammalian species. Further, the viability of the drug depends on its bioavailability and release kinetics *in*

*vivo*. Hence, animal models need to be developed for nasal drug delivery of the prepared formulations.

As a further development the use of phospholipids in LbL scheme can be applied to insulin cores, which is proving a problem under the conditions used for preparation of LbL thin films on PROMAXX<sup>®</sup> insulin microparticles. This work used PEG buffer for preparation of the insulin drug formulation, the buffer also contains trace quantities of Zn<sup>2+</sup> ions, both PEG and zinc cause problems with phospholipid vesicle stability. Moreover the work presented in this dissertation involved the use of DI water for preparation of phospholipid-polyelectrolyte multilayer films adding a constraint to the use of the technique. An investigation on the suitability of other amphiphilic molecules may be required.

The calcium carbonate microparticles show good prospect for loading hydrophobic and surface active drugs. Testing the efficacy of the platform for drugs and a study of the rheology of the particles for air based delivery systems would be crucial for the development of the platform.

## REFERENCES

1. Colombo, P., *Mucosal Drug Delivery*. Encyclopedia of Controlled Drug Delivery, ed. E. Mathiowitz. 1999, New York: John Wiley & Sons, Inc.
2. Antipov, A.A., G.B. Sukhorukov, E. Donath, and H. Möhwald, Sustained Release Properties of Polyelectrolyte Multilayer Capsules *The Journal of Physical Chemistry B*, 2001. **105**(12): p. 2281-2284.
3. Moya, S., E. Donath, G.B. Sukhorukov, M.B. Auch, H., H. Lichtenfeld, and H. Möhwald, Lipid Coating on Polyelectrolyte Surface Modified Colloidal Particles and Polyelectrolyte Capsules *Macromolecules*, 2000. **33**(12): p. 4538-4544.
4. Speers, M. and C. Bonnano, *Economic Aspects of Controlled Drug Delivery*. Encyclopedia of Controlled Drug Delivery, ed. E. Mathiowitz. 1999, New York: John Wiley & Sons, Inc.
5. *Diabetes Action Now: an Initiative of the World Health Organization and International Diabetes Federation*. 2004, World Health Organization: Geneva, Switzerland.
6. in *MedAd News*. 1998. p. 94.
7. Banting, F.G. and C.M. Best, Pancreatic extracts. *Journal of Laboratory and Clinical Medicine*, 1922. **7**: p. 464-472.
8. Brange, J. and L. Langkjoer, *Insulin structure and stability*. Pharmaceutical Biotechnology; Stability and Characterization of Protein and Peptide Drugs: Case Histories Vol. 5. 1993, New York: Plenum Press. 315-350.
9. Hohanson, O.L. and M.L. Tracy, *Peptide and Protein drug delivery*. Encyclopedia of Controlled Drug Delivery, ed. E. Mathiowitz. 1999, New York: John Wiley & Sons, Inc.
10. Pitt, C.G., The controlled parenteral delivery of polypeptides and proteins. *International Journal of Pharmaceutics*, 1990. **59**: p. 173-196.
11. Lu, W. and T.G. Park, Protein release from poly (lactic-co-glycolic acid) microspheres: protein stability problems. *Journal of Pharmaceutical Science and Technology*, 1995. **49**(1): p. 13-19.
12. Oppenheim, R.C., N.F. Stewart, L. Gordon, and H.M. Patel, The production and evaluation of orally administered insulin nanoparticles. *Drug Development and Industrial Pharmacy*, 1982. **8**: p. 531-546.



13. Damgé, C., C. Michel, M. Aprahamian, and P. Couvreur, New approach for oral administration of insulin with polyalkylcyanoacrylate nanocapsules as drug carriers. *Diabetes*, 1988. **37**: p. 246-251.
14. Michel, C., M. Roques, P. Couvreur, H. Vranckx, P. Baldschmidt, and C. Damge, Isobutyl cyanoacrylate nanoparticles as drug carrier for oral administration of insulin. *Proceedings of the International Symposium of Bioactive Materials*, 1991. **18**: p. 97-98.
15. Al-Khoury Fallouh, N., L. Roblot-Treupel, H. Fessi, J.P. Devissaguet, and F. Puisieux, Development of a new process for the manufacture of polyisobutylcyanoacrylate nanocapsules. *International Journal of Pharmaceutics*, 1986. **28**: p. 125-132.
16. Morishita, M., I. Morishita, K. Takayama, Y. Machida, and T. Nagai, Novel oral microspheres of insulin with protease inhibitor protecting from enzymatic degradation. *International Journal of Pharmaceutics*, 1992. **78**: p. 1-7.
17. Morishita, I., M. Morishita, K. Takayama, Y. Machida, and T. Nagai, Enteral insulin delivery by microspheres in 3 different formulations using Eudragit L100 and S100. *International Journal of Pharmaceutics*, 1993. **91**: p. 29-37.
18. Morishita, I., M. Morishita, K. Takayama, Y. Machida, and T. Nagai, Hypoglycemic effect of novel oral microspheres of insulin with protease inhibitor in normal and diabetic rats. *International Journal of Pharmaceutics*, 1992. **78**: p. 9-16.
19. Behl, C.R., H.K. Pimplaskar, A.P. Sileno, J. deMeireles, and V.D. Romeo, Effects of physicochemical properties and other factors on systemic nasal drug delivery *Advanced Drug Delivery Reviews*, 1998. **29**: p. 89-116.
20. *Physicians' Desk Reference*. 1996, Montvale, N.J.: Medical Economics Data Production Company.
21. Corbo, D.C., J.C. Liu, and Y.W. Chien, Characterization of the barrier properties of mucosal membranes. *Journal of Pharmaceutical Sciences*, 1990. **79**: p. 202-206.
22. Dyer, A.M., M. Hinchcliffe, P. Watts, J. Castile, Jabbal-Gill, R. Nankervis, A. Smith, and L. Illum, Nasal delivery of insulin using novel chitosan based formulations: a comparative study in two animal models between simple chitosan formulations and chitosan nanoparticles. *Pharmaceutical Research*, 2002. **19**: p. 998-1008.
23. Hussain, A.A., Intranasal drug delivery *Advanced Drug Delivery Reviews*, 1998. **29**(1-2): p. 39-49.
24. Merkus, F.W.H.M., N.G.M. Schipper, and J.C. Verhoef, The influence of absorption enhancers on intranasal insulin absorption in normal and diabetic subjects. *Journal of Controlled Release*, 1996. **41**(1-2): p. 69-75.
25. Merkus, F.W.H.M., J.C. Verhoef, S.G. Romeijn, and N.G.M. Schipper, Absorption Enhancing Effect of Cyclodextrins on Intranasally Administered Insulin in Rats. *Pharmaceutical Research*, 1991. **8**: p. 588-592.

26. Callens, C. and J.P. Remon, Evaluation of starch–maltodextrin– Carbopol 974 P mixtures for the nasal delivery of insulin in rabbits. *Journal of Controlled Release*, 2000. **66**: p. 215- 220.
27. Callens, C., E. Pringels, and J.P. Remon, Influence of multiple nasal administrations of bioadhesive powders on the insulin bioavailability. *International Journal of Pharmaceutics*, 2003. **250**: p. 415-422.
28. Mandal, T.K., Inhaled insulin for diabetes mellitus. *American Journal of Health-System Pharmacy*, 2005. **62**: p. 1359-1364.
29. Lorenz, R. and J. Silverstein, *Managing Insulin Requirements at School*, in *School Nurse News*. March 2005.
30. Heinemann, L., Variability of insulin absorption and insulin action. *Diabetes Technology & Therapeutics*, 2002. **4**: p. 673-682.
31. Fu, K., A.M. Klibanov, and R. Langer, Protein stability in controlled-release systems. *Nat. Biotechnol.*, 2000. **18**: p. 24-25.
32. Carrasquillo, K.G., A.M. Stanley, J.C. Aponte-Carro, P. De Jesus, H.R. Costantino, C.J. Bosques, and K. Griebenow, Nonaqueous encapsulation of excipient-stabilized spray-freeze dried BSA into poly(lactide-co-glycolide) microspheres results in release of native protein. *Journal of Controlled Release*, 2001. **76**: p. 199-208.
33. Chen, L., R.N. Apte, and S. Cohen, Characterization of PLGA microspheres for the controlled delivery of IL-1 alpha for tumor immunotherapy. *Journal of Controlled Release*, 1997. **43**: p. 261-272.
34. Edelman, E., L. Brown, J. Taylor, and R. Langer, In vitro and in vivo kinetics of regulated drug release from polymer matrices by oscillating magnetic fields. *Journal of Biomedical Materials Research*, 1987. **21**: p. 339-353.
35. Kost, J., J. Wolfrum, and R. Langer, Magnetically enhanced insulin release in diabetic rats. *Journal of Biomedical Materials Research*, 1987. **21**(12): p. 1367-1373.
36. Hsieh, D., R. Langer, and J. Folkman, Magnetic Modulation of Release of Macromolecules from Polymers. *Proceedings of the National Academy of Sciences*, 1981. **78**: p. 1863-1867.
37. Kost, J., R. Noecker, E. Kunica, and R. Langer, Magnetically controlled release systems: Effect of polymer composition. *Journal of Biomedical Materials Research*, 1985. **19**(8): p. 935-940.
38. Saslavski, O., P. Couvrer, and N. Peppas. *Controlled Release of Bioactive Materials*. in *Controlled Release Society*. 1988. Basel.
39. Edelman, E., J. Kost, H. Bobeck, and R. Langer, Regulation of drug release from polymer matrices by oscillating magnetic fields. *Journal of Biomedical Materials Research*, 1985. **19**(1): p. 67-83.

40. Brown, L., C. Munoz, L. Siemer, E. Edelman, and R. Langer, Controlled release of insulin from polymer matrices. Control of diabetes in rats. *Diabetes*, 1986. **35**: p. 692-697.
41. Kost, J., K. Leong, and R. Langer, Ultrasound-Enhanced Polymer Degradation and Release of Incorporated Substances. *Proceedings of the National Academy of Sciences*, 1989. **86**: p. 7663-7666.
42. Kost, J. Electronically-Controlled Drug Delivery, ed. B. Berner and S. Dinh. 1998, Boca Raton, Fla.: CRC Press.
43. Brownlee, M. and A. Cerami, A glucose-controlled insulin-delivery system: semisynthetic insulin bound to lectin. *Science*, 1979. **206**(4423): p. 1190-1191.
44. Kokufata, E., Y.-Q. Zhang, and T. Tanaka, Saccharide-sensitive phase transition of a lectin-loaded gel *Nature*, 1991. **351**: p. 302-304.
45. Lvov, Y., G. Decher, and H. Möhwald, Assembly, structural characterization and thermal behavior of layer-by-layer deposited ultrathin films of poly(vinylsulfate) and poly(allylamine). *Langmuir*, 1993. **9**(2): p. 481-486.
46. Lvov, Y., K. Ariga, I. Ichinose, and T. Kunitake, Assembly of Multicomponent Protein Films by Means of Electrostatic Layer-by-Layer Adsorption *Journal of the American Chemical Society*, 1995. **117**(22): p. 6117-6123.
47. Decher, G., Fuzzy Nanoassemblies: Toward Layered Polymeric Multicomposites. *Science*, 1997. **227**: p. 1232-1237.
48. Sukhorukov, G.B., *Multilayer Hollow Microspheres Dendrimers* Vol. 5. 2002, London: MML-Series Citus Books.
49. Shchukin, D.G., A.A. Patel, G.B. Sukhorukov, and Y.M. Lvov, Nanoassembly of Biodegradable Microcapsules for DNA Encasing. *Journal of the American Chemical Society*, 2004. **126**(11): p. 3374-3375.
50. Lvov, Y. and F. Caruso, Biocolloids with ordered urease multilayer shells as enzymatic reactors. *Analytical Chemistry*, 2001. **73**(17): p. 4212-4217.
51. Lvov, Y. and F. Caruso, Biocolloids with Ordered Urease Multilayer Shells as Enzymatic Reactors. *Analytical Chemistry*, 2001. **73**: p. 4212-4217.
52. Lvov, Y., K. Ariga, I. Ichinose, and T. Kunitake, Assembly of multicomponent protein films by means of electrostatic layer-by-layer adsorption. *Journal of the American Chemical Society*, 1995. **117**: p. 6117-6123.
53. Sukhorukov, G.B., D.V. Volodkin, A.M. Günther, A.I. Petrov, D.B. Shenoy, and H. Möhwald, Porous calcium carbonate microparticles as templates for encapsulation of bioactive compounds. *Journal of Materials Chemistry*, 2004. **14**: p. 2073-2079.
54. Pargaonkar, N., Y. Lvov, N. Li, J. Steenekamp, and M. de Villiers, Controlled Release of Dexamethasone from Microcapsules Produced by Polyelectrolyte Layer-by-Layer Nanoassembly. *Pharmaceutical Research*, 2005. **22**: p. 826-835.

55. Ai, H., S.A. Jones, and Y.M. Lvov, Biomedical applications of electrostatic layer-by-layer nano-assembly of polymers, enzymes, and nanoparticles. *Cell Biochemistry And Biophysics*, 2003. **39**(1): p. 23-43.
56. Ai, H., S. Jones, M. de Villiers, and Y. Lvov, Nanoencapsulation of Furosemide Microcrystals for Controlled Drug Release. *Journal of Controlled Release*, 2003. **86**: p. 59-66.
57. Uneo, Y., H. Futagawa, Y. Takagi, A. Uneo, and Y. Mizushima, Drug-incorporating calcium carbonate nanoparticles for a new delivery system. *Journal of Controlled Release*, 2005. **103**: p. 93-98.
58. Majeti, N.V.R.K., Nano and microparticles as controlled drug delivery devices. *Journal of Pharmacy and Pharmaceutical Sciences*, 2000. **3**: p. 234-258.
59. Akerman, M.E., W.C. Chan, P. Laakkonen, S.N. Bhatia, and E. Ruoslahti, Nanocrystal targeting in vivo. *Proceedings of the National Academy of Sciences*, 2002. **99**: p. 12617-12621.
60. Paul, W. and C.P. Sharma, Ceramic drug delivery: a prespective. *Journal of Biomaterials Applications*, 2003. **17**: p. 253-264.
61. Itokazu, M., T. Sugiyama, T. Ohno, E. Wada, and Y. Katagiri, Development of porous apatite ceramic for local delivery of chemotherapeutic agents. *Journal of Biomedical Materials Research*, 1998. **39**: p. 536-538.
62. Yanagawa, A., T. Kudo, and Y. Mizushima, A novel particle carrier for transnasal peptide absorption. *Japanese Journal of Clinical Pharmacology and Therapeutics*, 1995. **26**: p. 127-128.
63. Ishikawa, F., M. Murano, M. Hiraishi, T. Yamaguchi, I. Tamai, and A. Tsuji, Insoluble powder formulation as an effective nasal delivery system. *Pharmaceutical Research*, 2002. **19**: p. 1097-1104.
64. Haruta, S., T. Hanafusa, H. Fukase, H. Miyajima, and T. Oki, An effective absorption behavior of insulin for diabetic treatment following intranasal delivery using porous spherical calcium carbonate in monkeys and healthy human volunteers. *Diabetes Technology & Therapeutics*, 2003. **5**: p. 1-9.
65. Ozin, G.A., N. Varaksa, N. Coombs, J.E. Davies, D.D. Perovicd, and M. Ziliox, Bone mimetics: a composite of hydroxyapatite and calcium dodecylphosphate lamellar phase. *Journal of Materials Chemistry*, 1997. **7**(8): p. 1601-1607.
66. Ozin, G.A., Panoscopic materials: synthesis over 'all' length scales. *Chemical Communications*, 2000: p. 419-432.
67. Kankare, J., Sauerbrey Equation of Quartz Crystal Microbalance in Liquid Medium. *Langmuir*, 2002. **18**: p. 7092.
68. Axelrod, D., D.E. Koppel, J. Schlessinger, E. Elson, and W.W. Webb, Mobility measurement by analysis of fluorescence photobleaching recovery kinetics. *Biophysical Journal*, 1976. **16**: p. 1055-1069.

69. Blonk, J.C.G., A. Don, H. Van Aalst, and J.J. Birmingham, Fluorescence photobleaching recovery in confocal scanning light microscope. *Journal of Microscopy*, 1993. **169**(3): p. 363-374.
70. Rashba-Step, J., R. Darvari, and T.L. Scott, *Methods for encapsulating small spherical particles prepared by controlled phase separation in US Patent*. 2005, Baxter Health Care Corporation: USA.
71. Brown, L., J.K. McGeehan, J. Rashba-Step, and T.L. Scott, *Methods for fabrication, uses and compositions of small spherical particles prepared by controlled phase separation in US Patent*. 2005, Baxter Health Care Corporation: USA.
72. Donath, E., G.B. Sukhorukov, F. Caruso, S.A. Davis, and H. Möhwald, Novel Polymer Shells via Colloid-Templated Assembly of Polyelectrolytes. *Angewandte Chemie International Edition*, 1998. **37** p. 2201-2205.
73. Caruso, F., R.A. Caruso, and H. Möhwald, Nanoengineering of Inorganic and Hybrid Hollow Spheres by Colloidal Templating. *Science*, 1998. **262**: p. 1111-1114.
74. Peyratout, C. and L. Dähne, Tailor-Made Polyelectrolyte Microcapsules: From Multilayers to Smart Containers. *Angewandte Chemie International Edition*, 2004(43): p. 3762-3783.
75. Balabushevitch, N., G. Sukhorukov, N. Moroz, D. Volodkin, N. Larionova, E. Donath, and H. Möhwald, Encapsulation of proteins by layer-by-layer adsorption of polyelectrolytes onto protein aggregates. *Biotechn. Bioengineering.*, 2001. **76**: p. 209-214.
76. Qiu, X.P., S. Leporatti, E. Donath, and H. Möhwald, Studies on the drug release properties of polysaccharide multilayers encapsulated ibuprofen microparticles. *Langmuir*, 2001. **17**: p. 5375-5380.
77. Shchukin, D., G. Sukhorukov, and H. Möhwald, Biomimetic Fabrication of Nanoengineered Composite Shells. *Chemistry of Materials*, 2003. **15**: p. 3947-3950.
78. Ye, S., C. Wang, X. Liu, and Z. Tong, Deposition Temperature Effect on Release of Indomethacin from Microcapsules of Layer-by-Layer Assembled Chitosan and Alginate. *Journal of Controlled Release*, 2005. **88**: p. 678-683.
79. Dai, Z., A. Heilig, H. Zastrow, E. Donath, and H. Möhwald, Novel Formulation of Vitamins and Insulin by Nanoengineering of Polyelectrolyte Multilayers around Microcrystals. *Chemistry - A European Journal*, 2004. **10**: p. 6369-6374.
80. Balabushevich, N. and N. Larionova, Fabrication and Characterization of Polyelectrolyte Microparticles with Protein. *Biochemistry (Russ)*, 2004. **69**: p. 757-763.
81. Xia, J., P.L. Dubin, and V.A. Kabanov, *Chapters 15 and 10. Protein Polyelectrolyte Complexes in Chemistry and Biology*, ed. P.L. Dubin, J. Bock, R.M. Davis, D. Schulz, and C. Thies. 1994, Berlin: Eds. Springer-Verlag.

82. Krishna, G., T. Shutava, and Y. Lvov, Lipid Modified Polyelectrolyte Microcapsules with Controlled Diffusion. *Chemical Communications*, 2005: p. 2796-2799.
83. *Sigma standard fluorescent labeling procedure for amine labeling with fluorescein isothiocyanate*, in *Sigma-Aldrich Catalog*. 2005. p. 374.
84. Abbott, N.L., D. Blankshtein, and A.T. Hatton, Protein partitioning in two-phase aqueous polymer systems. 1. Novel physical pictures and a scaling thermodynamic formulation *Macromolecules*, 1991. **24**(15): p. 4334-4348.
85. Yap, H.P., J.F. Quinn, S.M. Ng, J. Cho, and F. Caruso, Colloid Surface Engineering via Deposition of Multilayered Thin Films from Polyelectrolyte Blend Solutions. *Langmuir*, 2005. **21**(10): p. 4328-4333.
86. Cho, J., J.F. Quinn, and F. Caruso, Fabrication of Polyelectrolyte Multilayer Films Comprising Nanoblended Layers *Journal of the American Chemical Society*, 2004. **126**(8): p. 2270-2271.
87. Chausmer, A.B., Zinc, Insulin and Diabetes. *Journal of the American College of Nutrition*, 1998. **17**: p. 109-115.
88. Ichinose, I., K. Fujiyoshi, S. Mizuki, Y. Lvov, and T. Kunitake, Layer-by-Layer Assembly of Aqueous Bilayer Membranes on Charged Surfaces *Chemistry Letters*, 1996. **25**: p. 257-258.
89. Kabanov, V.A. and A.A. Yaroslavov, What happens to negatively charged lipid vesicles upon interacting with polycation species? *Journal of Controlled Release*, 2002. **78**: p. 267-271.
90. Lvov, Y., F. Essler, and G. Decher, Combination of polycation/polyanion self-assembly and Langmuir-Blodgett transfer for the construction of superlattice films *The Journal of Physical Chemistry*, 1993. **97**(51): p. 13773-13777.
91. Moya, S., W. Richter, S. Leporatti, H. Baumler, and E. Donath, Freeze-Fracture Electron Microscopy of Lipid Membranes on Colloidal Polyelectrolyte Multilayer Coated Supports. *Biomacromolecules*, 2003. **4**(3): p. 808-814.
92. Wong, J.Y., J. Majewski, M. Seitz, C.K. Park, J.N. Israelachvili, and G.S. Smith, Polymer-Cushioned Bilayers. I. A Structural Study of Various Preparation Methods Using Neutron Reflectometry *Biophysical Journal*, 1999. **77**: p. 1445-1457.
93. Wong, J.Y., C.K. Park, M. Seitz, and J. Israelachvili, Polymer-Cushioned Bilayers. II. An Investigation of Interaction Forces and Fusion Using the Surface Forces *Biophysical Journal*, 1999. **77**: p. 1458-1468.
94. Mornet, S., O. Lambert, E. Duguet, and A. Brisson, The Formation of Supported Lipid Bilayers on Silica Nanoparticles Revealed by Cryoelectron Microscopy. *Nano Letters*, 2005. **5**(2): p. 281-285.
95. Feng, Z.V., S. Granick, and A.A. Gewirth, Modification of a Supported Lipid Bilayer by Polyelectrolyte Adsorption *Langmuir*, 2004. **20**(20): p. 8796-8804.

96. Rinia, H.A., R.A. Kik, R.A. Demel, M.M.E. Snel, J.A. Killian, J.P.J.M. van der Eerden, and B. de Kruijff, Visualization of Highly Ordered Striated Domains Induced by Transmembrane Peptides in Supported Phosphatidylcholine Bilayers. *Biochemistry*, 2000. **39**: p. 5852 - 5858.
97. Ibarz, G., L. Dähne, E. Donath, and H. Möhwald, Controlled Permeability of Polyelectrolyte Capsules via Defined Annealing *Chemistry of Materials*, 2002., **14**(10): p. 4059-4062.
98. Vogt, B.D., E.K. Lin, W.-l. Wu, and C.C. White, Effect of Film Thickness on the Validity of the Sauerbrey Equation for Hydrated Polyelectrolyte Films *The Journal of Physical Chemistry B*, 2004. **108**(34): p. 12685-12690.
99. Shashkov, S.N., M.A. Kiselev, S.N. Tioutiounnikov, A.M. Kiselev, and P. Lesieur, The Study of DMSO/Water and DPPC/DMSO/Water System by Means of the X-ray, Neutron Small-angle Scattering, Calorimetry and IR Spectroscopy *Physica B: Condensed Matter*, 1999. **271**(1-4): p. 184-191
100. Zein, M. and R. Winter, Effect of temperature, pressure and lipid acyl chain length on the structure and phase behaviour of phospholipid-gramicidin bilayers. *Physical Chemistry Chemical Physics*, 2000. **2**(20): p. 4545-4551.
101. Carion-Taravella, B., S. Lesieur, J. Chopineau, P. Lesieur, and M. Ollivon, Phase Behavior of Mixed Aqueous Dispersions of Dipalmitoylphosphatidylcholine and Dodecyl Glycosides: A Differential Scanning Calorimetry and X-ray Diffraction Investigation *Langmuir*, 2002. **18**(2): p. 325-335.
102. Uhrikova, D., N. Kucerka, A. Islamov, A. Kuklin, V. Gordeliy, and P. Balgavy, Small-angle neutron scattering study of the lipid bilayer thickness in unilamellar dioleoylphosphatidylcholine vesicles prepared by the cholate dilution method: n-decane effect. *BBA - Biochimica et Biophysica Acta: Biomembranes*, 2003. **1611**(1-2): p. 31-34
103. Fragneto, G., F. Graner, T. Charitat, P. Dubos, and E. Bellet-Amalric, Interaction of the Third Helix of Antennapedia Homeodomain with a Deposited Phospholipid Bilayer: A Neutron Reflectivity Structural Study. *Langmuir*, 2000. **16**(10): p. 4581-4588.
104. Rabea, E.I., M.E.-T. Badawy, C.V. Stevens, G. Smagghe, and W. Steurbaut, Chitosan as Antimicrobial Agent: Applications and Mode of Action *Biomacromolecules*, 2003. **4**(6): p. 1457-1465.
105. and, M.Z. and R. Winter, 2000, 2, 4545, Effect of temperature, pressure and lipid acyl chain length on the structure and phase behaviour of phospholipid-gramicidin bilayers. *Physical Chemistry Chemical Physics*, 2000. **2**(20): p. 4545-4551.
106. Antipov, A.A., D. Shchukin, Y. Fedutik, A.I. Petrov, G.B. Sukhorukov, and H. Möhwald, Carbonate microparticles for hollow polyelectrolyte capsules fabrication *Colloids and Surfaces A: Physicochemical and Engineering Aspects*, 2003. **224**: p. 175-183
107. Garidel, P., G. Förster, W. Richter, B.H. Kunst, G. Rapp, and A. Blume, 1,2-Dimyristoyl-sn-glycero-3-phosphoglycerol (DMPG) divalent cation complexes:

- an X-ray scattering and freeze-fracture electron microscopy study. *Physical Chemistry Chemical Physics*, 2000. **2**(20): p. 4537-4544.
108. Fang, N., V. Chan, H.-Q. Mao, and K.W. Leong, Interactions of Phospholipid Bilayer with Chitosan: Effect of Molecular Weight and pH *Biomacromolecules*, 2001. **2**(4): p. 1161-1168.
  109. Sukhorukov, G.B., D.G. Shchukin, W.-F. Dong, H. Möhwald, V.V. Lulevich, and O.I. Vinogradova, Comparative Analysis of Hollow and Filled Polyelectrolyte Microcapsules Templated on Melamine Formaldehyde and Carbonate Cores *Macromolecular Chemistry and Physics*, 2004. **205**: p. 530-535.
  110. Addadi, L. and S. Weiner, Biomineralization: A pavement of pearl. *Nature*, 1997. **389**: p. 912-915.
  111. Litvin, A.L., L.A. Samuelson, D.H. Charych, and D.L. Kaplan, Influence of Supramolecular Template Organization on Mineralization. . *The Journal of Physical Chemistry*, 1995. **99**(32): p. 12065-12068. .
  112. Malkaj, P. and E. Dalas, Calcium Carbonate Crystallization in the Presence of Aspartic Acid. *Journal of Crystal Growth*, 2004. **4**: p. 721-723.
  113. Dalas, E. and P.G. Koutsoukos, The crystallization of vaterite on cholesterol. *Journal of Colloid and Interface Science*, 1989. **127**: p. 273-280
  114. Manoli, F. and E. Dalas, Calcium carbonate crystallization in the presence of glutamic acid. *Journal of Crystal Growth*, 2001. **222**: p. 293-297
  115. Manoli, F., J. Kanakis, P. Malkaj, and E. Dalas, The effect of aminoacids on the crystal growth of calcium carbonate. *Journal of Crystal Growth*, 2002. **236**: p. 363-370.
  116. Manoli, F. and E. Dalas, Spontaneous precipitation of calcium carbonate in the presence of chondroitin sulfate. *Journal of Crystal Growth*, 2000 **217**: p. 416-421
  117. Damle, C., A. Kumar, S.R. Sainkar, M. Bhagawat, and M. Sastry, Growth of Calcium Carbonate Crystals within Fatty Acid Bilayer Stacks *Langmuir*, 2002. **18**(16): p. 6075-6080.
  118. Mann, S., J.P. Hannington, and R.J.P. Williams, Phospholipid vesicles as a model system for biomineralization *Nature*, 1986. **324**: p. 565-567.
  119. Tracy, L.S., C.J.P. Francois, and H.M. Jennings, The growth of calcite spherulites from solution: I. Experimental design techniques. *Journal of Crystal Growth*, 1998. **193**: p. 374-381.
  120. Koga, N., Y. Nakagoe, and H. Tanaka, Crystallization of amorphous calcium carbonate. . *Thermochimica Acta*, 1998. **318**: p. 239-244
  121. Horn, D. and J. Rieger, Organic Nanoparticles in the Aqueous Phase - Theory, Experiment, and Use. *Angewandte Chemie International Edition*, 2001. **40**: p. 4330-4361.



122. Spanos, N. and P.G. Koutsoukos, The transformation of vaterite to calcite: effect of the conditions of the solutions in contact with the mineral phase. *Journal of Crystal Growth*, 1998. **191**: p. 783-790.
123. Kitamura, M., Crystallization and Transformation Mechanism of Calcium Carbonate Polymorphs and the Effect of Magnesium Ion. *Journal of Colloid and Interface Science*, 2001. **236**: p. 318-327
124. Kitamura, M., H. Konno, A. Yasui, and H. Masuoka, Controlling factors and mechanism of reactive crystallization of calcium carbonate polymorphs from calcium hydroxide suspensions. . *Journal of Crystal Growth*, 2002. **236**: p. 323-332.
125. Antipov, A.A., D. Shchukin, Y. Fedutik, A.I. Petrov, G.B. Sukhorukov, and H. Möhwald, Carbonate microparticles for hollow polyelectrolyte capsules fabrication. *Colloids and Surfaces A: Physicochemical and Engineering Aspects*, 2003. **224**: p. 175-183.
126. Zarif, L., J. Graybill, D. Perlin, and R. Mannino, Cochleates: new lipid-based drug delivery system. *Journal of Liposome Research.*, 2000. **10(4)**: p. 523-538.
127. Papahadjopoulos, D., Surface properties of acidic phospholipids: Interaction of monolayers and hydrated liquid crystals with uni- and bi-valent metal ions. *BBA - Biochimica et Biophysica Acta: Biomembranes*, 1968. **163(2)**: p. 240-254.
128. Van Wazer, J.R. and D.A. Campanella, 1950, 72, 655., Structure and Properties of the Condensed Phosphates. IV. Complex Ion Formation in Polyphosphate Solutions *Journal of the American Chemical Society*, 1950. **72**: p. 655-663.

## VITA

Mr. Krishna Gopal was born in Amalapuram, A P, India. He did his bachelors in Chemical Engineering at Osmania University, College of Technology, (1997-2001) Hyderabad, AP, India. Following which he enrolled in PhD program in Biomedical Engineering at Louisiana Tech University (2001-2006).

### Journal Publications

- T. Shutava, R. Darvari , **K. Gopal**, N. Pargaonkar, Q. Lin, A. Sullivan, Y. Lvov and J. Rashba-Step, 2006 “Layer-by-Layer Polyelectrolyte Nanocoating of Insulin Microparticles for Sustained Release” *manuscript in preparation*
- **K. Gopal**, Z. Lu, M. M. de Villiers, and Y. Lvov, *The Journal of Physical Chemistry : B*. 2006, **110**, p 2471-2474 “Composite Phospholipid-Calcium Carbonate Microparticles: Influence of Anionic Phospholipids on the Crystallization of Calcium Carbonate”
- **K. Gopal**, T. Shutava, Y. Lvov, *Chemical Communications*, 2005, **22**, p 2796–2798, “Lipid Modified Polyelectrolyte Microcapsules with Controlled Diffusion”
- D. S. Patel , R. K. Aithal , **K. Gopal**, Y. Lvov, M. Tien and D. Kuila, *Colloids and Surfaces B: Biointerfaces*, 2005, **43**, p13–19 “ Nano-assembly of manganese peroxidase and lignin peroxidase from *P. chrysosporium* for biocatalysis in aqueous and non-aqueous media”.

### Conference Proceedings

- D. Kuila, M. Tien, **K. Gopal**, Y Lvov, M McShane, S. Singh, A. Potluri, S. Kaul, **SPIE-Proceedings**, (SPIE International Nanofabrication Conference) 2005, Philadelphia, “Nanoassembly of Immobilized Lignolytic Enzymes for Biocatalysis, Bioremediation and Biosensing,”

### Conference Presentations

- **K. Gopal**, Z. Lu, and Y. Lvov 231<sup>st</sup> ACS National Meeting, Atlanta GA “Phospholipid Mediated Synthesis of Calcium Carbonate Microparticles as a Carrier for Hydrophobic Molecules.” March 2006.
- Z. Lu, Z. Zheng, G. A. Grozdits, E. Lvova, **K. Gopal**, S. Eadula, and Y. M. Lvov 231<sup>st</sup> ACS National Meeting, Atlanta GA, “Layer-by-Layer Nanocoating of Wood Fibers with Polyelectrolytes and Nanoparticles.” March 2006.
- M. Prouty, Z. Lu, N. Veerabadran, **K. Gopal**, Alex Yaroslavov, Challa Kumar and Yuri Lvov, Louisiana Materials and Emerging Technologies Conference, Ruston LA, “Drug Layer-by-Layer Nanoencapsulation and Controlled Release.” December 2005.
- **K. Gopal**, Z. Lu, S. R. Eadula and Y. Lvov, 61<sup>st</sup> Southwest and the 57<sup>th</sup> Southeast ACS Joint Regional Meeting, Memphis TN, “Phospholipid-Calcium Carbonate nanocomposite microparticles: Blending Organic and Inorganic Materials.” November 2005.
- T. G. Shutava, M. D. Prouty, D. S. Kommireddy, **K. Gopal**, and Y. Lvov. 230<sup>th</sup> ACS National Meeting Washington DC, “Multilayered Polyelectrolyte/Natural Polyphenol Nanofilms and Microcapsules for Protein Encapsulation and Protection Against Free Radical Oxidation.” August 2005.
- **K. Gopal**, T. Shutava and Y. Lvov., 30<sup>th</sup> Annual Meeting, Society for Biomaterials, Memphis TN, Lipid-Polyelectrolyte Composite Films for Diffusion Control.” April 2005.
- D. S. Patel, R. Aithal, **K. Gopal**, Y. Lvov, T. Mester, M. Tien and D. Kuila, 226<sup>th</sup> ACS National Meeting, New York NY, “Nano-assembly of Lignin Peroxidase and Manganese Peroxidase from Phanerochaete Chrysosporium for Oxidation of Organic Compounds.” September 2003.
- K. Aithal, D. Patel, **K. Gopal**, Y. Lvov and D. Kuila. 225<sup>th</sup> ACS National Meeting, New Orleans, LA, “Nano-Assembly of Novel Enzymes for Biocatalysis and Degradation of Environmental Pollutants.” March 2003
- K. Aithal, D. Patel, **K. Gopal**, Y. Lvov and D. Kuila. 226<sup>th</sup> ACS National Meeting, New York NY, “Nano-assembly of Novel Enzymes for Bio-catalysis in Non-aqueous Media.” September 2003.
- **K. Gopal**, Y. Lvov and D. Kuila. 226<sup>th</sup> ACS National Meeting, New York NY, “Microreactor and microseparator research at Louisiana Tech's Institute for Micromanufacturing.” September 2003.

- **K. Gopal**, Q. Brown, T. Shutava, M. McShane and Y. Lvov. 2003 BMES National Annual Fall Meeting, Nashville TN, “Nano Sensor Based on Controlled Deposition of Glucose Oxidase and  $[\text{Ru}(\text{bpy})_3]^{2+}$  Entrapped in Zeolite.” October 2003.
- D. S. Patel, **K. Gopal**, K. R. Aithal Y. Lvov, T. Mester, M. Tien and D. Kuila. Governor’s Biotechnology Initiative Symposium, Shreveport, LA “Nano-assembly of novel enzymes for bio-catalysis and degradation of environmental pollutants.” November 2002.
- K. R. Aithal, D. S. Patel, **K. Gopal**, Y. Lvov, T. Mester, M. Tien and D. Kuila. LSU Health Sciences Retreat, Shreveport, LA “Nano-assembly of novel enzymes for bio-catalysis and degradation of environmental pollutants.” March 2003.
- R.I. Wadke, N. Palwai, K. Gajula, , **K. Gopal**, and D. Haynie. Louisiana NSF-EPSCoR conference, Baton Rouge LA “Role of tensin in structure and function of the focal adhesions.” May 2002.